ACUTE INTERMITTENT HYPOXIA – A NOVEL NON-INVASIVE THERAPY THAT PROMOTES REGENERATION AKIN TO BRIEF ELECTRICAL STIMULATION IN PERIPHERAL NERVE REPAIR

A Thesis Submitted to the College of Graduate and Postdoctoral Studies in Partial Fulfillment of the Requirements for the Degree of Doctorate of Philosophy in the Department of Anatomy and Cell Biology

University of Saskatchewan

Saskatoon, Saskatchewan, Canada

Joëlle Renée Nadeau

Permission to Use

In presenting this thesis in partial fulfillment of the requirements for the degree of Doctorate of Philosophy from the University of Saskatchewan, I consent that the library makes it freely available for review. I further agree that permission for copying of this thesis in any manner, in whole or in part, for scholarly purposes may be granted by the professor or professors who supervised this thesis work or, in my absence, by the Head of the Department or the Dean of College in which my thesis work was done. It is understood that any copying or publication or use of this thesis or parts thereof for financial gain shall not be allowed without my written permission. It is also understood that due recognition shall be given to me and to the University of Saskatchewan in any scholarly use which be made of any material in my thesis.

Dean
College of Graduate and Postdoctoral Studies
University of Saskatchewan
116 Thorvaldson Building, 110 Science Place
Saskatoon, Saskatchewan S7N 5C9
Canada

Requests for permission to copy or to make other use of material in this thesis to whole or part should be addressed to:
Head of the Department of Anatomy and Cell Biology
University of Saskatchewan, 2D01 Health Science Building, 107 Wiggins Road
Saskatoon, Saskatchewan S7N 5E5

Abstract

Peripheral nerve regeneration often results in poor functional outcomes, a reality we aim to change. Injured peripheral neurons mount an intrinsic repair response as they undergo regenerative neuronal reprogramming, which can be enhanced by brief electrical stimulation (ES) of the injured nerve at the time of surgical repair, resulting in improved regeneration in rodents and humans. However, this approach is invasive.

Acute intermittent hypoxia (AIH) - breathing alternate cycles of regular air and air with ~50% normal oxygen levels (11% O_2) is emerging as a promising non-invasive intervention that promotes respiratory and non-respiratory motor function in spinal cord injured rats and humans. However, this therapy has the potential to globally impact the nervous system beyond the motor system. Of note, hypoxic conditions can increase neural activity in injured sensory neurons and peripheral axons and promote repair. Thus, I hypothesized that an AIH paradigm similar to that used for spinal cord repair, will improve peripheral nerve repair in a manner akin to ES, including its impact on regeneration-associated gene (RAG) expression – a predictor of growth states. To this end, alterations in early RAG expression (growth-associated protein 43, brain-derived neurotrophic factor, hypoxia-inducible factor alpha and a neural specific growth-associated protein, superior cervical ganglion 10) were examined for rats that had undergone tibial nerve transection and repair with either 2 days of normoxia treatment or AIH treatment begun two days post-repair, or 1 hour continuous ES treatment (20 Hz) at the time of repair. Three days post-repair, AIH or ES treatments effected significant and parallel elevated RAG expression relative to normoxia control treatment, most evident at the growing axon front. Behavioural, thermal and mechanical sensitivity assessments revealed that neither ES nor AIH elevated regeneration-associated pain states. Finally, ES showed significant impacts on functional recovery relative to normoxia controls in mid (25 day)- and late (70 day)-regeneration stages and AIH in mid (25 day)-regeneration stages. These indicators of an enhanced regenerative state for AIH and ES were supported by significantly increased numbers of newly myelinated fibers detected 20 mm distal to the tibial nerve repair site at 25 days post nerve repair.

Collectively, these results support a role for brief AIH treatment, as a promising noninvasive adjunct therapy for improved peripheral nerve repair in a manner consistent with that observed with the more invasive direct nerve stimulation.

Acknowledgements

I would like to especially thank my two supervisors, Drs. Valerie Verge and Gillian Muir, for all of their support as well as all of their wonderful staff and students. To the two dear technicians of the Cameco MS Neuroscience Research Center, Dr. Ruiling Zhai and Jayne Johnston; your patience, guidance and support are very appreciated. Thank you to my lab moms for taking care of me as well as Dr. Erin Prosser-Loose, Dr. Atiq Hassan, Dr. Nikki McLean and Shannon Berko. Dr. Valerie Verge, in addition, I've truly appreciated having you as a mentor, encouraging multi-disciplinary research and introducing me to so many specialists that eventually led me to where I am now.

I would also like to thank my PhD committee: Dr. Helen Nichol, Dr. David Schreyer, Dr. Brian Eames and Dr. Gary Linassi, as well as my external advisor, Dr. Raj Midha, for their guidance, insight and feedback. Additionally, many thanks go to Dr. Breanna Arnold for performing the behavioural testing and handling of the rats in the long-term study section. Without her expertise, inadequate footprints would have been obtained, as I had absolutely no idea that one could successfully clip rat nails.
To my family and husband, thank you for your support, love and almost giving up on asking me "are you going to get a job now?"; I'm getting a job now, well after just one more degree, I promise.

The work for this thesis was done at both the Cameco MS Neuroscience Research Center and the Veterinary Biomedical Sciences Department at the University of Saskatchewan. Funding for this research was provided by the University of Saskatchewan, the Saskatchewan Health Research Foundation and the Canadian Institutes of Health Research. Scholarship support was provided by the University of Saskatchewan College of Medicine and the College of Graduate Studies. Additional financial support as travel awards for conference presentations was provided by the College of Medicine and the University of Saskatchewan.

Table of Contents

List of Figures

List of Abbreviations

AIH	Acute Intermittent Hypoxia
ATF3	Activating transcription factor 3
ATP	Adenosine triphosphate
BDNF	Brain-derived neurotrophic growth factor
Ca^{2+}	Calcium
DRG	Dorsal root ganglion
GAP43	Growth-associated protein 43
GDNF	Glial-derived neurotrophic factor
GFAP	Glial fibrillary acidic protein
HIF-1α	Hypoxia-inducible factor-1α
L2	Lumbar segment 2
L3	Lumbar segment 3
L4	Lumbar segment 4
L5	Lumbar segment 5
mRNA	Messenger ribonucleic acid
NGF	Nerve growth factor
NTRK1	Neurotrophic receptor tyrosine kinase 1 (aka trkA)
NTRK2	Neurotrophic receptor tyrosine kinase 2 (aka trkB)
NTRK3	Neurotrophic receptor tyrosine kinase 3 (aka trkC)
NT-3	Neurotrophin 3
NT-4/5	Neurotrophin 4/5
p75NTR	p75 neurotrophin receptor
PNS	Peripheral nervous system
RAG	Regeneration-associated gene
S2	Sacral segment 2
SCG10	Superior cervical ganglion 10; stathmin 2
s.e.m.	Standard error of the mean

1. Introduction

A century ago, Santiago Ramón y Cajal described in his 'Degeneration and Regeneration of the Nervous System' the regenerating capability of the axons of the peripheral nervous system (PNS) following nerve damage. This characteristic of the PNS to regenerate, unlike that of the central nervous system, has lead to the generalization that peripheral nerves fully regrow when, in fact, only 10% of adults regain normal function after injury to a major peripheral nerve even with surgical intervention (Brushart et al. 1998). Peripheral reinnervation is thus described as 'often delayed and seldom complete' (Zochodne 2012). In addition to slow growth and incomplete reinnervation, regenerating axons are often misdirected to functionally inappropriate target organs with efferent motor axons innervating sensory end organs or sensory axons being misdirected to inappropriate organs or locations (Brushart and Mesulam 1980, Koerber, Seymour, and Mendell 1989, Witzel, Rohde, and Brushart 2005). Thus, along with the diminishment or loss of limb or organ function, neuropathic pain states may develop.

Despite this intrinsic ability for peripheral nerves to regenerate, it remains fraught with challenges often maladaptive in nature. However, the intrinsic repair mechanisms can be greatly enhanced by the use of alternative therapies in conjunction with surgery. Brief electrical nerve stimulation (ES) applied at the time of surgical repair results in better functional outcomes in both rodents and humans (Al-Majed et al. 2000, Gordon et al. 2010). However, ES is invasive and becomes difficult if the nerve is not readily accessible. An emerging non-invasive therapy, acute intermittent hypoxia (AIH), promotes respiratory and non-respiratory motor function in spinal cord injured rats and humans (reviewed in Dale, Ben Mabrouk, and Mitchell 2014). This AIH paradigm

consists of breathing 5 minute alternating periods of air with half oxygen (11%) and regular air for ten cycles and results in increased phrenic nerve output activity in the rat (reviewed in Mitchell and Johnson 2003). The impact of this AIH treatment paradigm is presumably systemic with recent studies showing regeneration-associated changes in non-respiratory motor neurons in spinal cord injured rats (Satriotomo et al. 2016). In addition to that documented in the central nervous system, impacts in the PNS have been observed. Using a more aggressive AIH protocol (10 min cycles of air with significantly reduced oxygen (8%) alternating with regular air for 6 cycles) begun immediately at the time of sciatic nerve crush, positive effects of AIH were observed on transcriptional and regeneration-associated (RAG) expression and the regenerative capacity of the nerves in mice at the early 3 day time-point examined (Cho et al. 2015). While the Cho et al. (2015) study demonstrated the potential for AIH in enhancing early regenerative responses and also revealed a direct involvement of hypoxia-inducible factor-1α (HIF-1α) in regulation of these responses, the level of hypoxia employed in this study falls within what is considered a severe hypoxia range (reviewed in Astorino, Harness, and White 2015). Also, the injury and treatment paradigm employed do not address the realities of human application, such as level of hypoxia tolerated by humans and clinical pathologies requiring nerve coaptation. To this end, at the time of the Cho et al. (2015) publication, we had already begun studies examining whether a more subtle 2 day treatment of AIH using oxygen levels of 11%, similar to that currently employed in spinal cord injured patients, might prove beneficial to the more clinically relevant challenge of repairing completely severed peripheral nerves requiring coaptation, with treatment begun in a delayed manner. These studies were conducted in parallel with 1

hour ES, which although being a more invasive therapeutic intervention, is one that has been shown to promote enhanced peripheral nerve regeneration in both rodents and humans and to induce changes in RAG expression in motor neurons shown to be elevated in response to AIH (Gordon, Brushart, and Chan 2008, Gordon et al. 2009, Gordon et al. 2010, Satriotomo et al. 2016). Thus, my thesis reports these findings and discusses the potential of employing this AIH approach as a therapeutic intervention for peripheral nerve repair.

1. Introduction to the peripheral nervous system

The central nervous system consists of the brain and spinal cord with the PNS comprised of the cranial nerves and spinal nerves (reviewed in Snell 2010). The latter is a complex network of specialized cells and supporting elements that effectively and efficiently serve as a communication relay transmitting signals to and from parts of the body and the central nervous system (Figure 1.1; reviewed in Snell 2010). The major divisions of the PNS are the autonomic, somatic motor and sensory nervous systems. The autonomic nervous fibers innervate the arrectores pilarum muscles, the blood vessels and the sweat glands; the somatic motor fibers send axons to the motor end plates in skeletal muscles while the sensory fibers terminate in skin, tendons, muscles and joints (reviewed in Blumenfeld 2011). All spinal nerves are 'mixed' nerves in that they contain both somatic motor and sensory fibers. Signals along these fibers are conveyed via action potentials established by ionic gradients across the neuronal membrane.

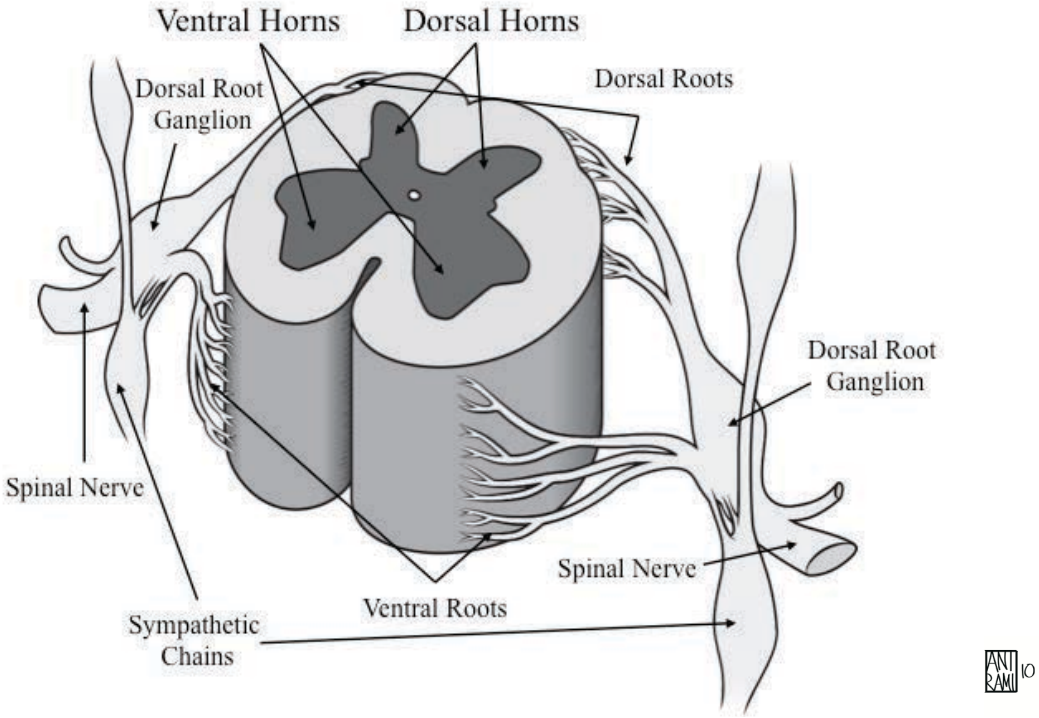

Figure 1.1 Anatomical representation of peripheral nervous system components (© Stephanie Ramirez, reproduced with permission). Sensory afferents in the dorsal roots enter into the dorsal/posterior side of the spinal cord, with the fibers largely terminating in the regions referred to as the dorsal horns. The cell bodies of the sensory nerves are located just outside the spinal cord in a structure known as the DRG, which are dorsal to the sympathetic ganglia chain. The motor neuron cell bodies and their efferents housed in the ventral horn, exit the spinal cord on the ventral/anterior side via the ventral roots. The fibers from the motor, sensory and sympathetic components join together to form the spinal nerves, which then go on to join and form the various peripheral nerves.

1.2 Functional anatomy of the peripheral nerve

Action potentials are propagated along the smallest anatomical subunit of the nerve, the nerve fiber or axon (Figure 1.2.1). A delicate matrix known as the endoneurium surrounds groups of these nerve fibers or axons to form fascicles, the innermost layer of the peripheral nerve (reviewed in Daroff et al. 2015). Each fascicle is held together by a membrane known as the perineurium that maintains intra-fascicular pressure and delineates the second anatomical layer. The innermost portion of the epineurium encloses groups of fascicles, facilitating the gliding of fascicles in relation to one another, while the external portion of the epineurium protects the entire nerve from longitudinal stress, forming the outermost layer of the nerve. Understanding these various layers is important especially in determining the extent of peripheral nerve injuries; the individual degrees of the classification system, used by clinicians to ascertain treatment and outcome, are demarcated by damage to the endoneurium, perineurium or epineurium (discussed in Section 1.5).

The sciatic nerve is the largest nerve in the body and innervates a large portion of the hind limb. In the rat, it is composed of afferent sensory axons originating from the L3 to L6 dorsal root ganglion (DRG) neurons with some variability amongst strains and individual animals (Asato et al. 2000, Rigaud et al. 2008) and efferent motor axons originating from spinal motor neurons located within spinal cord segments L3/L4 to S2 (Janjua and Leong 1984). An injury to any portion of the sciatic nerve or its branches will therefore affect motor and/or sensory function and generate an axonal retrograde response in the associated DRG and spinal cord neurons.

The sciatic nerve splits just proximal to the popliteal fossa into three branches: the

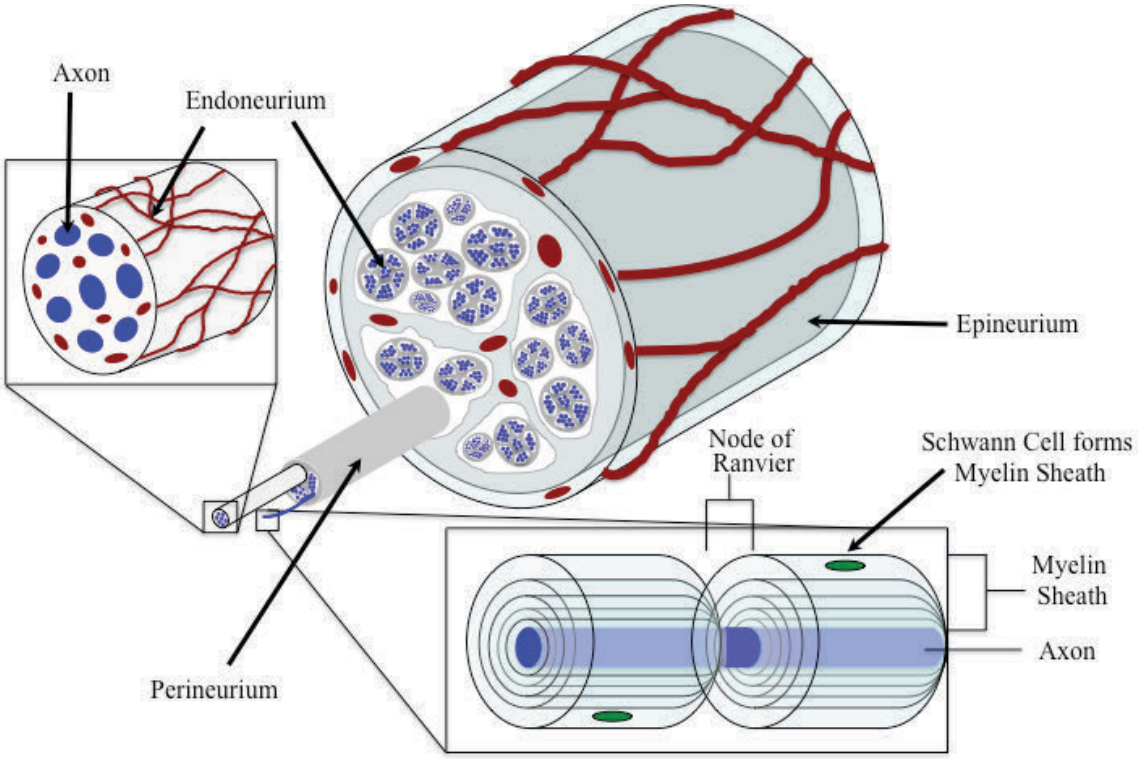

Figure 1.2.1 Schematic of peripheral nerve anatomy. Once the nerve exits the intervertebral foramen at the level of the vertebral column, the arachnoid and dura merge to form the epineurium. The outer portion known as the epineurium (light blue gray) helps to absorb longitudinal stress on the nerve. The connective tissue of the epineurium surrounds blood vessels (red) that supply the nerve. Some smaller branches of these blood vessels penetrate into the sheath that groups the axons of each fascicle together known as the perineurium (gray). Within these fascicles, the endoneurium (white) is the delicate matrix present between individual axons (blue), which acts as a structure to support a mesh-like network of blood vessel capillaries. Peripheral axons with a diameter greater than 1 μm are myelinated. Schwann cells (green) produce myelin as a spiraled sheet of cellular membrane and each Schwann cell makes one segment of myelin. There is discontinuity between each myelin segment and this space is known as a 'node of Ranvier'.

largest being the tibial nerve, the second, the common peroneal nerve and the smallest being the sural nerve. The tibial continues behind the knee then the first branch innervates the medial gastrocnemius muscle, then a large branch innervates the lateral gastrocnemius, soleus and plantaris muscles and another large branch innervates the posterior tibialis, flexor hallucis longus and the flexor digitorum longus muscles (Badia et al. 2010). The tibial then continues intact until it reaches the level of the ankle where it splits into two terminal branches, the medial plantar nerve and the lateral plantar nerve (Figure 1.2.2; Badia et al. 2010).

1.3 Motor neurons

Voluntary mechanical movement of the body relies on the efferent component of the nervous system, the motor system. The motor system is charged with relaying a multitude of impulses to a wide variety of muscles. These impulses are initiated by lower somatic motor neurons whose cell bodies are either situated in the ventral horn of the spinal cord grey matter or in the case of the cranial nerves, in the motor nuclei of the brainstem. The lower somatic motor neurons are the final conduit for transmitting signals to the musculature and this signaling activity can be modulated by a variety of inputs. The first of these inputs is the upper motor neurons, influencing the lower motor neurons by contacting local circuit neurons in the brainstem and spinal cord, which in turn synapse onto a specific grouping of lower motor neurons (reviewed in Blumenfeld 2011). These upper motor neurons have their cell bodies located in either the brain cortex or other brain structures including the superior colliculus, vestibular nucleus or the reticular

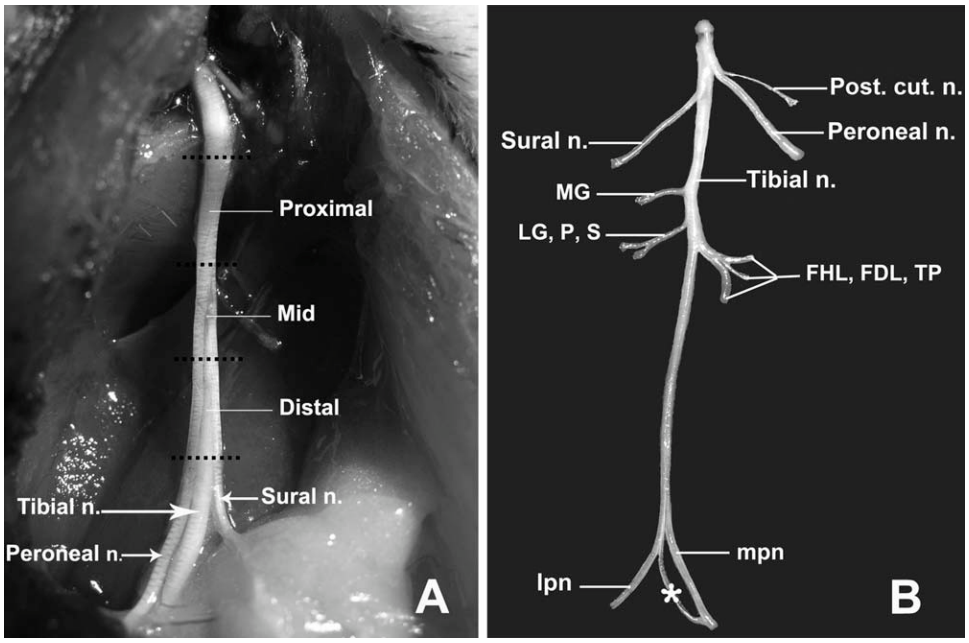

Figure 1.2.2 *In situ* anatomy sciatic nerve with tibial nerve and its branches highlighted (Badia et al. 2010, reproduced with permission). **(A)** Photomicrograph of the rat sciatic nerve (of the left hind limb) in the thigh, with indication of the proximal, middle, and distal levels. The sciatic nerve divides in the mid-segment into tibial, peroneal, and sural nerves that separate proximal to the popliteal space. **(B)** Photomicrograph of the dissected rat sciatic nerve in the leg, from the knee (top) to the ankle (bottom), showing the tibial nerve branches which innervate the medial gastrocnemius muscle (MG), the lateral gastrocnemius (LG), soleus (S) and plantaris (P) muscles, and the tibialis posterior (TP), flexor halluces longus (FHL) and the flexor digitorum longus (FDL) muscles. The tibial then continues intact until it reaches the level of the ankle where it splits into two terminal branches, the medial plantar nerve (mpn) and the lateral plantar nerve (lpn).

formation. The second of these inputs is the sensory neurons as they also terminate on these local circuit neurons, thus mediating lower somatic motor neuron activity.

The lower somatic motor neuron is multipolar (Figure 1.3). Although their cell bodies are mostly found in the ventral horn of the spinal cord within the central nervous system, lower motor neurons are considered to be part of the PNS because their axons project to the periphery of the body to form part of the spinal nerves and innervate skeletal muscles. There are three types of motor neurons: alpha, beta and gamma. These three types of neurons have significantly different conduction velocities of their action potentials owing to different axonal properties (Villiere and McLachlan 1996, reviewed in Millan 1999). Alpha motor neurons initiate contractions of the extrafusal fibers of skeletal muscle at a very fast rate, with a conduction velocity of 70-120 m/s, owing to their large axonal diameter (12-20 μm), which is highly myelinated. Beta motor neurons, medium in size with an axonal diameter of 5-12 μm and a conduction rate of 30-70 m/s, and gamma motor neurons, smaller in size with an axonal diameter of 3-6 μm and a conduction rate of 15-30 m/s, both innervate the intrafusal fibers of muscle spindles which serve as proprioceptive sensory organs to detect changes in the length of a muscle with beta motor neurons having some collaterals to extrafusal skeletal muscle fibers.

1.4 Sensory neurons

The perception of one's environment relies directly on the afferent component of the nervous system, the sensory system. The sensory system is charged with relaying a variety of sensations such as proprioception, mechanoception and nociception and thus, consists of a heterogeneous population of neurons. The cell bodies of these neurons are

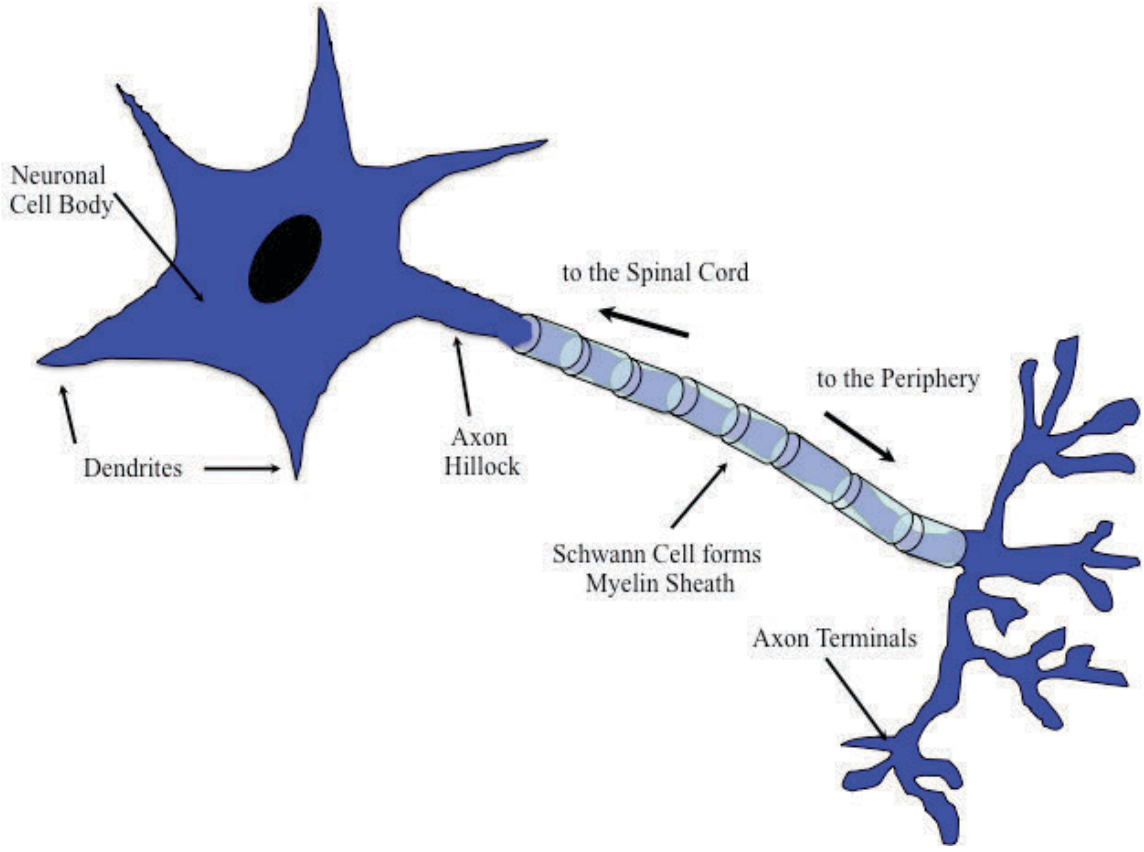

Figure 1.3 Schematic representation of a somatic motor neuron. Somatic motor neuron cell bodies are housed in the spinal cord and innervate skeletal muscle tissue. They receive information peripherally from target tissues or centrally via their dendrites or cell bodies. The axon hillock is a specialized unmyelinated region that is involved in action potential generation.

situated in structures located just outside the spinal cord parenchyma called the DRG (Figure 1.1). A single pseudounipolar process extends from the cell body of each neuron, and this branches into two axonal processes: one projects distally to the peripheral tissues and the other branches centrally to terminate within the dorsal horn of the spinal cord or within the brainstem nuclei via the dorsal columns (Figure 1.4). Sensory information is consequently transmitted from the peripheral tissues to the brainstem and then onwards to the thalamus, cerebellum and cerebral cortex. This directly influences both an organism's perception and response to external stimuli (reviewed in Kandel, Schwartz, and Jessell 2000).

The sensory system is comprised of subpopulations of neurons that express different receptors, allowing response to different types of stimuli. Thus, sensory neurons are commonly classified by the type of stimulus that activates them: proprioceptive, mechanoreceptive or nociceptive. These three types of neurons are not necessarily distinct subpopulations, but in general have significantly different conduction velocities of their action potentials owing to different axonal properties (Villiere and McLachlan 1996, reviewed in Millan 1999). Proprioceptive neurons' axons are known as A-α fibers, are large in diameter (12-20 μm), are highly myelinated and have a conduction velocity of 70-120 m/s. Mechanoreceptive neurons' axons known as A-β fibers, are medium in diameter (5-15 μm), are myelinated and have a conduction velocity of 30-100 m/s. Lastly, nociceptive neurons' axons can be subdivided into two groups: the first are known as A-δ fibers, are small in diameter (2-6 μm), are myelinated and have a conduction velocity of 12-30 m/s and the second, known as C fibers, are very small in diameter (0.4-1.2 μm), are unmyelinated and have a conduction velocity of 0.5-2.0 m/s. The cell bodies

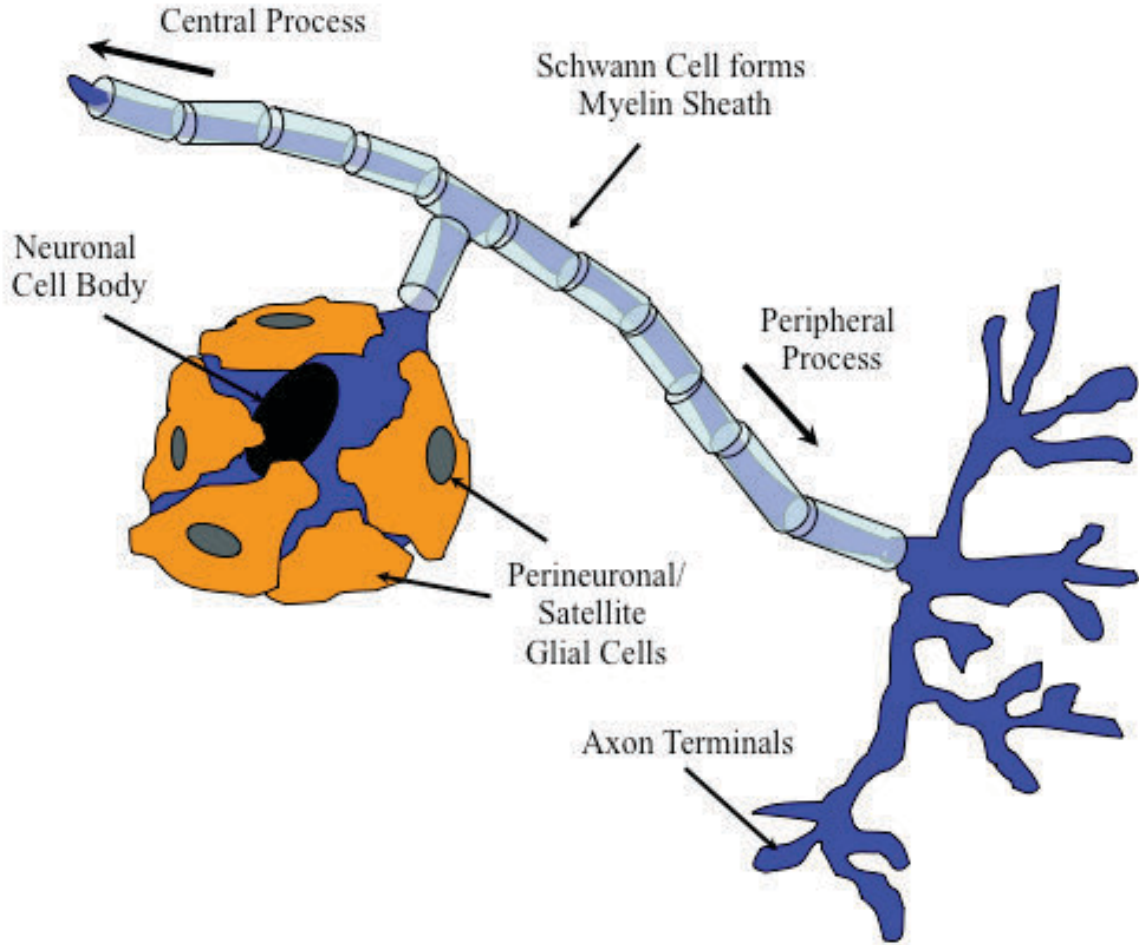

Figure 1.4 Schematic representation of a primary sensory neuron. The sensory neuron is pseudo-unipolar in structure. One apparent process extends from the cell body and then branches into the peripheral process/axon that projects to the periphery of the body and the central process/axon that projects to the spinal cord and sometimes to the brain as well. Some of these sensory neurons have myelinated axons (as shown above), while others do not. All sensory neuron cell bodies are encapsulated by supporting perineuronal/satellite glial cells unique to the PNS.

of the sensory neurons are mostly aggregated along the periphery of the DRG structure with their processes located more medially. In parallel with the diameters of their axons, the cell bodies of the various sensory neurons can roughly be separated by their diameters: proprioceptive neurons are ~40-80 μm, mechanoreceptive are ~25-40 μm and nociceptive neurons are ~10-25 μm, with some overlap between the three (Crowley et al. 1994, Smeyne et al. 1994). For example, there are some small-medium sized cells that are low threshold mechanoreceptors and some medium-large cells that are nociceptors (Djouhri et al. 2003, Fang et al. 2002).

The PNS contains two well-known types of glial cells, Schwann cells and perineuronal satellite glial cells, and a few poorly characterized cells that resemble microglia and less differentiated Schwann cells. A large portion of the Schwann cells envelop the axons of the majority of neurons, specifically those with an axonal diameter greater than 1 μm, producing an insulating substance called myelin, which increases the conduction velocity of action potentials (reviewed in Jessen and Mirsky 2005). Each Schwann cell ensheaths only a small segment of one axon. The smaller axons remain unmyelinated and lie in grooves created by the membrane of a category of Schwann cells that are non-myelin forming.

The satellite glial cells encapsulate the cell body of each sensory neuron within the DRG structure, forming a cellular envelope (Hanani 2005, reviewed in Pannese 1981) usually one to three layers thick (Pannese 1960) allowing the diffusion of most molecules (Shinder and Devor 1994). These satellite glial cells are also present in the autonomic nervous system, in both sympathetic and parasympathetic ganglia.

1.5 Peripheral nerve repair

Prior to the last century, over a period of 2000 years, neuroanatomical knowledge was limited and reports of peripheral nerve regeneration were correspondingly sparse (reviewed in Battiston et al. 2009). As far back as ancient Greece, Hippocrates of Kos warned physicians of nerve injuries when attempting to mend soldier's dislocated shoulders (460-370 BC). In Aelius Galenus' writings in the 2nd century, the first reports of peripheral nerve repair and regeneration appeared. In the 7th century, Paul of Aegina reported suturing of nerves as well as Islamic physicians Muhammad ibn Zakariya al-Razi and Ali Abu Ibn Sina in the 9th and 10th century respectively and a Catholic monk, Gabriele Ferrara, provided a thorough written description of his nerve suturing technique in the 17th century (reviewed in Battiston et al. 2009), proposed by some as the birth date of nerve repair (Artico et al. 1996).

Unfortunately, despite this early anatomical and surgical knowledge of the PNS, the consensus before the 19th century was that amputation or no intervention was the best option for peripheral nerve injury, as nerves typically did not regenerate. The first landmark studies to publish findings about peripheral nerve regeneration were both in 1915, during World War I, by French neurologist Jules Tinel and on the opposite side, Paul Hoffman, a German physiologist (Hoffmann, Buck-Gramcko, and Lubahn 1993). They developed a technique to detect irritated nerves by lightly tapping over the nerve to elicit a tingling sensation/paresthesias, known as the Hoffman-Tinel sign and still used today to detect entrapment of either the median nerve within the carpal tunnel or the ulnar nerve in the postcondylar groove. Based on reports ascertained during World War II by Sir Herbert Seddon (1954, 1948a, b) and his various colleagues, he published the first

classification system of peripheral nerve injuries, dividing them into three distinct types: *neurapraxia*, a temporary loss of nerve conduction that fully recovers within days to weeks with the endoneurium, perineurium and epineurium remaining intact; *axonotmesis*, no nerve conduction distal to the injury site with some axonal regeneration possible without surgical intervention, epineurium remains intact ; *neurotmesis*, no nerve conduction distal to the injury site, no regeneration possible without surgical intervention, partial or complete severance of endoneurium, perineurium and epineurium. In 1951, Sir Sidney Sunderland published his findings on the topographic organization of peripheral nerves and later on, his 5 degrees of nerve injury classification system (Sunderland 1978) which is still used by surgeons today:

- *1st degree*: equivalent to *neurapraxia*
- *2nd degree*: equivalent to *axonotmesis*
- *3rd degree*: *axonotmesis* with endoneurium injury
- *4th degree*: *axonotmesis* with perineurium injury
- *5th degree*: equivalent to *neurotmesis*
- *6th degree*: suggested by MacKinnon and Dellon (1988) as one that combines several of these degrees of injuries per fascicle and one that is the most frequently seen clinically

The main challenge of most surgical repairs of severed axons is attempting to restore the continuity between the proximal and distal stumps, known as end-to-end repair. Four main steps are undertaken (reviewed in Griffin et al. 2014): 1) preparation of the nerve ends to remove necrotic tissue, 2) approximation of the nerve ends while trying to avoid tension (repairs without tension have better outcomes), 3) rotational alignment of

the nerve ends taking the blood vessels into account, and 4) maintenance by using 9-0 or 10-0 non-absorbable suture to perform an epineurial repair or individual fascicular groups in the case of larger nerves. If the nerve ends cannot be approximated without significant tension, grafts are required. Autologous grafts are typically used as they are harvested from the patient's own body but are limited in amount and create complications at the donor site. Unfortunately, the standard grafts are the medial antebrachial cutaneous or the sural nerves, both sensory, when outcomes could be significantly improved with the architecture of motor nerve grafts (Moradzadeh et al. 2008). To meet this need, decellularized nerve allografts have recently become available (reviewed in Szynkaruk et al. 2013). These decellularized nerve allografts have been supplemented with stem cells (Wang et al. 2012), Schwann cells (Santosa et al. 2013) and growth factors (Boyer et al. 2015, Tajdaran et al. 2016). Another product used to bridge a short injury gap is polyethylene glycol. By exposing the proximal and distal axonal ends to a saline solution without calcium (Ca^{2+}) while trimming them to then fuse them with polyethylene glycol, it helped restore short- and long-term function in addition to preventing some distal axon disintegration known as Wallerian degeneration (See Section 1.5.1; Ghergherehchi et al. 2016).

In this thesis, all nerve injuries involve complete transection of the tibial nerve in rats and are therefore classified as *5th degree* or *neurotmesis*. An end-to-end epineurial repair was performed using 10-0 suture within a 4 mm silastic tube. The factors that influence the level of success of nerve repairs are age, time of primary repair, regeneration distance, proprioceptive feedback and rehabilitation. As surgical repair techniques and treatments create a more favorable regenerative microenvironment and

improve the coaptation region that the regenerating axons must traverse, the distance regenerating axons must travel, from injury region to target, remains the same and a definite challenge. Thus, recent therapies, including approaches used in this thesis, focus on modulating the neurobiological axes of Wallerian degeneration, cellular injury and/or regeneration responses in an effort to improve regenerative outcomes in the least invasive way.

1.5.1 Peripheral nerve regeneration

Following a nerve crush or a transection injury, the distal axons are separated from their cell bodies and undergo a process known as Wallerian degeneration where they begin to disintegrate within their endoneurial tubes (Waller 1850). The initial injury initiates a transient local Ca^{2+} wave that travels into the proximal stump and the distal axon fragment, disrupting the mitochondria within the vicinity. This initial Ca^{2+} wave, along with others produced if subsequent injuries are inflicted, was shown to not be necessary to induce the degeneration process of the distal axon fragment (Vargas et al. 2015). In contrast, the terminal phase of Ca^{2+} influx, affecting the cytoplasm and mitochondria of the entire axon, precedes the degeneration of the distal axon fragment by minutes. If blocked, this process is either delayed or significantly reduced (Vargas et al. 2015).

In response to injury, Schwann cells dedifferentiate/become activated as part of an adaptive response that facilitates nerve regeneration. They initially participate in the clearance of myelin and disintegrated axonal fragments within the first few days, eventually being replaced by infiltrating macrophages (Gaudet, Popovich, and Ramer

2011). More recently a study by Gomez-Sanchez et al. (2015) has revealed that the Schwann cells actually digest the myelin through a novel form of selective autophagy that is referred to as myelinophagy, a property of peripheral but not central myelinating cells, as transected optic nerve showed little evidence of autophagy. The Schwann cells are key players in the regeneration process as they undergo mitosis to form a structure to support the regenerating axons along the remnants of endoneurial sheaths, with the Schwann cells aligned as structures known as bands of Büngner. During regeneration, Schwann cells promote axon growth through the production of extracellular matrix molecules and increased levels of chemokines, cytokines and growth factors, the latter including nerve growth factor (NGF), brain-derived neurotrophic factor (BDNF), neurotrophin 4/5, vascular endothelial growth factor, pleiotrophin, artemin and glial-derived neurotrophic factor (GDNF) as well as expression of the common neurotrophin receptor p75 and the cell adhesion molecule N-cadherin (reviewed in Jessen and Mirsky 2016). There is a coordinated series of events that enables the injured axon to regenerate into the Wallerian degenerating distal portion of the injured nerve, with delays in the repair further challenged by a waning responsiveness of this region to support axon regeneration (reviewed in Fu and Gordon 1995).

1.5.2 Regeneration-associated genes

In order for regeneration to commence post-peripheral nerve injury, there is a major shift in gene expression, collectively known as the cell body response, that must occur in the injured sensory and motor neurons, whereby a class of genes known as RAGs becomes significantly upregulated. These RAGs include activating transcription

factor 3 (ATF3), growth-associated protein 43 (GAP43), the cytoskeletal proteins tubulin and actin, superior cervical ganglion 10 (SCG10; aka stathmin 2) in sensory neurons, BDNF and its high-affinity receptor, NTRK2, more commonly referred to as trkB, in motor neurons ((reviewed in Verge et al. 1996, Zochodne 2012, Shin, Geisler, and DiAntonio 2014).

Following a nerve injury, ATF3 is rapidly upregulated in sensory and motor neurons in both rats and humans (Tsujino et al. 2000, Gey et al. 2016). It is considered an excellent marker for neuronal injury as it cannot be induced trans-synaptically (Tsujino et al. 2000). The induction of approximately 20 to 25% of RAGs have been shown to be dependent on ATF3 levels (Gey et al. 2016).

In rats at birth, *GAP43* mRNA is present in high levels in both spinal cord motor neurons and DRG neurons (Chong et al. 1992). This persists for seven days postnatal, followed by a decline to adult baseline levels. In a non-injured adult rat, GAP43 is expressed at low levels in the lumbar motor neurons with substantial labeling of the neuropil (Schreyer and Skene 1991, Chong et al. 1992). Peak levels of GAP43 in the lumbar motor neurons were observed 3 days after a sciatic nerve transection (Chong et al. 1992). In the uninjured DRG, a mean of 46% of the neurons in L4 and L5 ganglia display some degree of GAP43 immunohistochemical labeling (Schreyer and Skene 1991). Most are lightly labeled by immunohistochemistry with the highest level of mRNA expression generally being found in the small/medium sensory neurons (Verge et al. 1990). A high proportion of the sensory neurons in the L4 and L5 DRG, over 80%, express GAP43 after a sciatic nerve injury (Verge et al. 1995, Schreyer and Skene 1991).

SCG10 is an axonal maintenance factor that is highly expressed during the development of the nervous system as it regulates protein transport and microtubule stability (reviewed in Ozon, Maucuer, and Sobel 1997). After development, it is expressed as a punctate pattern throughout the peripheral nerves whereas after an injury, its expression pattern changes dramatically (Shin, Geisler, and DiAntonio 2014). Only 3 hours post-injury, levels of SCG10 decrease by more than 70% in the distal nerve stump whereas degeneration of the axons is only observed after 48 hours (Beirowski et al. 2005, Shin et al. 2012). In contrast, on the growing axon front, SCG10 levels rise dramatically within half an hour, continue to rise until 3 hours where they plateau and at 5 hours, labeling can be observed in the central region of individual growth cones (Shin, Geisler, and DiAntonio 2014). The mechanism underlying this phenomenon appears to be the continuous anterograde transport of SCG10, replenishing protein levels within the axon from the cell body at a rate of 1.16 μm/s (Shin et al. 2012). The severance of this conduit would lead to the accumulation of SCG10 in the growing axon front. Thus, SCG10 can be used as a very early marker for peripheral nerve injuries with preferential expression in sensory versus motor axons, elevated in the proximal stump and reduced in the distal stump, when at those early time-points of 4 or 8 hours for example, GAP43 expression levels remain moderate (Shin, Geisler, and DiAntonio 2014).

BDNF plays a crucial role in plasticity promoting sprouting and regeneration of the PNS. Unlike the other neurotrophins, BDNF expression rises sharply in ~80% of sensory neurons following a nerve injury, followed by a reduction in expression in the small, NTRK1, more commonly referred to as trkA, expressing nociceptive population and an induction in the medium to large, NTRK2 and/or NTRK3 (also commonly known

as trkC) expressing population (Karchewski et al. 2002). The rapid increase in BDNF expression in the majority of sensory neurons is critically linked to the ability of these neurons to transition to a regenerating state (Geremia et al. 2010) while the induction in larger size neurons aids in remyelination of the regenerating nerves. BDNF promotes myelination during both development and after an injury via the common neurotrophin receptor p75 present in sensory neurons, injured motor neurons and Schwann cells *in vitro* and *in vivo* (Chan et al. 2001, Cosgaya, Chan, and Shooter 2002, Zhang et al. 2000).

Another molecule, GDNF, a member of the transforming growth factor β family, also has trophic effects on motor neurons and some sensory neurons, despite being structurally different from the neurotrophin family, thus is in a class of its own. It acts primarily on the ~40% of small and large sensory neurons that express the GDNF receptors RET and GFRα (Bennett et al. 1998, reviewed in Baloh et al. 2000). GDNF was first purified in 1993 and it was initially believed that it was a survival factor for only dopaminergic neurons (Lin et al., 1993). GDNF has a strong trophic effect on Schwann cells and sensory neurons (Matheson et al., 1997; Naveilhan et al., 1997). However, too much GDNF can actually impede regeneration in neurons. The induced overexpression of GDNF by Schwann cells implanted into acellular nerve allografts used for nerve repair actually trapped regenerating axons in the graft, preventing them from reaching the distal stump, perhaps due to the lack of a trophic gradient to lure the axons into it (Santosa et al. 2013).

Of interest to our laboratories, and initially investigated by Dr. Atiq Hassan (2015), is a heterodimeric transcriptional RAG linked to oxygen homeostasis within the cell: hypoxia-inducible factor-1α (HIF-1α). HIF-1 was identified by Semenza et al.

(1991) when investigating transcriptional activation of erythropoietin in response to hypoxia. HIF-1α protein synthesis is regulated by a multitude of growth and other factors (reviwed in Masoud and Li 2015). HIF-1α is quickly degraded by the ubiquitin-proteasome system in the cell under conditions of normoxia (at atmospheric oxygen levels), having a half life of only approximately 5 minutes, (Salceda and Caro 1997). In contrast, under hypoxic conditions, HIF-1α is activated within the cell, translocated from the cytoplasm to the nucleus where it forms the HIF heterodimer complex protein by binding with HIF-1β which is constitutively expressed (Lando et al. 2002, reviewed in Masoud and Li 2015).

Recent work by Cho et al. (2015) has established a link between induction of HIF-1α using hypoxia and the regenerative capacity of sensory neurons and accelerating the reinnervation of neuromuscular junctions. They demonstrated that HIF-1α is not required for the early phase of regeneration as its absence did not hinder the outgrowth of SCG10-expressing axons 1 day post-crush lesion. When a conditioning lesion was performed 3 days prior, a 2 fold increase in axon regeneration was observed, supporting HIF-1α's role as a transcriptional regulator, activating the pro-regenerative program. In addition to HIF-1α, the regenerative response is linked to the activation of a number of important transcriptional regulators including ATF3, STAT3, c-Jun and Luman/cAMP response element binding protein 3 (Ying, Misra, and Verge 2014, Zigmond 2012;, reviewed in Raivich 2011). This activation, coupled with local translation of proteins including cytoskeletal modifiers, neuropeptides, adhesion and guidance molecules, is instrumental to the growing axon quickly transitioning and maintaining a regenerative state (reviewed in Raivich 2011). Increases in regeneration-

associated proteins such as GAP43 and BDNF are often associated with increased plasticity required for induction and mediation of the nerve regeneration (Geremia et al. 2007, Udina et al. 2008, Bomze et al. 2001, Geremia et al. 2010). It is thus necessary to identify the optimal parameters for regeneration to occur *in vivo,* in the hopes of being able to recreate these ideal conditions as best as possible in clinical scenarios.

1.6 Electrical stimulation and nerve regeneration

Our laboratory and colleagues have previously employed an approach using ES to enhance the regenerative/plasticity capacity of peripheral nerves. The application of electrical current directly to the sciatic nerve post-injury at 20 Hz for one hour activates both sensory and motor neurons and a significant cellular response is induced. This response involves an influx of Ca^{2+} into the neurons followed by the upregulation of regeneration/plasticity-associated genes such as BDNF, cAMP, GAP43, tα1-tubulin, actin in motor and sensory neurons, and the BDNF receptor NTRK2 in motor neurons (Al-Majed, Brushart, and Gordon 2000, Gordon et al. 2009, Wenjin et al. 2011). These cellular mechanisms are believed to be responsible for the enhanced growth and target specificity. BDNF is thought to be upregulated with ES treatment through the activation of L-type voltage sensitive Ca^{2+} channels of the non-N-methyl-D-aspartate subtype of glutamate receptor (reviewed in Al-Majed, Brushart, and Gordon 2000). Another factor upregulated by ES, responsible for enhanced neurite outgrowth and regeneration, is cAMP (reviewed in Batty, Fenrich, and Fouad 2017). Drugs that increase neuronal cAMP levels, as well as activating phosphokinase A, promote axon proliferation akin to that observed with ES (reviewed in Gordon et al. 2009).

Initial studies were performed to identify the optimal duration and timing of ES therapy. When applying low frequency stimulation directly to a peripheral nerve, one hour has been shown to be as effective as a continuous two week protocol for motor neurons (Al-Majed et al. 2000). In contrast, single stimulation protocols beyond an hour of continuous stimulation negate the optimal positive regenerative effects of the treatment in sensory neurons (Geremia et al. 2007). In terms of timing, one hour of ES when applied successive to a sciatic nerve repair with a biodegradable conduit 1 day or 1 week after a nerve transection is effective at promoting regeneration. But, when performed 1 or 2 months post-injury, a repair using the same conduit paradigm is not enhanced by ES. This is believed to be a consequence of distal stump degeneration and/or fibrosis due to increased collagen (Han et al. 2015). Comparatively, when a direct nerve-to-nerve repair was performed 3 months after a nerve transection, one hour of ES was still capable of improving axonal outgrowth and target reinnervation (Elzinga et al. 2015).

ES also promotes earlier sprouting of neurites and more accurate reinnervation (Al-Majed et al. 2000, Brushart et al. 2005, Geremia et al. 2007). Collectively, the stimulated axons appear to grow out as a front as opposed to the staggered type of regrowth normally observed (Geremia et al. 2007). ES thus promotes an earlier onset of axons regenerating across the nerve repair site without increasing its overall elongation speed through the distal stump, as assessed by isotopically labeling proteins transported to the growing axon front (Gordon, Brushart, and Chan 2008). Further, if lumbar motor neurons are remotely activated by application of 1 hour of ES to the cervicothoracic spinal cord, regenerating motor axons of the femoral nerve show greater target specificity at 6 weeks post-repair (Franz et al. 2013). The effect that ES has on DRG neurons can be

cell autonomous, as accelerated more robust neurite outgrowth is also observed when DRG neurons are isolated and cultured *in vitro* on a microelectrode array that applies the same 1 hour stimulation paradigm used in our *in vivo* studies (Singh et al. 2012).

Promoting regeneration into the distal nerve stump while it remains in a growth permissive state is a major goal of treatment. This state includes the neurotrophic support provided by the distal stump, which expresses a multitude of growth factors, many of them by Schwann cells, as well as surface adhesion molecules, and the increased expansion of basement membrane extracellular matrix proteins such as laminin, fibronectin, among many others. Because this state cannot be sustained indefinitely, one must be cognizant of this challenge when designing delayed nerve repair strategies or ones where distance to target is great (Fu and Gordon 1997).

A complementary strategy to direct nerve stimulation has been recently employed, with the hopes that it will impact reinnervation of the denervated target tissue, namely stimulation of target tissue. ES of the target muscle rather than the nerve directly, resulted in significantly increased numbers of reinnervated motor units and improved functional outcomes (Willand et al., 2015). Here, the gastrocnemius muscle was stimulated with a biphasic train of 40 pulses at 100 Hz for an hour a day, described as more suitable for fast twitch muscle, which elicits a contraction every 6 seconds (Willand et al. 2011). The improved outcomes are speculated to be influenced by the increased intramuscular, but not nerve levels of *BDNF* and *GDNF* mRNA (Willand et al. 2016). This therapy has also been shown to be sufficient in increasing the number of axons in the distal stump, possibly due to the support of trophic factors diffusing from the target muscles (Willand et al. 2016)

1.7 Acute intermittent hypoxia as an adjunct therapy

Another potential therapeutic intervention that has come to light for nervous system repair is AIH. Intermittent hypoxia has been the focus of research in recent years due to its negative implications in sleep-disordered breathing and its positive effects on athletic performance (Berger and Lavie 2011, Wilber, Stray-Gundersen, and Levine 2007). Therefore, it can be described as both beneficial and harmful, with the hypoxic dose determining the outcome. Because of exposure to chronic intermittent hypoxia over long periods of time, patients with sleep apnea may suffer from cognitive dysfunction, hypertension, and myocardial ischemia (reviewed in Chakrabarty 2006). With obstructive sleep apnea, the hypoxic episodes are brief but they are very frequent, with the adverse effects correlated with the total time patients are hypoxic (oxygen saturation <90%) (Gottlieb et al. 2009). In contrast, when athletes are exposed to alternating periods of hypoxia and normoxia for less than 90 minutes per day, most studies, mainly endurance ones, but not all endurance studies, report performance improvements of 1.7 to 8.2% (Kilding, Dobson, and Ikeda 2016). Protocols of intermittent hypoxia vary significantly by a number of parameters: the severity of the hypoxic exposure (reported as the levels of inspired reduced oxygen also known as hypoxemia) with levels varying from 2% to 16%, the length of each hypoxic versus normoxic exposure ranging from 15-30 sec to 12 hours, the number of cycles per day recorded as 3 to 2400, the exposure schedule (consecutive or alternating days, number of days per week), the total experimental hypoxic exposure (from less than an hour to 90 days) and other variables such as the arterial carbon dioxide levels (reviewed in Navarrete-Opazo and Mitchell 2014).

AIH therapy consists of repeatedly breathing low levels of oxygen for short

periods of time alternating with ambient levels of oxygen. This sets up a form of respiratory plasticity, known as long-term facilitation (LTF), that was first observed in rats following three short hypoxic episodes (Bach and Mitchell 1996, Hayashi et al. 1993). This LTF has been demonstrated in both rats and humans (McGuire et al. 2002, 2004, Pierchala et al. 2008) and is measured by an increase in phrenic or hypoglossal nerve amplitude that is maintained for at least 2 hours following AIH treatment (Baker-Herman and Mitchell 2002, Mitchell et al. 2001). The development of LTF is fundamentally pattern dependent. Importantly, continual hypoxia is not capable of invoking LTF (Baker and Mitchell 2000), with the required stimulus appearing to be repetitive changes in blood levels of oxygen (Fuller et al. 2000, Mahamed and Mitchell 2008). Varying protocols of hypoxia appear to exhibit comparable effects, as long as the hypoxic episodes administered are intermittent and acute (Mahamed and Mitchell 2007). The total length of treatment is also critical; if administered chronically, such as 5 min alternating episodes for 12 hours per night for a week in rats, this leads to deleterious consequences (Fuller et al. 2003). Therefore, investigations into hypoxic dosage to enhance positive and decrease negative outcomes have helped establish the optimal AIH parameters of 3 to 15 sequences of alternating air with modest levels of hypoxia of 9 to 16% oxygen (reviewed in Navarrete-Opazo and Mitchell 2014), while oxygen levels in the 2-8% are considered a severe hypoxia range (reviewed in Astorino, Harness, and White 2015).

In rats, an AIH treatment protocol consisting of only 3 to 10 hypoxic episodes in less than two hours per day is sufficient to elicit spinal plasticity of a relatively short duration in the Sprague-Dawley strain (Dale-Nagle et al. 2010, Lovett-Barr et al. 2012).

To increase the effects of treatment, they either treat rats with partial spinal cord injuries daily for 7 days (Wilkerson and Mitchell 2009, Lovett-Barr et al. 2012) or three times per week for 10 weeks (Satriotomo et al. 2012). These paradigms appear sufficient to induce spinal plasticity without obvious adverse consequences (Vinit, Lovett-Barr, and Mitchell 2009).

In addition to variations in AIH treatment protocol, attention should be paid to which inbred rat strains are used in each study as differences in phrenic responses to time-dependent hypoxia have been reported by Golder et al. (2005) who compared Brown-Norway, Fischer, Lewis and Piebald-viral-Glaxo strains. Additionally, AIH treatment is highly dependent on the time of its introduction post-injury and varies between rat strains. For example, four weeks post-injury, an AIH effect was observed in Lewis but not Sprague-Dawley rats (Golder and Mitchell 2005). This variability is not restricted to rats; genetic influences on hypoxic ventilatory response have been described in humans as well (Weil 2003).

Investigations at the cellular level revealed that the initiation of LTF is dependent on the activation of spinal serotonin receptors (Prabhakar 2001, Baker et al. 2001) and that serotonin-dependent synthesis of BDNF is necessary to maintain it after AIH treatment (Baker-Herman and Mitchell 2002). This phenomenon appears to be independent of increased phrenic nerve activity and is described as a ‘form of neuromodulator-induced plasticity’ (Mitchell and Johnson 2003). BDNF is highly associated with neuroplasticity and neuroregenerative states, however its increase in small and medium sensory neurons is also associated with an increase in pain sensation known as hyperalgesia (Coull et al. 2005, Tender, Li, and Cui 2010). Elevated levels of

BDNF in the dorsal horn of the spinal cord of rats with an injured sciatic nerve correspond with the timeline of thermal hyperalgesia, increased sensitivity to a noxious thermal stimulus, with a return to baseline levels of BDNF correlating with a return to baseline thermal sensitivity after 28 days (Miletic and Miletic 2002). If AIH causes a significant upregulation in serotonergic signaling, it is possible that sensory neurons, in addition to motor neurons will be affected by the treatment. While the actions of serotonin in pain pathways are complex and dependent on the complement of serotonin receptors, increased serotonin levels in the periphery have been linked to induction of mechanical hyperalgesia, increased sensitivity to a force applied to the foot pad of the hind paw, via increases in transient Ca^{2+} signaling in sensory neurons (Lin et al. 2011). By instigating a shift in the neural environment, alterations in protein expression associated with novel therapies hold the potential to increase pain. As such, the potential impact of AIH treatment on injury-associated mechanical and/or thermal hyperalgesia needs to be investigated.

It can also be postulated that AIH may have a systemic impact on neuronal activity; hypoxic conditions have been shown to increase neural activity (spontaneous impulse generation) in injured sensory neurons and peripheral axons (Burchiel 1984), and when exposed, sensory neurons produce nitric oxide to resist against the effects of hypoxia, a mechanism dependent on the activation of mitochondrial complex II and voltage gated Ca^{2+} channels (Henrich et al. 2004). AIH's ability to elevate RAG expression in spinal cord injury models that is consistent with the gene programs induced in peripheral nerve regeneration in response to ES, supports investigating AIH as a

possible treatment modality for enhancing repair following peripheral nerve injury in a manner akin to ES.

1.8 Rationale

It appears that these two independent treatments, ES and AIH, may have some underlying commonalities in terms of how they promote repair of the nervous system, namely their ability to increase neural activity and associated RAG expression, including a major regulator of regenerative events in peripheral nerve repair – BDNF (Al-Majed, Brushart, and Gordon 2000, Wenjin et al. 2011, Wilkerson and Mitchell 2009). BDNF has been shown to be critical for the induction of a regenerative state in sensory and motor neurons (Geremia et al. 2010, Verge 2004). This upregulation of BDNF does however appear to be via different mechanisms: In the case of ES, it is speculated to be directly elevated through the activation of L-type voltage sensitive Ca^{2+} channels of the non-N-methyl-D-aspartate subtype of glutamate receptor (Al-Majed, Brushart, and Gordon 2000) or with AIH treatment, BDNF has been shown to be upregulated in a serotonin-dependent manner (Baker-Herman et al. 2004). The increased neural activity evoked by AIH, thus, may upregulate BDNF and BDNF-dependent RAGs and serve to promote peripheral nerve repair. This is also supported by emerging data linking the hypoxia-induced transcription factor HIF-1α to downstream regulation of RAGs in the regenerating sciatic nerve (Cho et al. 2015).

The delivery of these therapies clinically is also very different. ES requires the application of sterile stainless steel wires directly to the injured nerve at the time of surgery and half an hour later, once the patient has recovered from anesthetic, a

continuous 20 Hz train is delivered for an hour with the wires subsequently pulled out (Gordon et al. 2010). AIH, on the other hand, is delivered via a non-rebreathing mask attached to an oxygen generator that provides variable inspired oxygen mixtures (Trumbower et al. 2012).

The extent to which AIH might serve as a clinically relevant adjunct therapy for PNS repair beyond the promising impact on phrenic nerve plasticity seen in cervical spinal cord injury models remained to be investigated at the start of this thesis. We therefore sought to identify whether AIH treatment may in fact promote regeneration in the PNS akin to that seen with ES, safely, without inducing mechanical or thermal hyperalgesia. To do so, we took a two step approach in an *in vivo* rat model: (i) assessing whether only two sessions of AIH treatment with 11% oxygen administered 48 and 72 hours post-injury, significantly increased RAG expression within the range currently seen with ES after the most acute nerve injury, namely a complete nerve transection followed by coaptation (classified as neurotmesis or 5^{th} degree nerve injury) and (ii) performing longer-term investigations to elucidate the physiological/behavioural affects of this AIH protocol on the regrowth of the tibial branch of the sciatic nerve in rats.

AIH has previously been shown to improve peripheral nerve regeneration outcomes by Cho et al. (2015). However, our approach differs significantly from that of the two protocols employed by Cho et al. (2015). The first Cho protocol utilized for investigation of axonal regeneration consisted of 3 sessions with 8% oxygen, the first session administered within 2 hours of surgery with the second and third treatments after 24 and 48 hours respectively. For studying the extent of muscle reinnervation, they used a second protocol - 7 consecutive days of AIH sessions with 8% oxygen beginning an hour

post-sciatic nerve injury. As mentioned before, 8% falls within the severe hypoxia treatment ranges for human applications.

Thus, in our studies we opted to investigate a more clinically relevant model of nerve repair and assess responses over protracted regeneration periods and longer distances. We also investigated cellular responses and regeneration for both motor and sensory neurons. To this end we are: (i) testing a hypoxia level within the range utilized in current human trials; (ii) because of the parallels of AIH with plasticity responses observed in regenerating motor neurons subjected to ES, we are directly comparing these two therapeutic interventions in a clinically relevant model of severe nerve injury - nerve transection and coaptation; (iii) we opted to not administer AIH until 48 hours post-surgery as isoflurane anesthesia has been shown to increase levels of HIF-1α potentially confounding results with treatment effects (Li, Zhu, and Jiang 2008); and (iv) we are examining the impacts of the two treatments on behavioral pain and regeneration responses, as this is important for patient compliance.

2. Hypothesis and Specific Aims

Supported by the data presented in the introduction, I hypothesize that ***AIH will serve as an effective adjunct therapy to promote improved regeneration of surgically repaired peripheral nerves in a manner akin to that observed with brief nerve ES.***

2.1 Specific Aims

To test this hypothesis, I addressed the following aims:

(i) Examine the impact of AIH versus ES on early expression of early RAG proteins in regenerating tibial nerve and associated motor and sensory neurons, and examine whether there are rat strain-dependent differences in this response;

(ii) Examine the impact of AIH versus ES on tibial nerve regeneration; and

(iii) Examine the impact of AIH versus ES on regeneration- and pain-associated behavioural responses.

To address these aims I:

(a) Quantified the early expression of regeneration-associated proteins at the short-term time-point of 72 hours post-repair of a tibial nerve transection subjected to immediate 1 hour ES, 2 days of AIH or normoxia treatment. This included examination of BDNF, GAP43 and HIF-1α expression in the injured and non-injured motor neurons; BDNF, GAP43 and HIF-1α expression in the injured and non-injured sensory neurons in the L4 DRG; BDNF, GAP43 and SCG10 expression in the proximal tibial nerve at the repair site.

(b) Evaluated regeneration at the mid-term regeneration time-point of 25 days. This included assessment of functional behavioural responses (ladder crossing test, walking footprint analysis, mechanical and thermal hyperalgesia tests), as well as the numbers of neurons regenerating 20 mm from the repair site with ES, 2 days of AIH or normoxia; quantification of the numbers of regenerating motor and sensory neurons versus total numbers of neurons contributing to the tibial nerve at the level of injury using a retrograde tracer introduced 28 mm distal from the repair site in injured rats or at the level of the injury site in naïve rats respectively; and assessment of the numbers of myelinated axon profiles detected 20 mm from the repair site in semi-thin transverse sections of nerve from the two experimental (AIH, ES) versus normoxia control animals; and

(c) Assessed regeneration functionally (ladder crossing test, walking footprint analysis, mechanical and thermalhyperalgesia) up to the long-term regeneration time-point of 10 weeks post-repair of a tibial nerve transection in the two treatment (AIH and ES) versus control (Normoxia or no injury) groups.

3. Materials and Methods

All animal procedures were approved by the University of Saskatchewan's Committee on Animal Care and Supply under the guidelines of the Canadian Council on Animal Care (protocol #19980012). A total of 134 rats, 45 male Wistar strain, 4 male Sprague Dawley strain and 85 male Lewis strain (Charles River Laboratories, St.Constant, QC) weighing 250–300g, between 3 to 5 months old, were used for the following set of experiments. All animals upon arrival were housed at the Animal Care Facility in the Western College of Veterinary Medicine at the University of Saskatchewan and acclimated for 7 days before handling or any procedures. They were then evenly distributed into experimental groups based on their weights. They were housed in groups of 2 or 3 per cage except for post-surgery where they were singly housed for 4 days to allow for post-operative observation and treatment. The Animal Care Facility maintained a controlled environment with a temperature of 20 +/- 1 degrees Celsius and an alternating 12 hour light/dark schedule. The cages measured 51 cm long by 28 cm wide with wood chip bedding. Environmental enrichment included hard wood blocks, willow sticks, Nylabone® toys and newspaper. Regular introduction of new enrichment items were deemed necessary for hind limb nerve injuries to reduce the incidence of autotomous behaviour. No autotomy was observed with any of the studies. Rats were fed rodent rat chow *ad libitum* upon arrival until they reached an average weight of 300 grams. Afterwards, they were fed 4-5 pellets each per day in order to slow their weight gain and allow for a more homogenous weight distribution over the longer experimental timelines.

3.1 Tibial nerve transection and repair

Animals were anesthetized with a gas mixture of 1.5-2.5% isoflurane/97.5-98.5% oxygen and given an analgesic, buprenorphine (Temgesic, sc, 0.1-0.2 mg/kg), post-surgically for 24 hours. Under aseptic conditions, the right sciatic nerve was exposed by splitting the gluteal muscle and gently spreading it apart with blunt tip scissors. The tibial nerve, once freed of surrounding tissue, was cleanly transected with Vanna micro scissors 5 mm distal from the sciatic trifurcation. The tibial nerve was then repaired under 40x magnification using 10-0 (Perma-Hand®) silk suture through the distal and proximal epineuriums to join the ends in the center of a 4 mm long section of Silastic® tubing (Dow Corning Inc., USA). The wound was then closed in layers with the muscles being sutured (5-0 Vicryl®) followed by the skin (4-0 Silk, Ethilon®) (See Figure 3.1.1). Procedure times were adjusted such that all treatment groups including ES were anesthetized for a similar total amount of time, ranging from an hour to an hour and thirty minutes total.

3.1.1 Electrical stimulation

For rats being treated with electrical stimulation, the sciatic nerve, 5 mm proximal to the trifurcation was cleared of surrounding tissue immediately after the tibial nerve transection and repair. The cathode stainless steel wire whose insulation is removed at the end was looped around the sciatic nerve whereas the anode wire was placed under the skin proximal to the surgical site. Electrical stimulation of supramaximal pulses (100 μs, 3V) delivered in a continuous 20-Hz train was applied for an hour. The wound was then closed as described above.

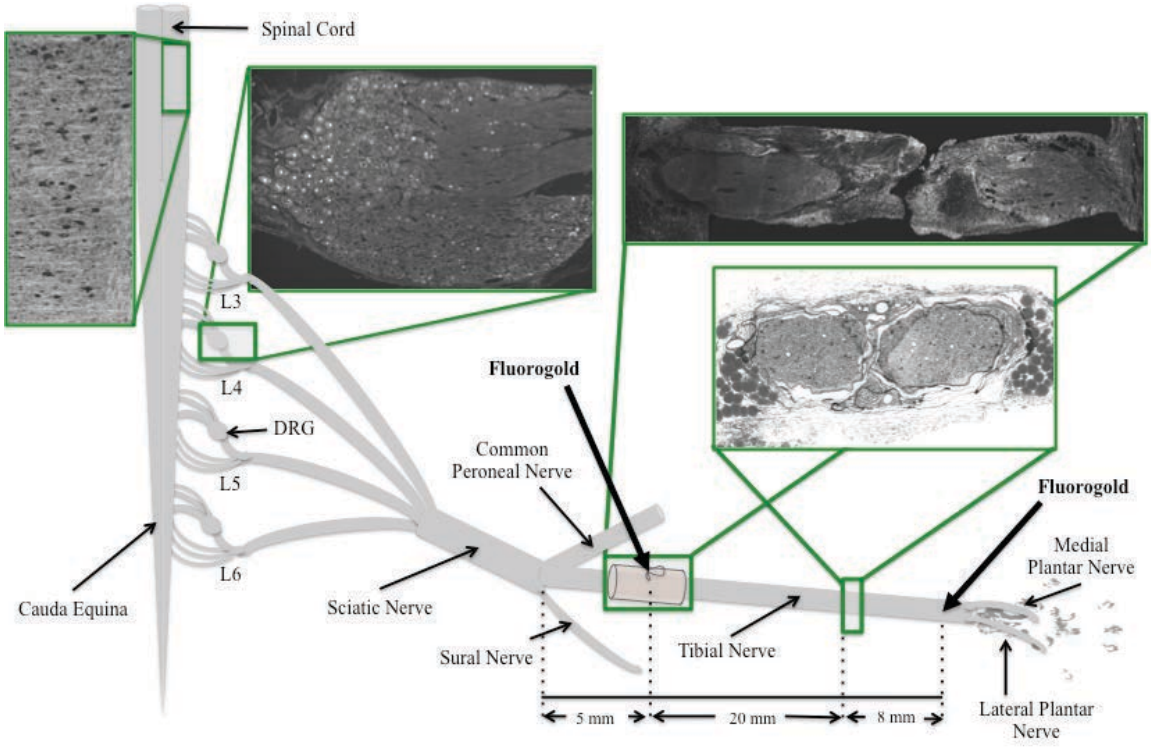

Figure 3.1.1 Experimental model used to examine impact of treatment on tibial nerve regeneration. A complete transection of the tibial nerve was done 5 mm distal from the sciatic nerve trifurcation followed immediately by a repair with suture and a 4 mm silastic cuff. Experimental treatments included either immediate nerve stimulation for one hour at 20 Hz (ES), or once daily normoxia (Norm) or AIH treatments for two days post-surgical repair. Tissue collected for regeneration analysis included the region of the spinal cord receiving tibial nerve inputs from L3-L5 sensory neuron afferents and sectioned longitudinally through the ventral horn to identify back-labeled motor neurons, the L4 DRG containing the majority of the tibial nerve sensory neuron cell bodies, the tibial nerve repair site and regions of nerve 20 mm distal to the tibial nerve repair site. The impact of treatment on early regeneration responses was done on tissue collected 3 days post tibial nerve repair. Retrograde labeling of regenerated sensory and motor afferents with FG was performed at 25 days post-tibial nerve repair 28 mm from the repair site, followed by perfusion and tissue collection 5 days later.

3.1.2 Acute intermittent hypoxia and normoxia

Rats were treated on day 2 and day 3, but not on day 1 to allow for recovery from isoflurane anesthetic, after the tibial nerve transection and repair surgery for all experimental timelines. They were individually placed in custom-made plexiglass chambers (WD Plastics, Saskatoon, SK) measuring 30 cm long by 17 cm wide by 12 cm high with brown paper towel on the floor (Figure 3.1.2). The AIH protocol is automated via a controller and delivers continuous gas flow of medical air (21% O_2) for 5 min, alternating with low oxygen (11% O_2) for 5 min with each switch preceded by a 1 min purge. The daily treatment protocol consists of 10 full cycles, a total duration of 2 hours. For the normoxia group, continuous medical air (21% O_2) flows into the chambers for the same duration as the AIH treatment group. The oxygen and carbon dioxide levels in the chambers were regularly monitored using a portable oxygen analyzer (Model AX300-1, Teledyne Analytical Instruments).

3.1.3 Experimental timelines

Short-term timeline

The impact of treatment on early regeneration responses was done on tissue collected 3 days post tibial nerve repair (Figure 3.1.3.1). All animals underwent a tibial nerve transection and repair at day 0 with 6 animals being treated with the ES treatment protocol immediately afterwards, 6 animals treated with the normoxia protocol on day 2 and 3 and the remaining 6 animals treated with the AIH protocol on day 2 and 3. All the animals from the 3 treatment groups (n=18) were perfused one hour after completion of the AIH/normoxia treatment protocol on day 3 (~72 hours post-repair). Tissues from the

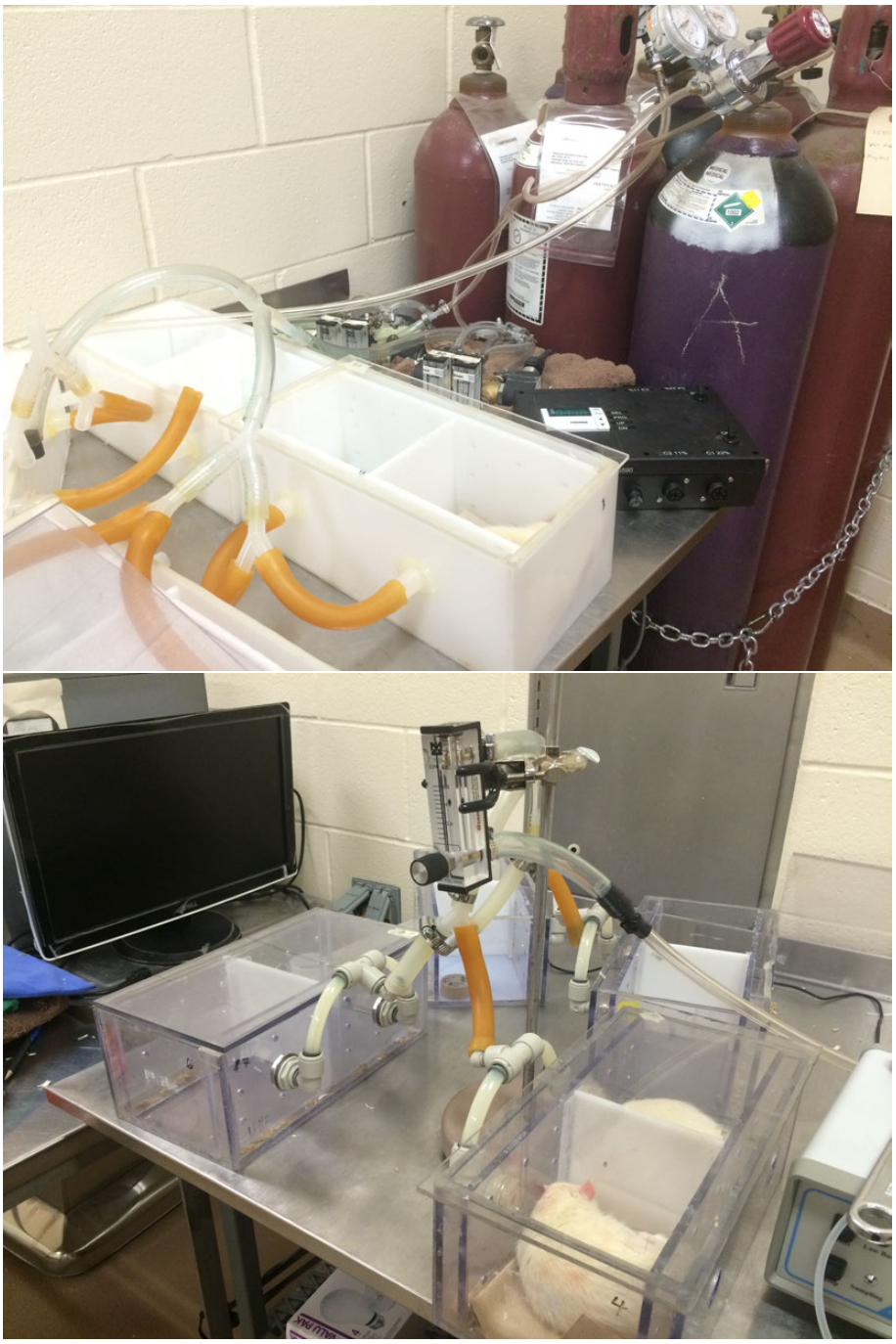

Figure 3.1.2 AIH and normoxia treatment chambers. Custom-made plexiglass chambers with clear lids are connected to gas cylinders via a digital controller that regulates air cycles. Half of the chambers are used for normoxia treatment which feeds continuous medical air (21% oxygen), while the other half are for AIH treatment with the controller set to deliver 5 minutes of alternating medical air (21% oxygen) and 5 minutes of low oxygen air (11% oxygen) preceded by a 1 min purge for each for a total of 10 cycles.

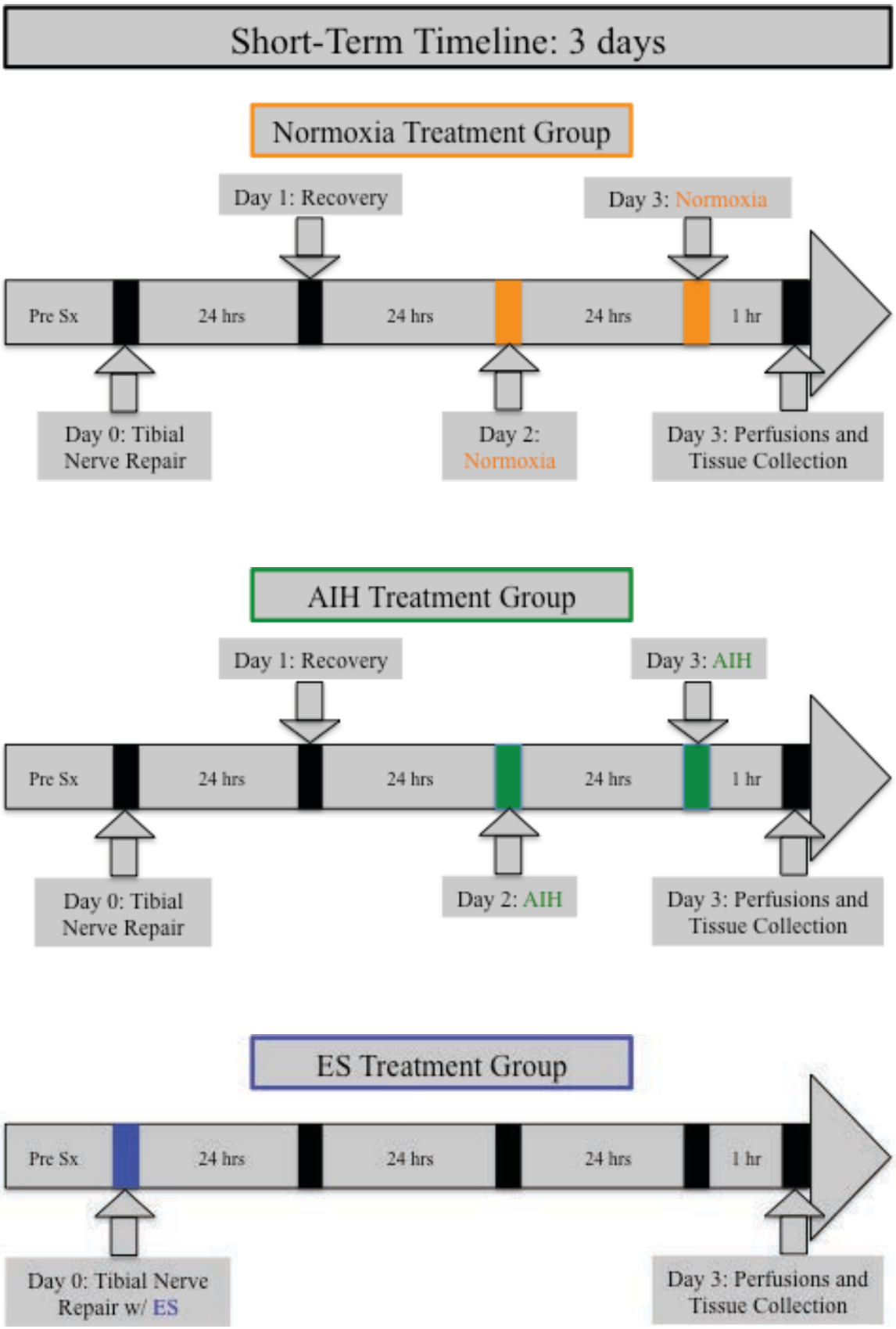
Short-Term Timeline: 3 days
Normoxia Treatment Group
Day 1: Recovery
Day 3: Normoxia
Pre Sx
24 hrs
24 hrs
24 hrs
1 hr
Day 0: Tibial Nerve Repair
Day 2: Normoxia
Day 3: Perfusions and Tissue Collection
AIH Treatment Group
Day 1: Recovery
Day 3: AIH
Pre Sx
24 hrs
24 hrs
24 hrs
1 hr
Day 0: Tibial Nerve Repair
Day 2: AIH
Day 3: Perfusions and Tissue Collection
ES Treatment Group
Pre Sx
24 hrs
24 hrs
24 hrs
1 hr
Day 0: Tibial Nerve Repair w/ ES
Day 3: Perfusions and Tissue Collection

Figure 3.1.3.1 Experimental timeline - summary of methodology used to investigate the short-term effect of AIH or ES on RAGs. All animals underwent tibial nerve transection and repair at day 0. **Top**: Six animals were treated with the normoxia treatment protocol (orange) on day 2 and day 3. **Middle:** Six animals were treated with the AIH treatment protocol (green) on day 2 and day 3. **Bottom:** Six animals were treated with ES treatment protocol (blue) immediately after the tibial nerve transection and repair. All the animals from the 3 treatment groups (n=18) were perfused one hour after completion of the AIH/normoxia treatment protocol on day 3 (72 hours post-repair). Tissues from the L3-L5 spinal cord region, L4 DRG and tibial nerve repair region were collected and processed for RAGs.

L3-L5 spinal cord region, L4 DRG and tibial nerve repair region were collected and processed for expression of RAGs.

Mid-term timeline for FG retrograde tracing

The effect of AIH or ES treatment on the regeneration of peripheral nerves was investigated using FG (Figure 3.1.3.2). In order to establish the total number of motor and sensory neurons contributing to the tibial nerve, a total of 12 animals had their right tibial nerve transected 5 mm distal from the sciatic trifurcation and the proximal stump soaked in 2% FG solution in saline for an hour (Day 0). Four of these animals were then immediately treated with the ES protocol. The remaining 8 animals were treated with either normoxia on day 2 and 3 (n=4) or AIH on day 2 and 3 (n=4). They were perfused on day 30 and tissues collected to observe dye distribution corresponding to the tibial nerve in motor neurons in the L3-L5 spinal cord region and in sensory neurons in the L4 DRG.

To establish the percentage of sensory and motor neurons that regenerated a significant distance from the tibial repair site 25 days post-repair, the tibial nerve was transected ~28 +/- 1 mm distal from the center of the silastic tube and soaked in 2% FG for an hour (See Figure 1.2.2 for tibial anatomical reference). A total of 21 animals underwent this procedure with their respective treatment protocols post-tibial nerve transection and repair: normoxia (n=6), AIH (n=6) and ES (n=9). On day 30, all of the animals were perfused and their tissues collected to observe dye distribution of the regenerated tibial nerve in motor neurons in the L3-L5 spinal cord region and in sensory neurons in the L4 DRG.

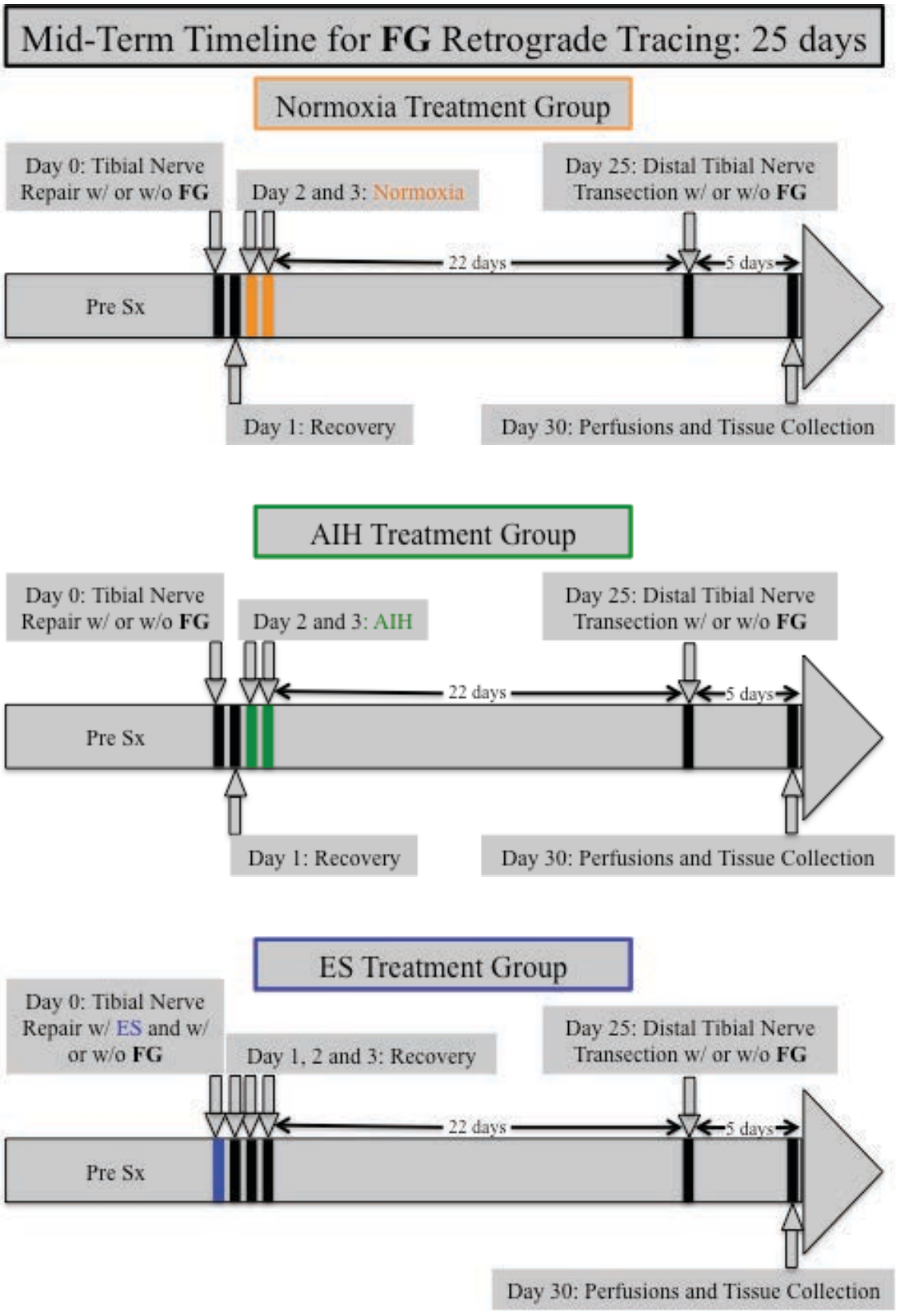
Mid-Term Timeline for FG Retrograde Tracing: 25 days
Normoxia Treatment Group
Day 0: Tibial Nerve Repair w/ or w/o FG
Day 2 and 3: Normoxia
Day 25: Distal Tibial Nerve Transection w/ or w/o FG
22 days
5 days
Pre Sx
Day 1: Recovery
Day 30: Perfusions and Tissue Collection
AIH Treatment Group
Day 0: Tibial Nerve Repair w/ or w/o FG
Day 2 and 3: AIH
Day 25: Distal Tibial Nerve Transection w/ or w/o FG
22 days
5 days
Pre Sx
Day 1: Recovery
Day 30: Perfusions and Tissue Collection
ES Treatment Group
Day 0: Tibial Nerve Repair w/ ES and w/ or w/o FG
Day 1, 2 and 3: Recovery
Day 25: Distal Tibial Nerve Transection w/ or w/o FG
22 days
5 days
Pre Sx
Day 30: Perfusions and Tissue Collection

Figure 3.1.3.2 Experimental timeline - summary of methodology used to investigate the effect of AIH or ES on peripheral nerve regeneration. Top: A total of 10 animals underwent tibial nerve transection and repair with normoxia treatment (orange) on day 2 and day 3. Of these 10 animals, 4 had the proximal stump of the tibial nerve at the repair site soaked in FG for an hour on day 0 and the remaining 6 had the tibial nerve 28 mm distal from the repair site transected and soaked in FG for an hour on day 25. **Middle**: A total of 10 animals underwent a tibial nerve transection and repair with AIH treatment (green) on day 2 and day 3. Of these 10 animals, 4 had the proximal stump of the tibial nerve at the repair site soaked in FG for an hour on day 0 and the remaining 6 had the tibial nerve 28 mm distal from the repair site transected and soaked in FG for an hour on day 25. **Bottom:** A total of 13 animals were treated with ES treatment protocol (blue) immediately after the tibial nerve transection and repair. Of these 13 animals, 4 had the proximal stump of the tibial nerve at the repair site soaked in FG for an hour on day 0 and the remaining 9 had the tibial nerve 28 mm distal from the repair site transected and soaked in FG for an hour on day 25. On day 30, all of the animals (n=33) were perfused and tissues collected to observe dye distribution in motor neurons in the L3-L5 spinal cord region and in sensory neurons in the L4 DRG.

Mid-term timeline for behavioural testing

The effect of AIH or ES treatment on behaviours associated with peripheral nerve regeneration in the hind limb was investigated (Figure 3.1.3.3). A total of 14 animals underwent training/acclimatization to the walking footprint analysis apparatus, Hargreaves thermal hyperalgesia testing chambers, Von Frey mechanical hyperalgesia testing chambers and the ladder crossing apparatus for 14 days. Seven days prior to tibial nerve transection and repair (day 0), baseline values were determined for all of the behavioural tests: Walking footprint analysis (3 days x 3 prints per hind limb), Hargreaves (1 day x 5 trials per hind limb), Von Frey (1 day x 4 trials per hind limb) and ladder crossing (3 days x 10 crossings per day). On day 0, two animals did not undergo a tibial nerve transection and repair (naïve controls) and 12 animals did, followed by ES treatment (n=4), normoxia treatment (n=4) or AIH treatment (n=4). Starting on day 4, all of the animals were behaviour tested for a 21 day period: Walking footprint analysis (9 days x 3 prints per hind limb), Hargreaves (5 days x 5 trials per hind limb), Von Frey (5 days x 4 trials per hind limb) and ladder crossing (9 days x 10 crossings per day). On day 30, the animals were perfused and tissues collected.

Long-term timeline for behavioural testing

With encouraging results obtained from the mid-term experimental timeline, the effect of AIH or ES treatment on behaviours associated with peripheral nerve regeneration in the hind limb was investigated over a 10 week recovery period (Figure 3.1.3.4). A total of 18 animals underwent training/acclimatization as previously described for the mid-term timeline. For one week prior to tibial nerve transection and repair, the following baseline values were obtained: Walking footprint analysis (2 days x 3 prints

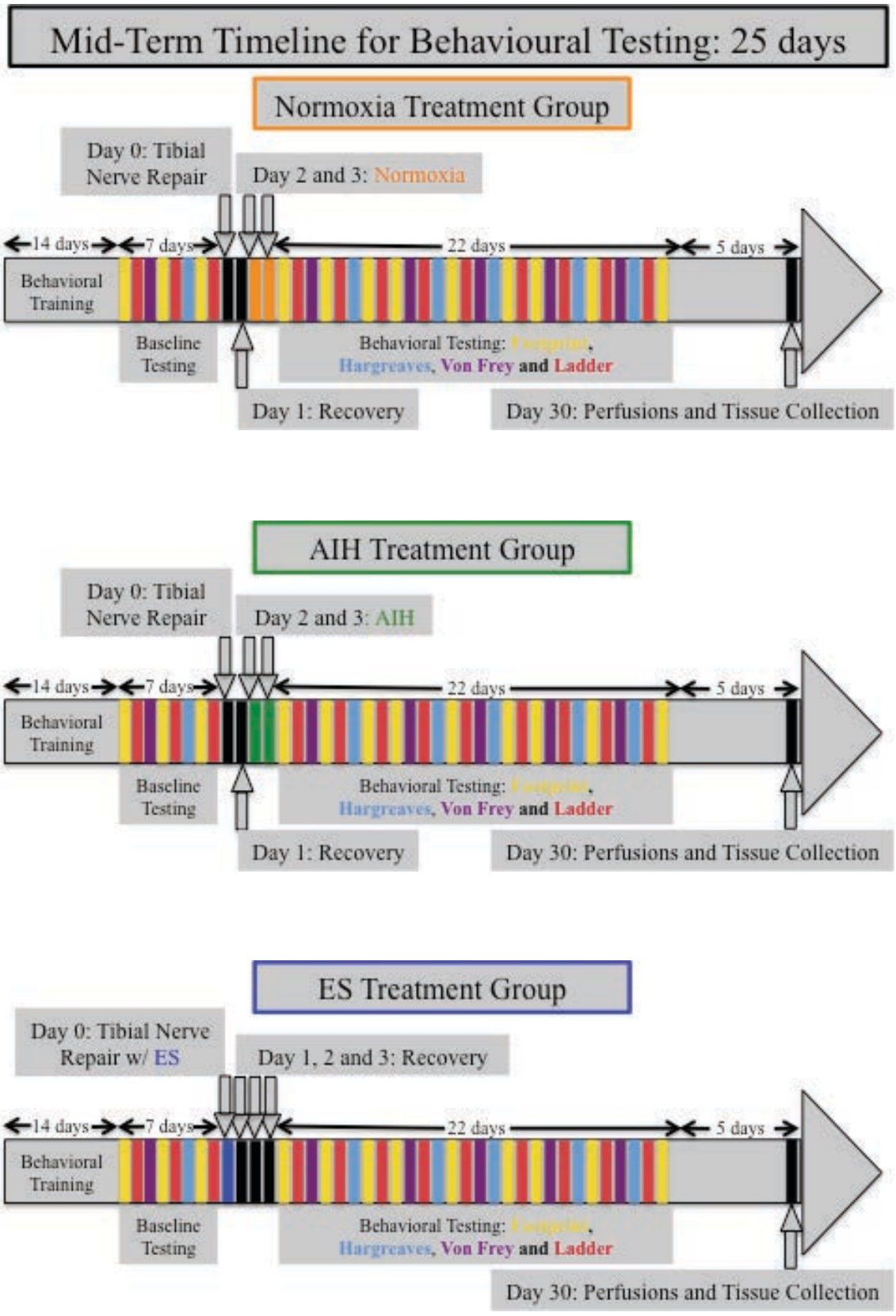
Mid-Term Timeline for Behavioural Testing: 25 days
Normoxia Treatment Group
Day 0: Tibial Nerve Repair
Day 2 and 3: Normoxia
14 days
7 days
22 days
5 days
Behavioral Training
Baseline Testing
Behavioral Testing: Footprint, Hargreaves, Von Frey and Ladder
Day 1: Recovery
Day 30: Perfusions and Tissue Collection
AIH Treatment Group
Day 0: Tibial Nerve Repair
Day 2 and 3: AIH
14 days
7 days
22 days
5 days
Behavioral Training
Baseline Testing
Behavioral Testing: Footprint, Hargreaves, Von Frey and Ladder
Day 1: Recovery
Day 30: Perfusions and Tissue Collection
ES Treatment Group
Day 0: Tibial Nerve Repair w/ ES
Day 1, 2 and 3: Recovery
14 days
7 days
22 days
5 days
Behavioral Training
Baseline Testing
Behavioral Testing: Footprint, Hargreaves, Von Frey and Ladder
Day 30: Perfusions and Tissue Collection

Figure 3.1.3.3 Experimental timeline - summary of methodology used to investigate the effect of AIH or ES on peripheral nerve regeneration-associated behaviours over 25 days. In the mid-term experiment, a total of 14 animals underwent training/acclimatization to the walking footprint analysis apparatus, Hargreaves thermal hyperalgesia testing chambers, Von Frey mechanical hyperalgesia testing chambers and the ladder crossing apparatus for 14 days. Baseline values were established for all tests for 7 days prior to tibial nerve transection and repair (day 0): Walking footprint analysis (3 days x 3 prints per hind limb), Hargreaves (1 day x 5 trials per hind limb), Von Frey (1 day x 4 trials per hind limb) and Ladder crossing (3 days x 10 crossings per day). Twelve animals underwent a tibial nerve transection and repair at day 0 and two animals remained uninjured (controls). **Top:** Four out of the 12 animals underwent normoxia treatment (orange) on day 2 and 3 following the tibial nerve transection and repair on day 0. **Middle:** Four out of the 12 animals underwent AIH treatment (green) on day 2 and 3 following the tibial nerve transection and repair on day 0. **Bottom:** Four out of the 12 animals underwent ES treatment (blue) for an hour immediately after the tibial nerve transection and repair on day 0. Four days after tibial nerve repair, all of the animals underwent behavioural testing throughout a 21 period: Walking footprint analysis (9 days x 3 prints per hind limb), Hargreaves (5 days x 5 trials per hind limb), Von Frey (5 days x 4 trials per hind limb) and Ladder crossing (9 days x 10 crossings per day). On day 30, the animals were perfused and tissues collected.

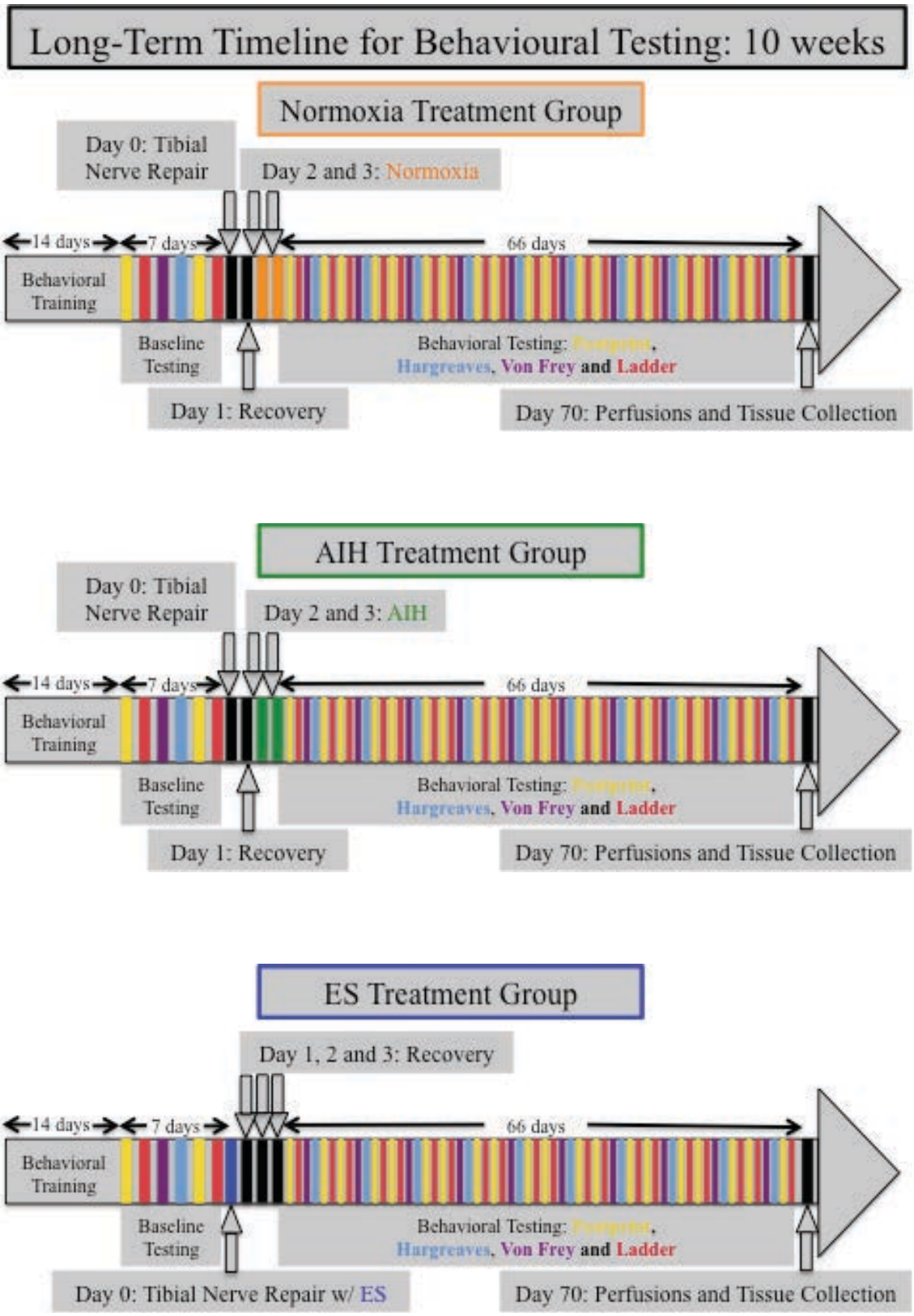
Long-Term Timeline for Behavioural Testing: 10 weeks
Normoxia Treatment Group
Day 0: Tibial Nerve Repair
Day 2 and 3: Normoxia
14 days
7 days
66 days
Behavioral Training
Baseline Testing
Behavioral Testing: Footprint, Hargreaves, Von Frey and Ladder
Day 1: Recovery
Day 70: Perfusions and Tissue Collection
AIH Treatment Group
Day 0: Tibial Nerve Repair
Day 2 and 3: AIH
14 days
7 days
66 days
Behavioral Training
Baseline Testing
Behavioral Testing: Footprint, Hargreaves, Von Frey and Ladder
Day 1: Recovery
Day 70: Perfusions and Tissue Collection
ES Treatment Group
Day 1, 2 and 3: Recovery
14 days
7 days
66 days
Behavioral Training
Baseline Testing
Behavioral Testing: Footprint, Hargreaves, Von Frey and Ladder
Day 0: Tibial Nerve Repair w/ ES
Day 70: Perfusions and Tissue Collection

Figure 3.1.3.4 Experimental timeline - summary of methodology used to investigate the effect of AIH or ES on peripheral nerve regeneration-associated behaviours over 10 weeks. In the long-term experiment, a total of 18 animals underwent training/acclimatization of the walking footprint analysis apparatus, Hargreaves thermalhyperalgesia testing chambers, Von Frey mechanical hyperalgesia testing chambers and the ladder crossing apparatus for 14 days. Baseline values were established for all tests for 7 days prior to tibial nerve repair: Walking footprint analysis (2 days x 3 prints per hind limb), Hargreaves (1 day x 5 trials per hind limb), Von Frey (1 day x 4 trials per hind limb) and Ladder crossing (2 days x 10 crossings per day). Fourteen animals underwent a tibial nerve transection and repair at day 0 and 4 animals remained uninjured (controls). **Top:** Five out of the 14 animals underwent normoxia treatment (orange) on day 2 and 3 following the tibial nerve transection and repair on day 0. **Middle:** Five out of the 14 animals underwent AIH treatment (green) on day 2 and 3 following the tibial nerve transection and repair on day 0. **Bottom:** Four out of the 14 animals underwent ES treatment (blue) for an hour immediately after the tibial nerve transection and repair on day 0. Four days after tibial nerve repair, all of the animals underwent behavioural testing for 66 days: Walking footprint analysis (2x per week x 3 prints per hind limb), Hargreaves (1x per week x 5 trials per hind limb), Von Frey (1x per week x 4 trials per hind limb) and ladder crossing (2x per week x 10 crossings per day). On day 70, the animals were perfused and tissues collected.

per hind limb), Hargreaves (1 day x 5 trials per hind limb), Von Frey (1 day x 4 trials per hind limb) and ladder crossing (2 days x 10 crossings per day). On day 0, four animals did not undergo a tibial nerve transection and repair (controls) and 14 animals did followed by ES treatment (n=4), normoxia treatment (n=5) or AIH treatment (n=5). Starting on day 4, all of the animals underwent behavioural testing for 66 days: Walking footprint analysis (2x per week x 3 prints per hind limb), Hargreaves (1x per week x 5 trials per hind limb), Von Frey (1x per week x 4 trials per hind limb) and ladder crossing (2x per week x 10 crossings per day). On day 70, the animals were perfused and tissues collected.

3.1.4 Fluorogold® nerve labeling

For the mid-term study, to identify the total number of sensory and motor neurons that contribute to the tibial nerve, the proximal end of the nerve, during the tibial nerve transection and repair procedure, was submerged in 4 μl of a 2% FG solution carefully pipetted into a Vaseline lined metal spatula for one hour. The tibial nerve was rinsed with sterile saline and was then repaired as described above using 10-0 silk suture and a 4 mm long section of Silastic® tubing. The muscle and skin were then sutured to close the wound as previously described.

In order to determine the number of sensory and motor neurons that regenerated, the tibial nerve was exposed above the level of the ankle 25 days after the tibial nerve transection and repair with the same anesthetic and analgesic conditions as the original tibial nerve transection and repair procedure. The membrane between the soleus and gastrocnemius muscles was gently spread apart with blunt tip scissors to allow better

exposure. The tibial nerve was cut 28 mm +/- 1mm distal from the original repair site with Vanna micro-scissors (approximately 10 mm proximal from the footpad). Two μls of a 2% FG solution were carefully pipetted into a 4 mm section of silastic tubing that had one end sealed with medical grade silicone glue. The proximal end of the transected tibial nerve was then submerged in the solution in the tube for an hour. It was rinsed with sterile saline and the muscle and skin were then sutured to close the wound. The rats were killed 5 days after the FG application. In addition to the standard tissues collected, a 3 mm section of the tibial nerve from both hind limbs located 20 mm distal from the original repair site was dissected and processed for Epon embedding as below.

3.1.5 Animal perfusion and tissue preparation

The rats were deeply anesthetized with an overdose of pentobarbital and perfused transcardially with 0.1 M PBS, pH 7.4, followed by 4% paraformaldehyde in 0.1 M PBS. The sciatic nerves, tibial nerves, spinal cord, bilateral L3, L4 and L5 DRG were carefully removed and post-fixed for 1-1.5h in 4% paraformaldehyde, then cryoprotected in 10% sucrose followed by 20 % sucrose overnight at 4°C. Initial studies of the DRG involved identifying the dorsal side of each ganglia with 10-0 suture prior to excision during dissection as well as leaving additional dorsal root attached to each to allow for consistent orientation when embedding for sectioning (Figure 3.1.3.5). It allowed for a better understanding of the location of the sensory neuron cell bodies associated with the tibial nerve.

Experimental and control ganglia, nerves or spinal cord were frozen with OCT compound (Tissue Tek; Miles Laboratories, Elkhart, IN) in a cryomold (Tissue Tek,

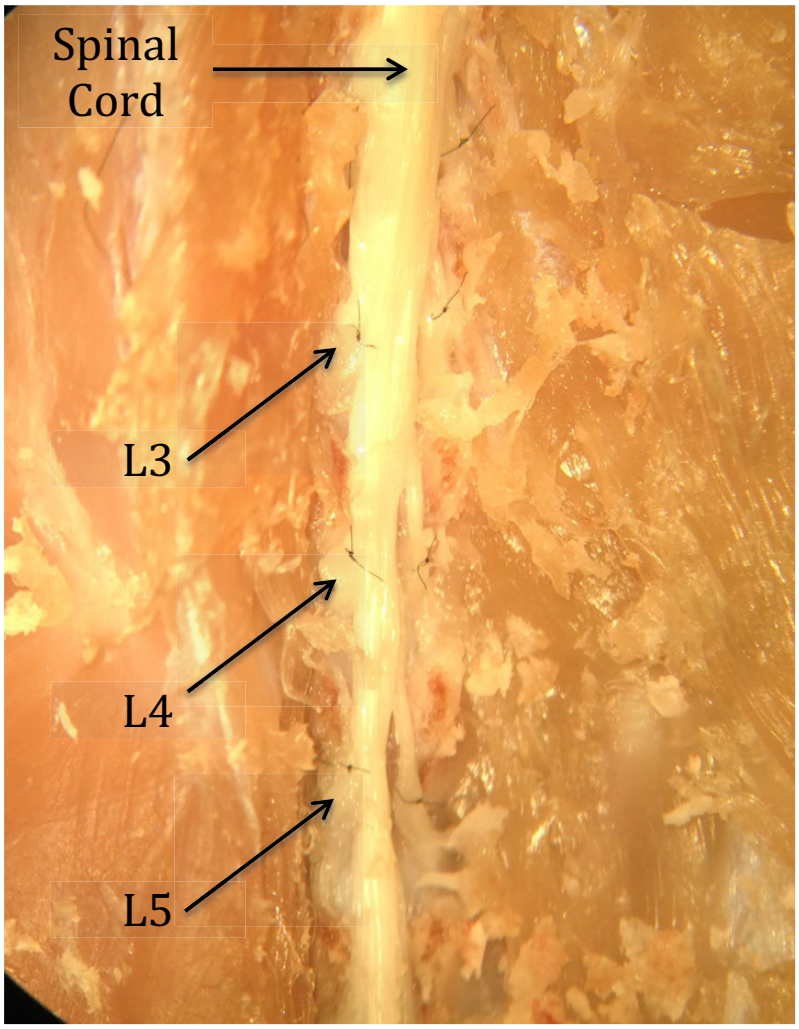

Figure 3.1.3.5 Dissection of DRG and spinal cord. Initial studies of the DRG and lumbar spinal cord involved identifying the dorsal side of each ganglia including L2-L6 with 10-0 suture prior to excision during dissection as well as leaving additional dorsal root attached to each to allow for consistent orientation when embedding for sectioning. Tissue collected for future studies included the region of the spinal cord receiving tibial nerve inputs from L3-L5 sensory neuron afferents, the L4 DRG containing the majority of the tibial nerve sensory neuron cell bodies, the tibial nerve repair site and a 3 mm region of nerve taken 20 mm distal to the tibial nerve repair site.

Miles Laboratories) as to ensure parallel processing. The L3, L4 and L5 ganglia were cut transversally and the tibial nerves and spinal cords were cut either longitudinally or transversally on a cryostat (Micron, Zeiss, Canada) into 8 or 10 μm sections and thaw mounted on Superfrost Plus slides (Fisher Scientific) for immunohistochemistry and Probe-On^{+} slides (Fisher Scientific) for in situ hybridization processing.

3.2 Immunohistochemistry

3.2.1 Visualization of protein expression with antibodies

Slides were blocked with SeaBlock (Calbiochem) for an hour and subsequently treated with the following primary antibodies: mouse anti-ATF3 (Abcam, 1:500), rabbit anti-ATF3 (Santa Cruz, 1:1000), chicken anti-BDNF (R&D Systems, 1:100), mouse anti-tubulin βIII isoform (Millipore, 1:100), rabbit anti-βIII tubulin (Millipore, 1:1000), mouse anti-GAP43 (Schreyer Lab, 1:1000), rabbit anti-HIF-1α (Genetex, 1:200) and rabbit anti-SCG10 (also known as phosphoprotein stathmin, MIM 151442, Novus Biologicals, 1:5000) in a solution comprised of 10% SeaBlock in 0.3% Triton X-100 in 0.1 M PBS overnight. The next day, slides were washed in 0.1 M PBS and antigen/antibody complexes were visualized with donkey anti-mouse alexa 488 (1:1000), donkey anti-mouse dylight 594 (1:2000), goat anti-rabbit dylight 488 (1:1000), donkey anti-rabbit Cy3 (1:2000) or donkey anti-chicken Cy3 (1:1000) (all Jackson Laboratories). The slides were then washed three times in 0.1M PBS and coverslipped using Prolong Gold anti-fade reagent with or without DAPI (Invitrogen – Molecular Probes, Carlsbad, CA) or using a 50% glycerol/50% 0.1M PBS solution. Control sections were processed in the same manner while omitting the primary antibody. All slides were stored at -20°C in

lightproof bags.

3.2.2 *In situ* hybridization

Hybridization was performed according to published procedures (Dagerlind et al., 1992) with a custom 48 mer oligonucleotide probe complementary to and selective for *HIF* mRNA with the following synthesized sequence (Univ. of Calgary DNA services, AB): CAGTTTCCGTGTCATCGCTGCCGAAGTCCAGTGATATGATCGTGTCCC The probes were labeled at the 3'-end with α-[^{35}S]dATP (New England Nuclear, Boston, MA) using terminal deoxynucleotidyl-transferase (Amersham Pharmacia Biotech, Piscataway, NJ) in a buffer containing 10 mM $CoCl_2$, 1 mM dithiothreitol, 300 mM Tris base and 1.4 M $C_2H_6AsKO_2$. The probes were purified using Bio-Spin Disposable Chromatograph Columns (Bio-Rad Laboratories, Hercules, CA) with 200 mg of NENSORB PREP Nucleic Acid Purification Resin. Dithiothreitol was added to obtain a final concentration of 10 nM. The sections were hybridized at 43°C for 14-18h in a buffer containing 10^7 cpm/ml of probe. After hybridization, the slides were washed, dehydrated, processed for radioautography as per Karchewski et al. (2002) and exposed for 7 days before developing in D-19 (Kodak, Rochester, NY). Slides were stained with 0.25% toluidine to visualize cell structure.

3.2.3 Visualization of Fluorogold® distribution

L4 DRGs (left and right) and ventral motor side of the L3 to L5 spinal cord were serially cut into 10 μm sections. Every second slide was used for counts. The DRGs were photographed using Northern Eclipse® (Empix Imaging Inc.) and the FG labeled sensory

neurons in the DRGs counted using Fiji® (Image J, Version 2.0.0, Open Source). The FG labeled motor neurons in the spinal cords were manually counted. The transverse nerve sections were photographed using Northern Eclipse® (Empix Imaging Inc.) to ensure that FG dye uptake was not systemic.

3.2.4 Visualization of axonal regeneration

The three mm sections of tibial nerves dissected 20 mm distal from the original repair site were processed for Epon resin embedding (Western College of Veterinary Medicine at the University of Saskatchewan). One micron transverse semi-thin sections were cut from each animal of both left and right tibial nerves and counterstained with Toluidine Blue to visualize the regenerating axons in each nerve section. Images were taken of the highest quality section from each nerve, absent tissue folds and with even staining, with a Zeiss Axio Imager 1 microscope system with Northern Eclipse® (Empix Imaging Inc.) software using a 40X objective and the images reassembled using Adobe® Photoshop® CS3 (Adobe Systems Inc., USA). The images were blinded and the thinly myelinated and medium myelinated as well as the degenerating axon profiles were individually identified and counted using Fiji® (Image J, Version 2.0.0, Open Source).

3.2.5 Quantification of immunohistochemical signal

All slides were initially analyzed qualitatively and relative changes in immunohistochemistry labeling intensity between experimental groups were noted within each slide to omit discrepancies in background labeling intensity. Slides were selected for experimental analysis such that they had similar numbers of neurons or tissue in the

sections representing each experimental group. Images were taken under identical conditions for each section on individual slides on a Zeiss Axio Imager 1 microscope system with Northern Eclipse® (Empix Imaging Inc.) software using a 40X objective for quantitative sensory neuron analysis and a 20x objective for quantitative motor neuron and tibial nerve analysis. After photographing all sections on a slide, images of each DRG or spinal cord were taken with a 10X objective to create photomontages of each section to be analyzed which were then assembled using Adobe® Photoshop® CS3 (Adobe Systems Inc., USA) to ensure that all neurons with a visible nucleus were only traced once. For neuronal profiles, the circumference of the neuron was traced as well as the nucleus using tablet tracing software (Bamboo, Wacom Ltd, Japan) with inputs into Northern Eclipse® (Empix Imaging Inc.) which computed the diameter of each individual neuron and its respective average cytoplasmic and nuclear immunohistochemical labeling intensity.

3.2.6 Statistical analysis

Each data point for individual neurons or nerves analyzed was normalized to the mean immunohistochemical labeling intensity from the normoxia treatment group using Microsoft Excel software (Microsoft Corp., USA). In the case of cells being double-labeled as ATF3-(uninjured) or ATF3+(injured), the individual neurons were normalized to the mean immunohistochemical labeling intensity of the ATF3- cells from the normoxia treatment group. A Kruskall-Wallis non-parametric ANOVA (Prizm 4.0, Graph Pad Software, San Diego, CA) was used to compare the cytoplasmic or nuclear immunohistochemistry labeling intensity as well as the number of cell bodies and axons

between treatment groups. Statistical significance was accepted at $p < 0.05$ level. Supplemental statistical and graphical manipulations were performed with Prizm 4.0 (Graph Pad Software, San Diego, CA) and Microsoft Excel (Microsoft Corp., USA).

3.3 Behavioural testing

Milk chocolate Ensure® was heated with gelatin to create 5 mm by 5 mm by 5 mm cubes as food rewards for both the mid-term and long-term behavioural testing sessions.

3.3.1 Thermal hyperalgesia test

The Hargreaves plantar test apparatus consists of three clear plexiglass boxes (22 cm long by 17 cm wide by 14 cm high each) whose clear plexiglass floor sits above a moveable infrared source connected to a controller that counts reaction time (Figure 3.3.1). The infrared source is placed under the center of both hind limb footpads and the thermal threshold of foot withdrawal is then displayed on the controller with a 5 minute rest period in between each hind limb recording. Five recordings were done per hind limb per testing session with two baselines and five testing sessions spread out within the three weeks post-surgery. For each of the three experimental groups, a repeated measures ANOVA was performed (Prizm 4.0, Graph Pad Software, San Diego, CA) with treatment and time as variables.

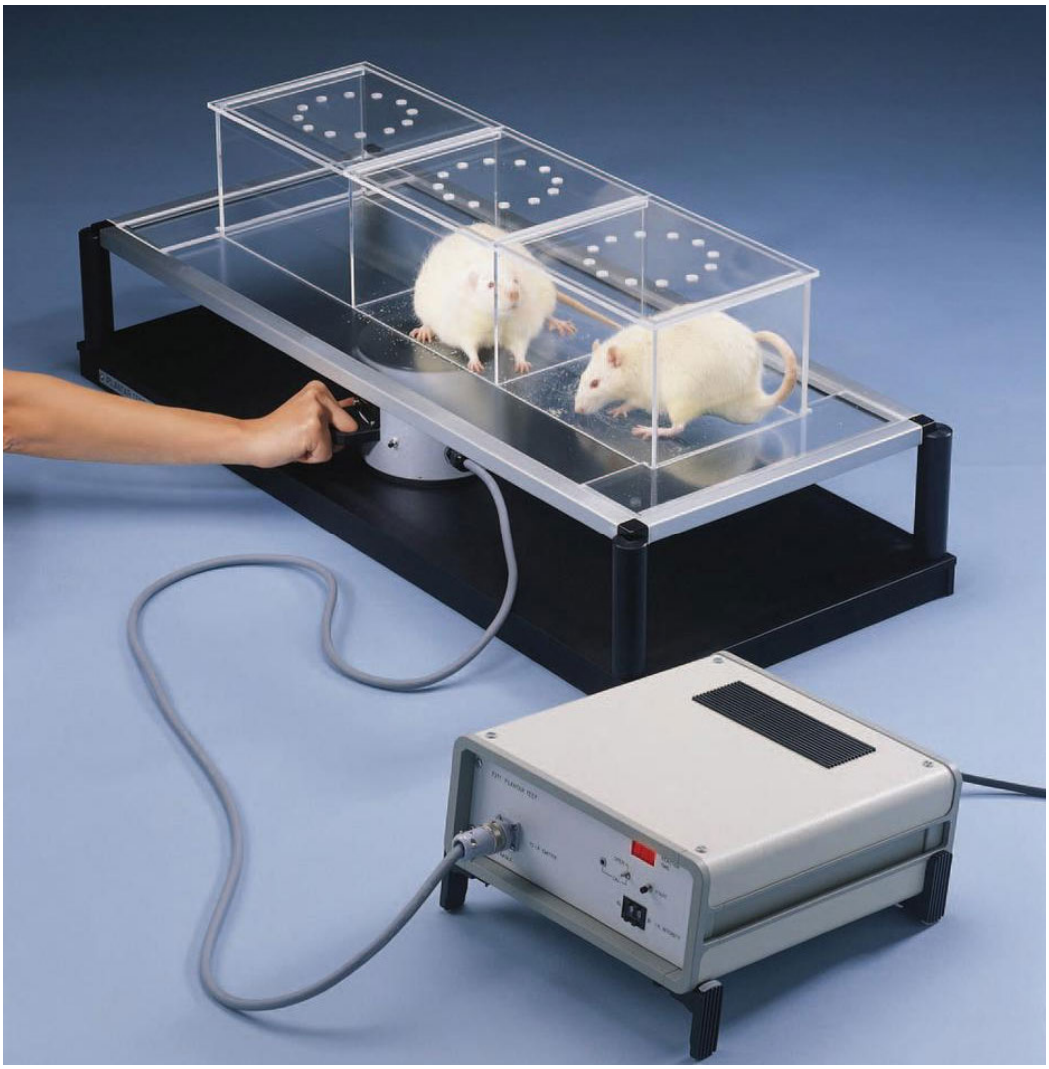

Figure 3.3.1 Thermal hyperalgesia testing apparatus. The Hargreaves testing apparatus consisted of three plexiglass chambers (22 cm long by 17 cm wide by 14 cm high each) on a raised plexiglass floor. An infrared heat source was placed in the center of the hind limb footpad producing heat with a timer running simultaneously. The withdrawal time of each hind limb from the heat source was recorded five times per testing session with a 5 minute rest period between each hind limb recording.

3.3.2 Mechanical hyperalgesia test

The Von Frey test apparatus consists of three clear plexiglass boxes (22 cm long by 17 cm wide by 14 cm high each) with the floor having 1.5 mm diameter holes that are evenly spaced (Figure 3.3.2). An electric von Frey filament is applied to the center of the hind limb footpads to establish mechanical force threshold (in grams) of foot withdrawal, which is then displayed on a controller. The von Frey filaments were applied in order of increasing stiffness for each rat to establish the smallest filament to evoke a withdrawal response. It was determined that the #14 28 gram super tip was optimal in producing a consistent withdrawal response without reaching maximal flex in the filament. The withdrawal pressure per hind limb was recorded four times per testing session with 5 minutes rest period in between each hind limb recording. Two baselines and five testing sessions were recorded spread out within the three weeks post-surgery. For each of the three experimental groups, a repeated measures ANOVA was performed (Prizm 4.0, Graph Pad Software, San Diego, CA) with treatment and time as variables.

3.3.3 Ladder crossing test

The ladder is 80 cm long with 20 cm opaque plexiglass platforms at both ends with clear plexiglass walls (Figure 3.3.3). The ladder consists of 2 mm diameter wire rungs that are spaced by 1 cm. The ladder sits above an angled mirror so that both the side and bottom aspects of the ladder can be video recorded. Rats were trained to cross the ladder to the opposite platform by having a food reward present when animals traversed. The ladder apparatus was wiped with 70% alcohol between sessions. Over ten ladder crossings were recorded with a video camera and video analysis was performed on

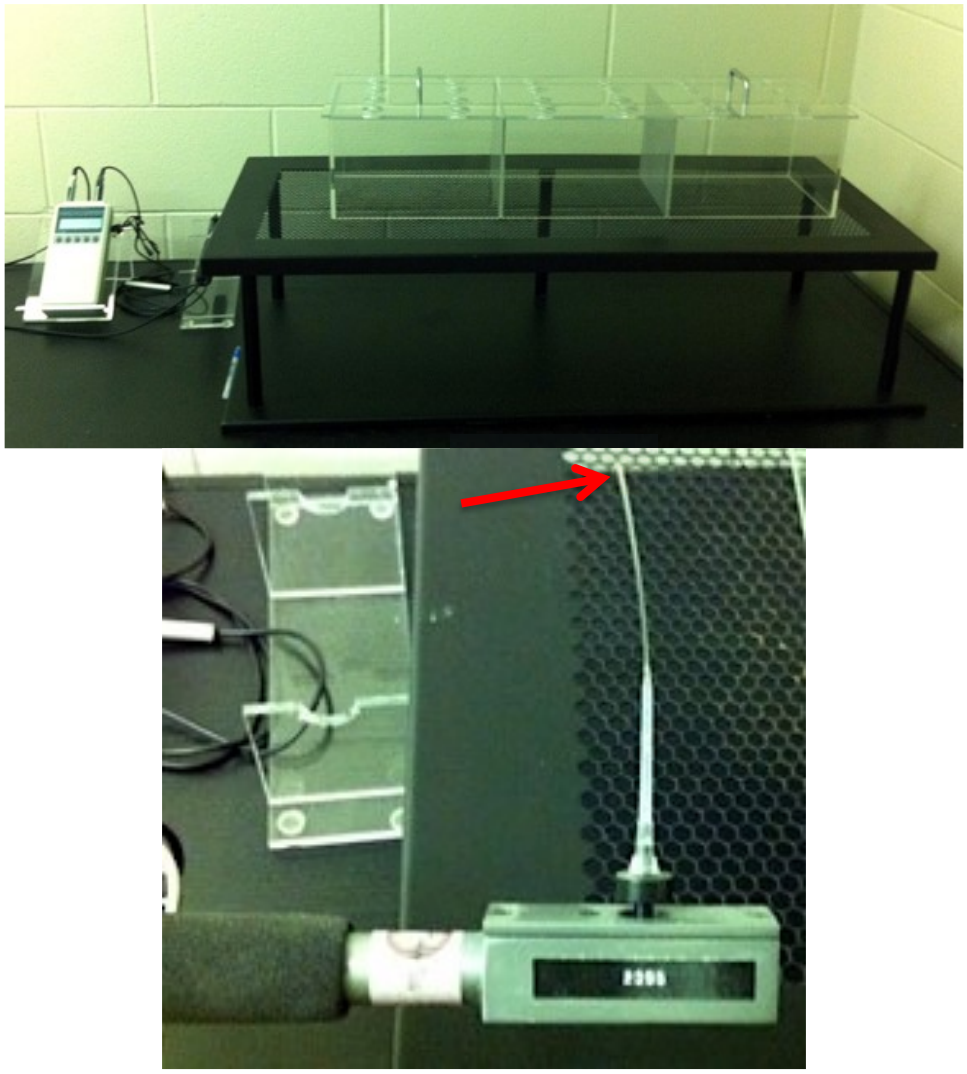

Figure 3.3.2 Mechanical hyperalgesia testing apparatus. The Von Frey testing apparatus consisted of three plexiglass chambers (22 cm long by 17 cm wide by 14 cm high each) on a raised metal floor with evenly spaced 1.5 mm holes (see grid pattern viewed from above on Bottom Figure). Through the holes from below, the tip of an electric von Frey filament (red arrow) was applied to both hind limbs to establish mechanical force threshold (in grams) of foot withdrawal, which is then displayed on a controller (left apparatus on Top Figure). The withdrawal pressure per hind limb was recorded four times per testing session with a 5 minute rest period in between each hind limb recording.

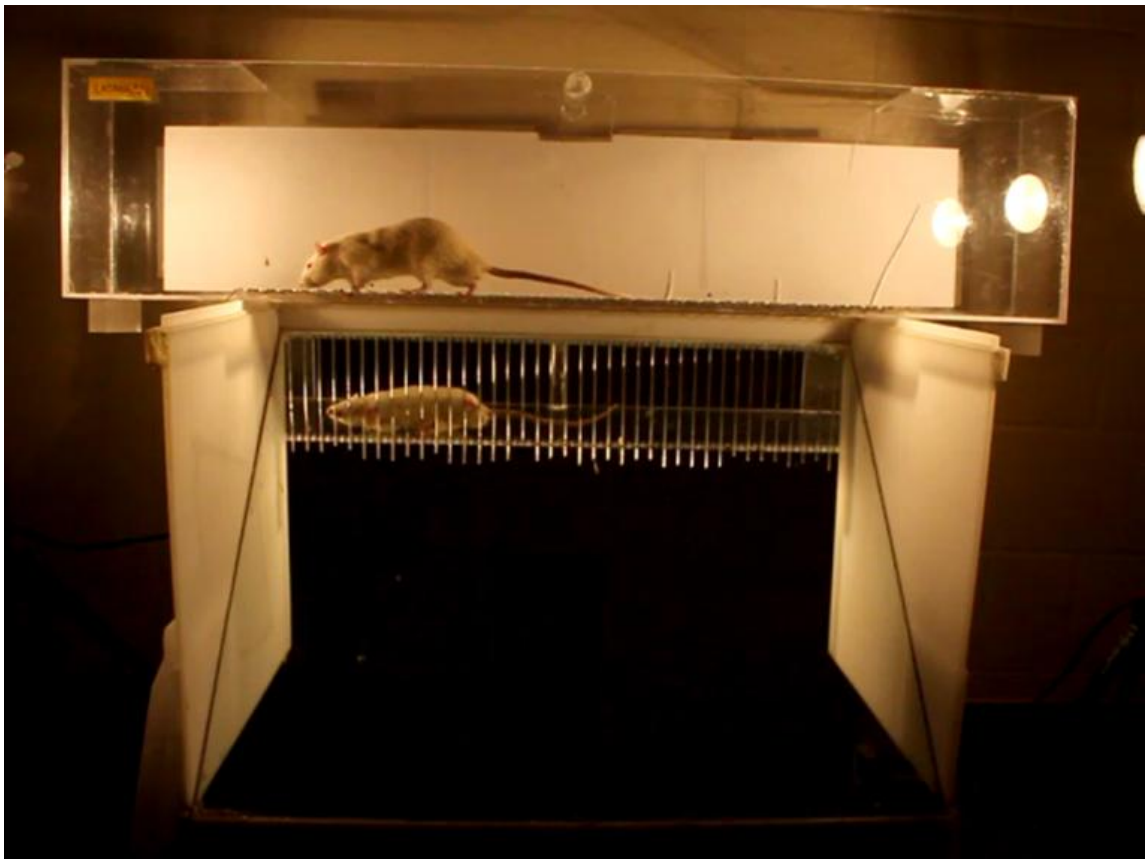

Figure 3.3.3 Ladder crossing testing apparatus. The ladder crossing testing apparatus was custom-made out of clear plexiglass and measured 80 cm long with 20 cm opaque platform at each end. Two millimeters metal pegs are evenly spaced by 1 cm along the track. It sits above an angled mirror so that video recordings can show the animal's positioning as well as their hind limb and toe placements on/between the pegs. Ten ladder crossings were recorded per testing session.

blinded videos on ten crossings with no breaks or stops. Each paw was scored at two occasions per crossing for positioning on the rings whether it was normal (grasps with both the digits and the plantar surface of the hind paw), mostly digits (uses digits only to contact the rung), wrist (no grasping with the digits, only the plantar surface is against the rung), a corrected step (the paw is initially placed on a rung and is immediately lifted and placed on another rung) or a slip (when the hind paw slips through the rungs). When a slip occurred, no quantification was done until the rat had done a full stride to prevent any rebalancing having an impact on subsequent hind limb placement. Three testing sessions were done per week for a baseline then for three weeks or 10 weeks post-surgery. For each of the three experimental groups, a repeated measures ANOVA was performed (Prizm 4.0, Graph Pad Software, San Diego, CA) on each of the scoring parameters (normal, mostly digits, wrist, corrected step or slip) with treatment and time as variables.

3.3.4 Walking footprint analysis test

The walking track is 50 cm long, 8 cm wide and 12 cm high with clear plexiglass walls set within a clear plastic basin (Figure 3.3.4). The rats' hind feet were covered with non-toxic water based black ink (Trodat®) using cotton balls for application, allowed to walk across a strip of white paper that was taped to the floor of the track then washed with dampened cotton balls. A food reward was placed at the end of the track to encourage a continuous set of prints without any stopping or swaying. Three (mid-term experiment) or two (long-term experiment) testing sessions were done for a week of baseline measurements then repeated weekly for three (mid-term experiment) or 10

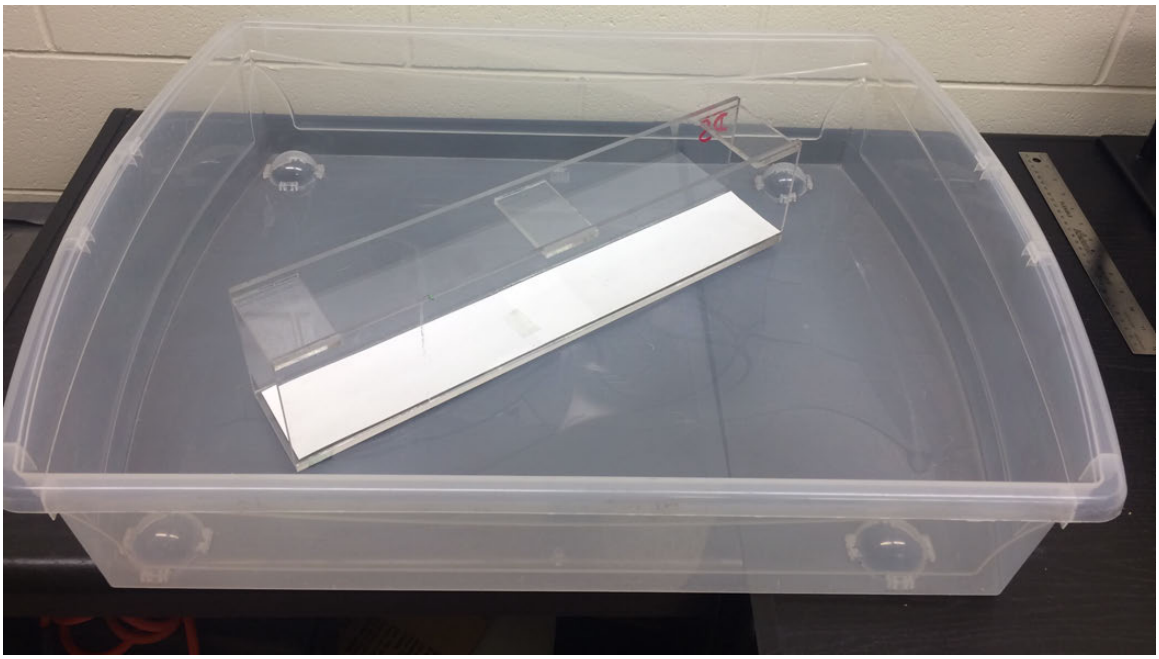

Figure 3.3.4 Walking footprint analysis testing apparatus. The footprint apparatus was custom-made out of clear plexiglass and measured 50 cm long, 8 cm wide and 12 cm high, placed within a clear plastic basin. The animal's hind feet were dabbed with black ink and they were encouraged to walk within the testing track with treats. Three paper strips of prints were collected per testing session.

(long-term experiment) weeks post-surgery. Three paper strips of prints were collected per testing session with the three prints that were the most defined with the least smearing from each hind limb were kept for analysis. Placement of each hind paw based on the ink prints was analyzed as follows (Bain, Mackinnon, and Hunter 1989):

a. Measurement of average print length on both the experimental (EPL) and normal side (NPL).
b. Measurement of toe spread between the first and fifth digits on both sides (ETS and NTS).
c. Measurement of the distance between the second and fourth toes on both sides (EIT and NIT).
d. The formula to calculate the tibial nerve function index (TFI) is:

   TFI = -38.8 (EPL-NPL)/NPL + 109.5(ETS-NTS)/NTS + 13.3(EIT-NIT)/NIT – 8.8
e. For each of the three experimental groups, a repeated measures ANOVA was performed (Prizm 4.0, Graph Pad Software, San Diego, CA) with treatment and time as variables.

4. Results

4.0 Analysis of plasticity-associated gene expression in lumbar sensory neurons from AIH treated spinal cord injured rats reveals potential of AIH to impact PNS

The preliminary studies that established the hypothesis in this thesis were initially done on PNS tissue from Lewis rats that had undergone a cervical partial spinal cord injury with or without one or 7 days AIH treatment one month following injury. Sensory neurons remote from the injury site were examined to see if AIH had an impact on RAGs. Thus, lumbar DRG were processed for immunofluorescence to detect AIH-associated changes in GAP43 and BDNF expression. Expression of both BDNF and GAP43 in sensory neurons was elevated in the animals that underwent cervical spinal cord injury coupled with 1 day (n=2) or 7 days (n=2) AIH treatment relative to those injured animals receiving normoxia treatment (n=2; Figure 4.0.1). Surprisingly, one day of AIH treatment was sufficient to induce these robust changes in RAGs in sensory neurons, with 7 days of AIH treatment not appearing to increase protein levels much beyond that observed with 1 day. Another member of our lab, Dr. Atiq Hassan, also observed similar alterations in gene expression in the lumbar motor neurons (Hassan 2015). The DRG RAG and AIH immunofluorescence were confirmed in repeat experiments and another marker induced by AIH and very recently linked to peripheral nerve repair (Cho et al. 2015), HIF-1α was examined using *in situ* hybridization (Figure 4.0.2). An increase in hybridization signal was observed over L5 DRG sections in rats that underwent AIH treatment relative to normoxia controls, that was most robust in spinal cord injured rats receiving 1 day AIH versus 7 days AIH treatment. No further *in situ* hybridization experiments were performed due to an ongoing inability to buy isotope

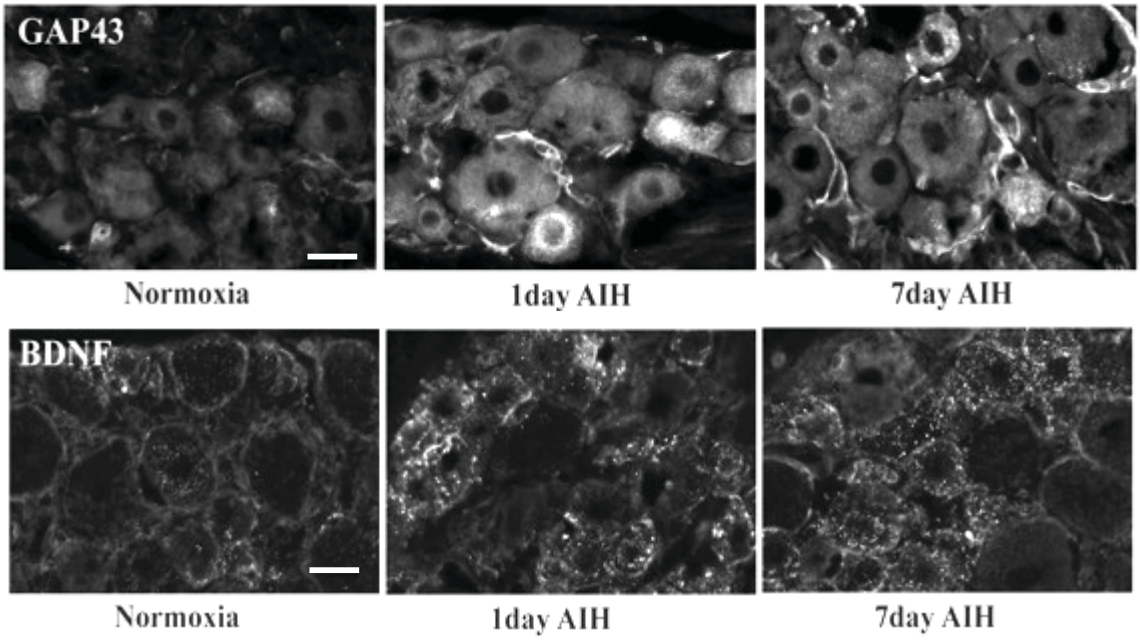

Figure 4.0.1 Preliminary data showing AIH treatment elevates expression of plasticity-associated genes in sensory neurons. Fluorescence photomicrographs of 10 μm lumbar DRG sections from Lewis rats processed for immunohistochemistry to detect GAP43 protein expression (top) and BDNF protein expression (bottom) in response to normoxia (left), 1 day AIH (middle) or 7 days AIH treatment (right). Note: AIH treatment for 1 day (n=2) or 7 days (n=2) one month following cervical spinal cord injury leads to an increase in neuronal GAP43 protein and BDNF protein expression compared to normoxia treated controls (n=2). Scale bar = 30 μm

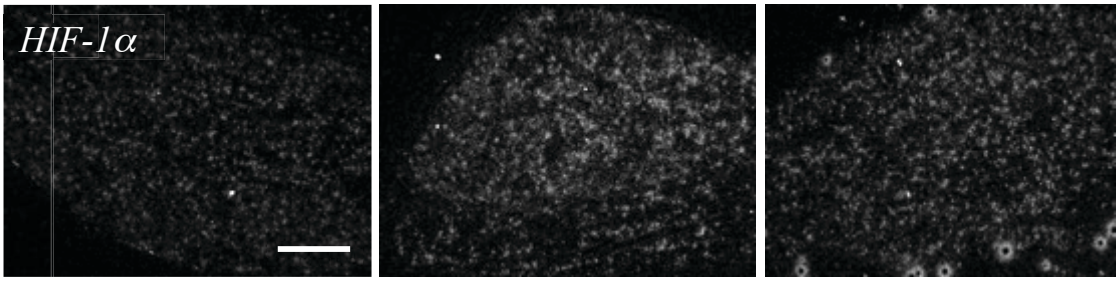

Figure 4.0.2 Preliminary data showing AIH treatment elevates expression of HIF-1α in sensory neurons. Dark field photomicrographs of 8 μm lumbar DRG sections processed for in situ hybridization depict levels of *HIF-1 α* mRNA treated with normoxia (left), 1 day of AIH (middle) and 7 days of AIH (right). Note: AIH treatment for 1 day (n=2) or 7 days (n=2) one month following cervical spinal cord injury leads to a widespread increase in *HIF-1 α* mRNA throughout the DRG relative to normoxia control (n=2). Unfortunately, due to supply unavailability of radioactive isotope that would reliability label any of our oligonucleotide probes, no in situ hybridizations were done to substantiate these results. Scale bar = 500 μm

that reliably labels the oligonucleotide probes.

Collectively, these exciting preliminary insights prompted further investigations and the development of my thesis project examining whether the heightened RAG expression induced by AIH might occur in injured and repaired sensory and motor neurons and prove beneficial to repair in a less invasive manner, but with results akin to that which we have observed in response to one hour brief electrical nerve stimulation (ES; 20Hz) at the time of nerve repair (Al-Majed et al. 2000, Geremia et al. 2007, reviewed in Gordon and Borschel 2016).

We chose to create an AIH tibial nerve repair model, where the tibial branch of the sciatic nerve was transected just distal to the sciatic nerve trifurcation and repaired in the same manner as that used for the femoral nerve in Geremia et al. (2007), followed by either immediate one hour ES of the sciatic nerve proximal or AIH treatment for either one or two consecutive days beginning one day post-injury and repair. The initial attempts to examine the potential of AIH treatment to improve peripheral nerve repair were conducted in the Wistar strain of rat utilized in our previous ES studies. However, unlike the Lewis rats, no significant increases in GAP43 immunofluorescence was observed in DRG neurons at 3 days post-injury and repair with either one day or two days of AIH treatment in these rats. However, the expected increases were observed in the ES group as previously published (Geremia et al. 2007) (Figure 4.0.3). Thus, all future investigations were conducted using the Lewis rat strain.

Due to the tibial nerve repair model being new to our research group, FG retrograde labeling of the tibial nerve was also done to examine the distribution of its sensory and motor neuron cell bodies in the Lewis rat. The L3, L4 and L5 DRG as well

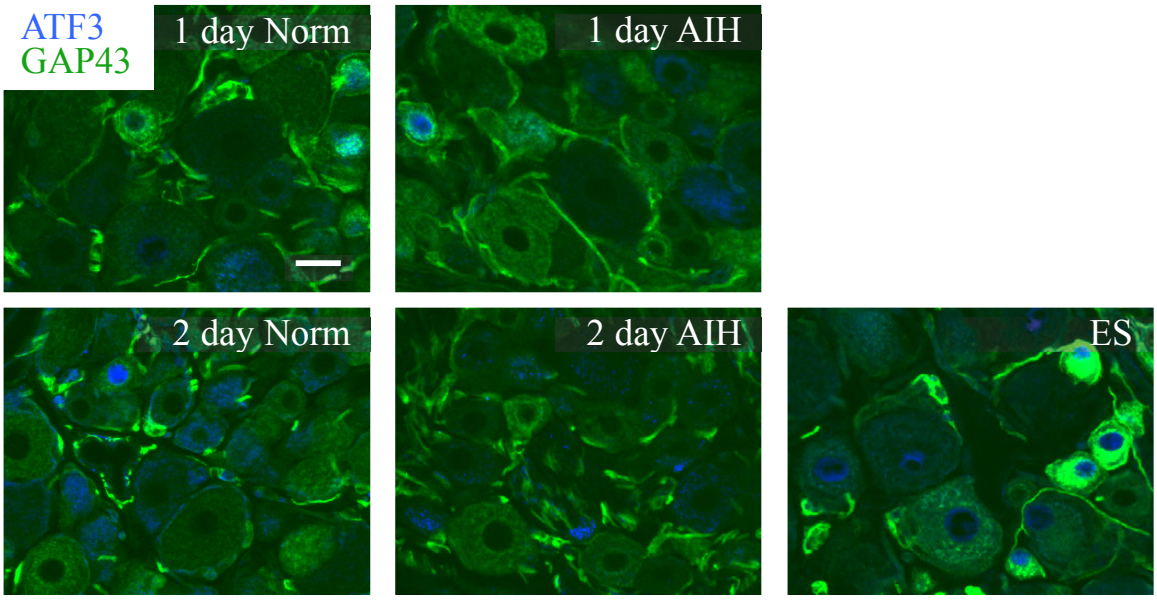

Figure 4.0.3 AIH treatments for 1 day or 2 days does not increase GAP43 protein expression in lumbar sensory neurons 3 days post nerve repair in Wistar rats. Fluorescence photomicrographs of L4 DRG 10 μm sections processed for dual immunofluorescence to detect cytoplasmic GAP43 (green) protein levels in injured activated transcription factor-3 (ATF3; blue) positive ($ATF3^{+ve}$) or uninjured ATF3 negative ($ATF3^{-ve}$) sensory neurons from rats that underwent tibial nerve repair followed by 1 day normoxia (top left), 1 day AIH (top middle), 2 day normoxia (bottom left), 2 day AIH (bottom middle) or 1 hour ES (bottom right) treatment. Note: ES treatment results in increased expression of GAP43 in the cytoplasm of sensory neurons, most notably in the smaller cells with a diameter of 12-30 μm, compared to normoxia controls. No changes in expression levels of GAP43 were observed with 1 or 2 days of AIH treatment, contrary to our preliminary results in Lewis rats and our hypothesis. GAP43 is also expressed in the sympathetic axons distributed throughout the DRG, appearing as fibers between the sensory neurons, however no qualitative changes were observed in their GAP43 expression levels with the various treatments. Scale bar = 30 μm.

as the L3 to L6 spinal cord were collected 5 days after dye application. The distribution of the tibial nerve to the DRGs has been reported within the following approximate ranges for the Sprague-Dawley and Sabra/Wistar strains of rats: L3 0-1%, L4 40-68%, L5 30-60% and L6 0-5% (Swett et al. 1991, Devor et al. 1985, Asato et al. 2000). In addition, a thorough literature search at the time did not yield any information as to whether any of the nerves are segregated/organized within the DRG, thus prior to dissection, by identifying the dorsal side of the DRG with suture and leaving the attached dorsal root longer than the attached spinal nerve, it allowed for topographical analysis of the DRGs (Figure 3.1.3.5).

The greatest number of FG-labeled sensory neurons in our Lewis rats was in the L4 DRG with over 50% of its population, whereas the L5 DRG, being smaller in size and in number of sensory neuron cell bodies than the L4, had less than 40% of its population FG-labeled (data not shown). Swett et al. (1991) reported that the L4 DRG contains more than twice the number of tibial neurons than the L5 in the Sprague-Dawley strain. This determined that the L4 was the primary DRG for all of our investigations. In addition, topographical orientation of the L4 DRG revealed that neurons with axons in the tibial branch of the sciatic nerve distribute closer to the dorsal root side of the L4 DRG and are predominantly on the ventral side with very few present on the dorsal side (data not shown). Our usual technique that involves laying the DRG on their ‘flat side’ in the molds for cryo-processing, has the dorsal sides of the DRGs sectioned first and thus many initial studies where only 10-20 sections were cut, missed the actual tibial neurons. Thus, our embedding and sectioning protocol was also modified.

4.1 Impact of AIH or ES versus normoxia treatment on early expression of RAG proteins in regenerating tibial nerve and associated motor and sensory neurons

It should be noted that for all markers examined, similar qualitative trends were observed between experimental groups for all animals in each experimental group. In regards to the sensory neurons, located in the L4 DRGs, three out of six groupings of different experimental animals were selected for detailed quantitative analysis. This selection was based on having a similar number of sensory neurons in each of the three DRG sections on the slide such that a minimum of 80 sensory neurons with $ATF3^{+ve}$ (positive) nuclei identifying those neurons contributing axons to the injured tibial nerve branch and another 80 with $ATF3^{-ve}$ (negative) nuclei identifying L4 DRG neurons not contributing axons to the injured tibial nerve could be traced and quantified for each animal. This yielded separate immunofluorescence signal intensity values for the nuclei and the cytoplasm for the marker examined.

In the motor neurons, located in the L4 region of the spinal cord, the protein expression levels were analyzed qualitatively in six animals and three of these animals that had the highest number of both $ATF3^{-ve}$ and $ATF3^{+ve}$ labeled nuclei in the processed sections were quantitatively analyzed. A minimum of 50 motor neurons that had $ATF3^{+ve}$ nuclei and another 50 motor neurons with $ATF3^{-ve}$ nuclei were traced per animal using the same image analysis program as for the sensory neurons. Each neuronal population was normalized to the mean immunofluorescence signal intensity of the uninjured $ATF3^{-ve}$ nuclei cells from the normoxia treatment group on the same immunohistochemical slide, containing a section from each treatment group . Further, all digital images were captured under identical conditions for ganglia or spinal cord sections from all

experimental groups mounted on the same slide, then images were blinded prior to quantification. These approaches to quantification were consistent with those employed in our previous ES studies (Geremia et al. 2007, Verge 2004, Pettersson et al. 2014).

4.1.1 Neuronal GAP43 expression

In sensory neurons, both AIH and ES treatments resulted in significant increases in cytoplasmic GAP43 protein levels in their cell bodies located in L4 DRG at 3 days post-repair relative to repair with normoxia treatment (Figure 4.1.1.1, Table 4.1.1.1). The graph and table summarize these findings which reveal that while small (9% AIH; 7% ES) but significant increases were observed in the uninjured neurons, there was a much larger response (62% AIH; 67% ES; 37% Norm) in the injured and repaired neurons contributing to the tibial nerve relative to the uninjured $ATF3^{-ve}$ neurons in the normoxia treatment group. The increased GAP43 expression in injured neurons in response to AIH or ES was most notable in the small size neurons, previously shown to already express GAP43 at moderate levels when uninjured (Verge et al. 1990, Schreyer and Skene 1991). In addition to the observed neuronal changes, it was noted that elevated GAP43 expression was evident in the perineuronal cells in the AIH treated animals relative to normoxia treatment (Figure 4.1.1.1).

In motor neurons at the level of the L4 spinal cord, it was observed that AIH as well as ES treatment increased GAP43 protein levels at 3 days post-repair in their cell bodies as compared to normoxia treatment and surprisingly, this effect was observed regardless of whether the motor neurons were injured ($ATF3^{+ve}$) or uninjured ($ATF3^{-ve}$) (Figure 4.1.1.2, Table 4.1.1.2). The graph and table summarize these findings depicting a

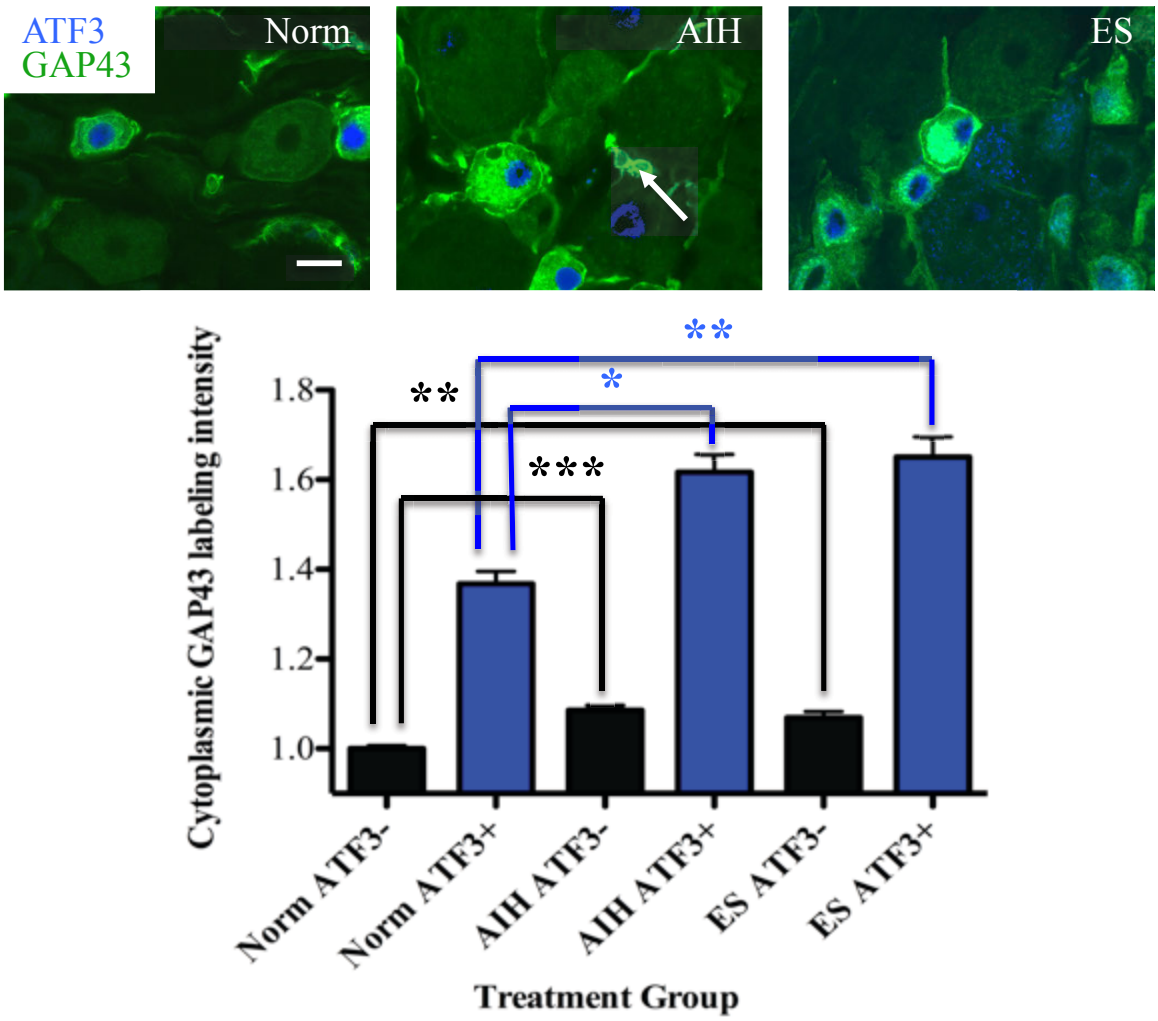

Figure 4.1.1.1 AIH or ES treatment results in increased GAP43 protein expression in sensory neurons 3 days post nerve repair. Top: Fluorescence photomicrographs of L4 DRG 10 μm sections processed for dual immunofluorescence to detect cytoplasmic GAP43 (green) protein levels in injured activated transcription factor-3 (ATF3; blue) positive ($ATF3^{+ve}$) or uninjured ATF3 negative ($ATF3^{-ve}$) sensory neurons from rats that underwent tibial nerve repair followed by 2 day normoxia, AIH or 1 hour ES treatment. Note: AIH treatment, unlike in the Wistar strain of rat, results in increased expression of GAP43 compared to normoxia controls. Increased labeling is also seen in the perineuronal cells (white arrow). ES treatment also had higher expression compared to normoxia controls. Higher levels of GAP43 expression are seen primarily in the smaller population of sensory neurons. Scale bar = 20 μm. Bottom: Graph depicts quantification of relative changes in the cytoplasmic immunofluorescence levels for GAP43 in neurons with or without $ATF3^{+ve}$ nuclei in L4 DRG from rats treated with either AIH or ES and compared to normoxia controls post-tibial nerve repair. The data is normalized to the mean of the sensory neurons from the normoxia treatment group without $ATF3^{+ve}$ nuclei (i.e. uninjured). Asterisks indicate significant differences between experimental groups (Kruskal-Wallis test with Dunn's Multiple Comparison test; * $p<0.05$, ** $p<0.01$, *** $p<0.001$; N=555-690 total neurons analyzed from 3 animals per treatment group).

GAP43 in Sensory Neurons			
Treatment	**Normoxia**	**AIH**	**ES**
Mean immunofluorescence signal intensity ATF3^{+ve} cells	1.37 +/- 0.0282 s.e.m.	1.62 +/- 0.0398 s.e.m.	1.65 +/- 0.0453 s.e.m.
# of cells	259	304	256
# of animals	3	3	3
Significance (p)	-	$p<0.05$	$p<0.01$
Mean immunofluorescence signal intensity ATF3^{-ve} cells	1.00 +/- 0.0070 s.e.m.	1.09 +/- 0.0114 s.e.m.	1.07 +/- 0.0133 s.e.m.
# of cells	337	385	298
# of animals	3	3	3
Significance (p)	-	$p<0.001$	$p<0.01$

Table 4.1.1.1 The mean cytoplasmic immunofluorescence signal intensity of GAP43 in uninjured sensory neurons (ATF3^{-ve} nuclei) with AIH treatment or ES treatment as normalized to normoxia treatment increased significantly. In addition, in the injured ATF3^{+ve} nuclei population of these cells, the cytoplasmic mean labeling intensity with AIH treatment or ES treatment compared to normoxia treatment also increased significantly.

GAP43 in Motor Neurons			
Treatment	**Normoxia**	**AIH**	**ES**
Mean immunofluorescence signal intensity ATF3^{+ve} cells	1.09 +/- 0.0153 s.e.m.	1.17 +/- 0.0087 s.e.m.	1.27 +/- 0.0106 s.e.m.
# of cells	159	154	196
# of animals	3	3	3
Significance (p)	-	$p<0.001$	$p<0.001$
Mean immunofluorescence signal intensity ATF3^{-ve} cells	1.00 +/- 0.0120 s.e.m.	1.10 +/- 0.0078 s.e.m.	1.13 +/- 0.0109 s.e.m.
# of cells	156	194	191
# of animals	3	3	3
Significance (p)	-	$p<0.001$	$p<0.001$

Table 4.1.1.2 The cytoplasmic mean labelling intensity in uninjured motor neurons with ATF3^{-ve} nuclei with AIH treatment or ES treatment as normalized to normoxia treatment increased significantly. The same relationship was observed in the injured ATF3^{+ve} nuclei population of these cells; the cytoplasmic mean labeling intensity with AIH treatment or ES treatment compared to normoxia treatment increased significantly.

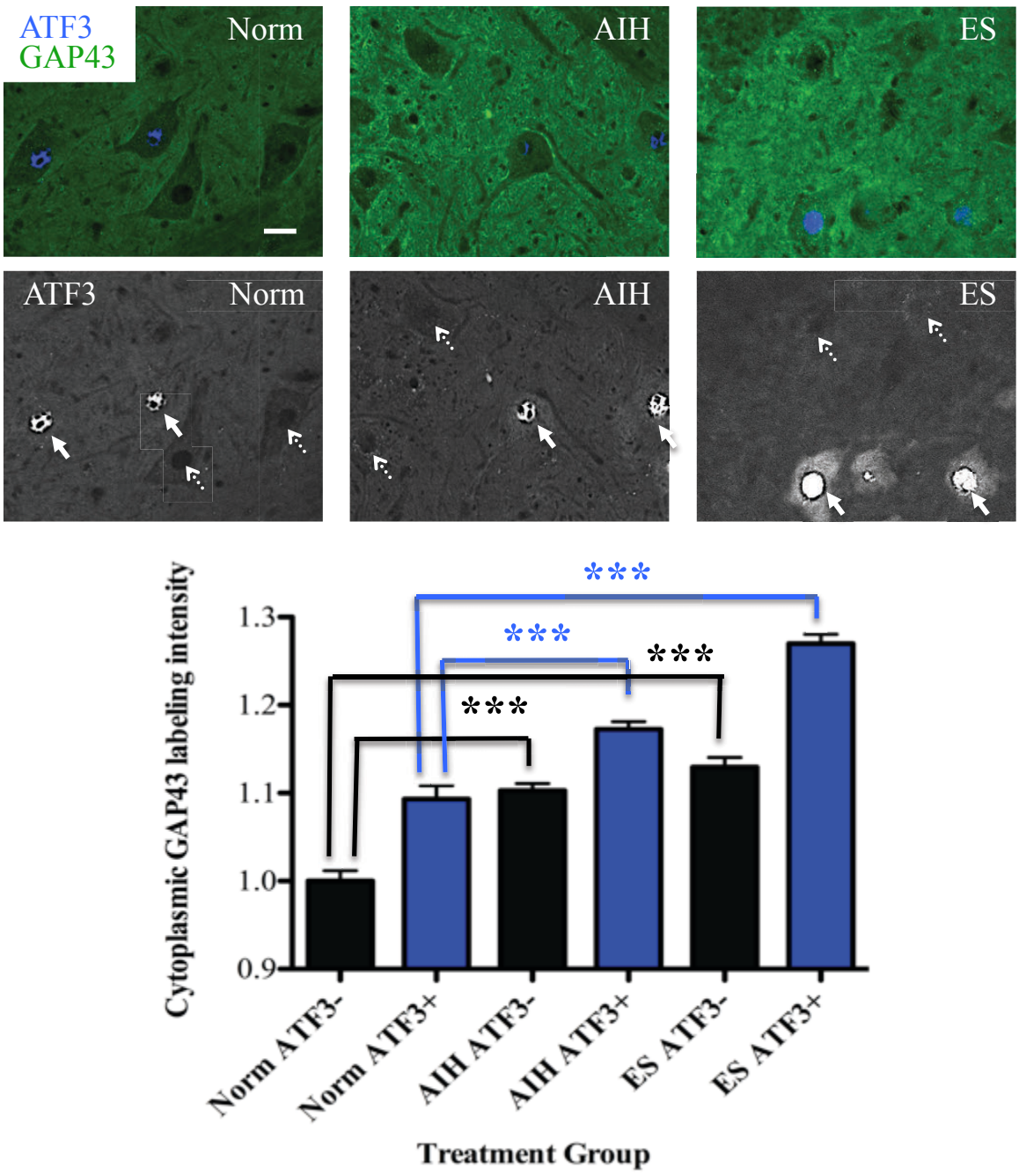

Figure 4.1.1.2 AIH or ES treatment results in increased GAP43 protein expression in motor neurons 3 days post nerve repair. Top: Fluorescence photomicrographs of 10 µm lumbar spinal cord sections processed for dual immunofluorescence to detect cytoplasmic GAP43 (green) protein levels in injured ATF3 (blue) positive ($ATF3^{+ve}$) or uninjured ATF3 negative ($ATF3^{-ve}$) motor neurons from rats that underwent tibial nerve repair followed by 2 day normoxia, AIH or 1 hour ES treatment. Arrows identify representative motor neurons with (injured, full arrows) or without (uninjured, dashed arrows) $ATF3^{+ve}$ nuclei. Note: AIH and ES treatment results in increased expression of GAP43 in the cytoplasm of injured and uninjured motor neurons as well as the neuropil

compared to normoxia controls. Additionally, ATF3 expression levels in ES treated injured motor neurons appears higher both in the cytoplasm and nucleus compared to AIH and normoxia treatment. Scale bar = 30 μm. Bottom: Graph depicts quantification of relative changes in the cytoplasmic immunofluorescence levels for GAP43 in motor neurons with or without $ATF3^{+ve}$ nuclei in spinal cord from rats treated with either AIH or ES and compared to normoxia controls post-tibial nerve repair. The data is normalized to the mean of the motor neurons from the normoxia treatment group without $ATF3^{+ve}$ nuclei (i.e. uninjured). Asterisks indicate significant differences between experimental groups (Kruskal-Wallis test with Dunn's Multiple Comparison test; *$p<0.05$, ** $p<0.01$, *** $p<0.001$; N=315-387 total neurons analyzed from 3 animals per treatment group).

significant effect in both the injured (ATF^{+ve}) (17% AIH; 27% ES; 9% Norm) and the uninjured ($ATF3^{-ve}$) (10% AIH; 13% ES) motor neuron populations relative to normoxia treatment. Beyond increased expression in the motor neuron cytoplasm there was an even larger rise in GAP43 protein levels in both the AIH and the ES treatment groups compared to the normoxia treatment group in the grey matter neuropil surrounding the quantified motor neurons (Figure 4.1.1.2). Additionally, ATF3 labeling was noted to be increased in the cytoplasm in both the sensory and motor neurons in the ES treatment group compared to the normoxia and AIH treatment groups (Figures 4.1.1.1 and 4.1.1.2).

4.1.2 Neuronal BDNF expression

In sensory neurons, it was observed that AIH treatment significantly increased cytoplasmic BDNF protein levels in the cell bodies in L4 DRG at 3 days post-repair (Figure 4.1.2.1, Table 4.1.2.1). The graph and table summarize these conclusions. The AIH treatment produced significant increases in BDNF expression in both the $ATF3^{-ve}$ and the $ATF3^{+ve}$ sensory neuron populations (5% and 21% respectively) compared to the normoxia treatment (0% and 9% respectively). Unlike GAP43 expression levels in the sensory neurons, the ES treatment did not significantly increase BDNF expression levels (Figures 4.1.1.1 and 4.1.2.1). More specifically, there was no significant effect on the $ATF3^{-ve}$ population (3%), however the $ATF3^{+ve}$ population was found to express significantly lower increases in levels of BDNF with ES treatment (17%) than the AIH treatment group (21%).

It was observed that AIH or ES increased BDNF protein levels in the motor neurons in L4 spinal cord (Figure 4.1.2.2, Table 4.1.2.2). The values in the graph and

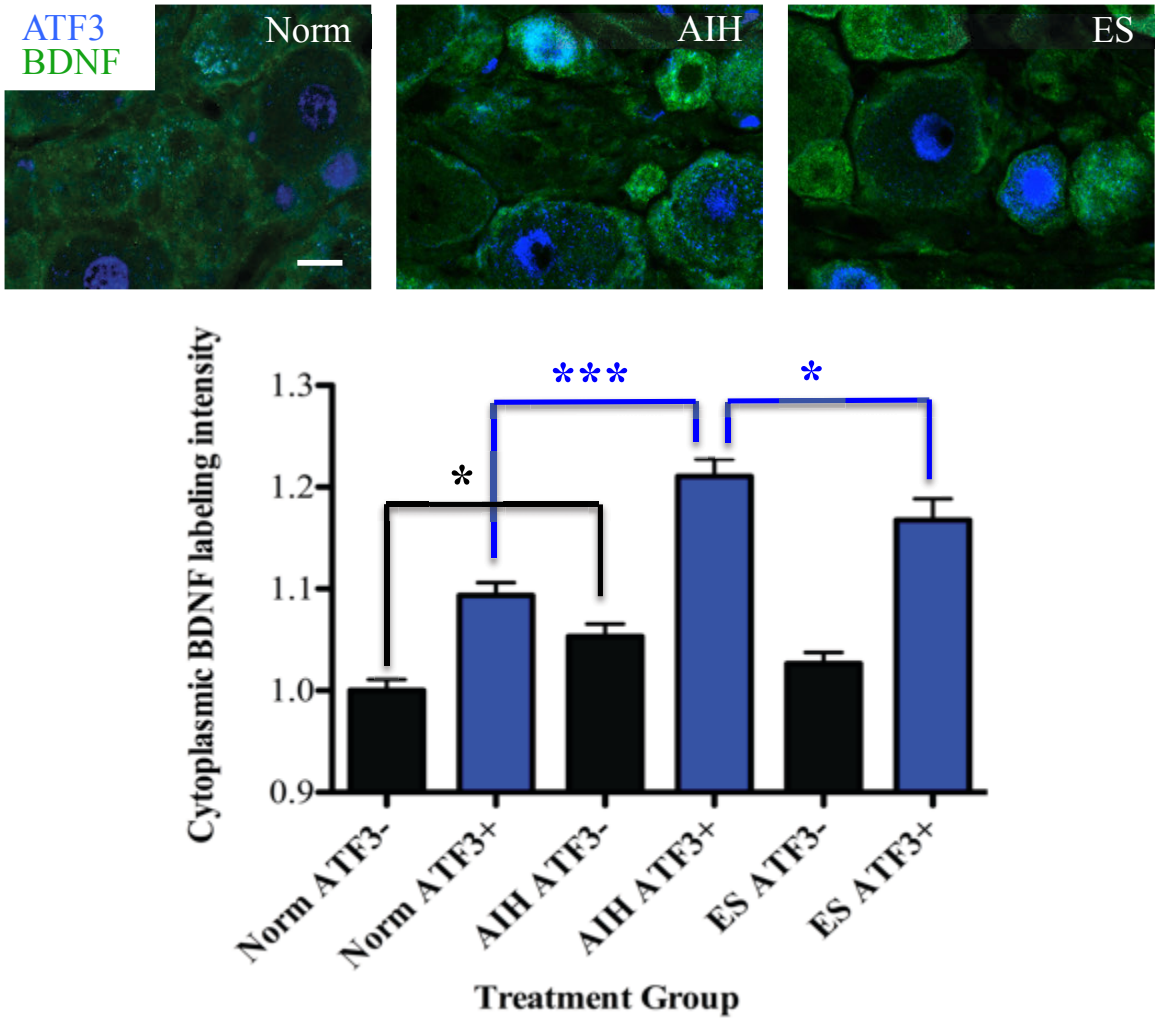

Figure 4.1.2.1 AIH treatment results in increased BDNF protein expression in sensory neurons 3 days post nerve repair. Top: Fluorescence photomicrographs of L4 DRG 10 μm sections processed for dual immunofluorescence to detect cytoplasmic BDNF (green) protein levels in injured ATF3 (blue) positive (ATF3+) or uninjured ATF3 negative (ATF3-) sensory neurons from rats that underwent a tibial nerve repair followed by 2 day normoxia, AIH or 1 hour ES treatment. Note: AIH and ES treatment results in increased expression of BDNF in the cytoplasm of sensory neurons compared to normoxia controls. BDNF is also expressed in the satellite glial cells which appear as semi-lunar structures wrapping the sensory neurons. Scale bar = 20 μm. Bottom: Graph depicts quantification of relative changes in the cytoplasmic immunofluorescence levels for BDNF in sensory neurons with or without ATF3 positive nuclei in L4 DRG from rats treated with either AIH or ES compared to normoxia controls post-tibial nerve repair. The data is normalized to the mean of the sensory neurons from the normoxia treatment group without ATF3 positive nuclei (i.e. uninjured). Asterisks indicate significant differences between experimental groups (Kruskal-Wallis test with Dunn's Multiple Comparison test; * $p<0.05$, ** $p<0.01$, *** $p<0.001$; N = 532-555 total neurons analyzed from 3 animals per treatment group).

BDNF in Sensory Neurons			
Treatment	**Normoxia**	**AIH**	**ES**
Mean immunofluorescence signal intensity ATF3^{+ve} cells	1.09 +/- 0.0130 s.e.m.	1.21 +/- 0.0171 s.e.m.	1.17 +/- 0.0209 s.e.m.
# of cells	277	264	282
# of animals	3	3	3
Significance (p)	-	$p<0.001$	$p<0.05$
Mean immunofluorescence signal intensity ATF3^{-ve} cells	1.00 +/- 0.0109 s.e.m.	1.05 +/- 0.0122 s.e.m.	1.03 +/- 0.0109 s.e.m.
# of cells	266	268	273
# of animals	3	3	3
Significance (p)	-	$p<0.05$	$p>0.05$

Table 4.1.2.1 The cytoplasmic mean labelling intensity in uninjured sensory neurons with ATF3^{-ve} nuclei increased significantly with AIH treatment as normalized to normoxia treatment but did not increase significantly with ES treatment. In the injured ATF3^{+ve} nuclei population of these cells, there was a significant impact of AIH treatment on BDNF expression as the cytoplasmic mean labeling intensity increased as compared to the ES treatment group and the normoxia treatment.

BDNF in Motor Neurons			
Treatment	**Normoxia**	**AIH**	**ES**
Mean immunofluorescence signal intensity ATF3^{+ve} cells	1.04 +/- 0.011 s.e.m.	1.17 +/- 0.0133 s.e.m.	1.27 +/- 0.0207 s.e.m.
# of cells	160	173	204
# of animals	3	3	3
Significance (p)	-	$p<0.001$	$p<0.001$
Mean immunofluorescence signal intensity ATF3^{-ve} cells	1.00 +/- 0.0094 s.e.m.	1.11 +/- 0.0098 s.e.m.	1.22 +/- 0.0193 s.e.m.
# of cells	180	176	206
# of animals	3	3	3
Significance (p)	-	$p<0.001$	$p<0.001$

Table 4.1.2.2 The cytoplasmic mean labelling intensity in uninjured motor neurons with ATF3^{-ve} nuclei with AIH treatment or ES treatment as normalized to normoxia treatment increased significantly. The same relationship was observed in the injured ATF3^{+ve} nuclei population of these cells; the cytoplasmic mean labeling intensity with AIH treatment or ES treatment compared to normoxia treatment also increased significantly.

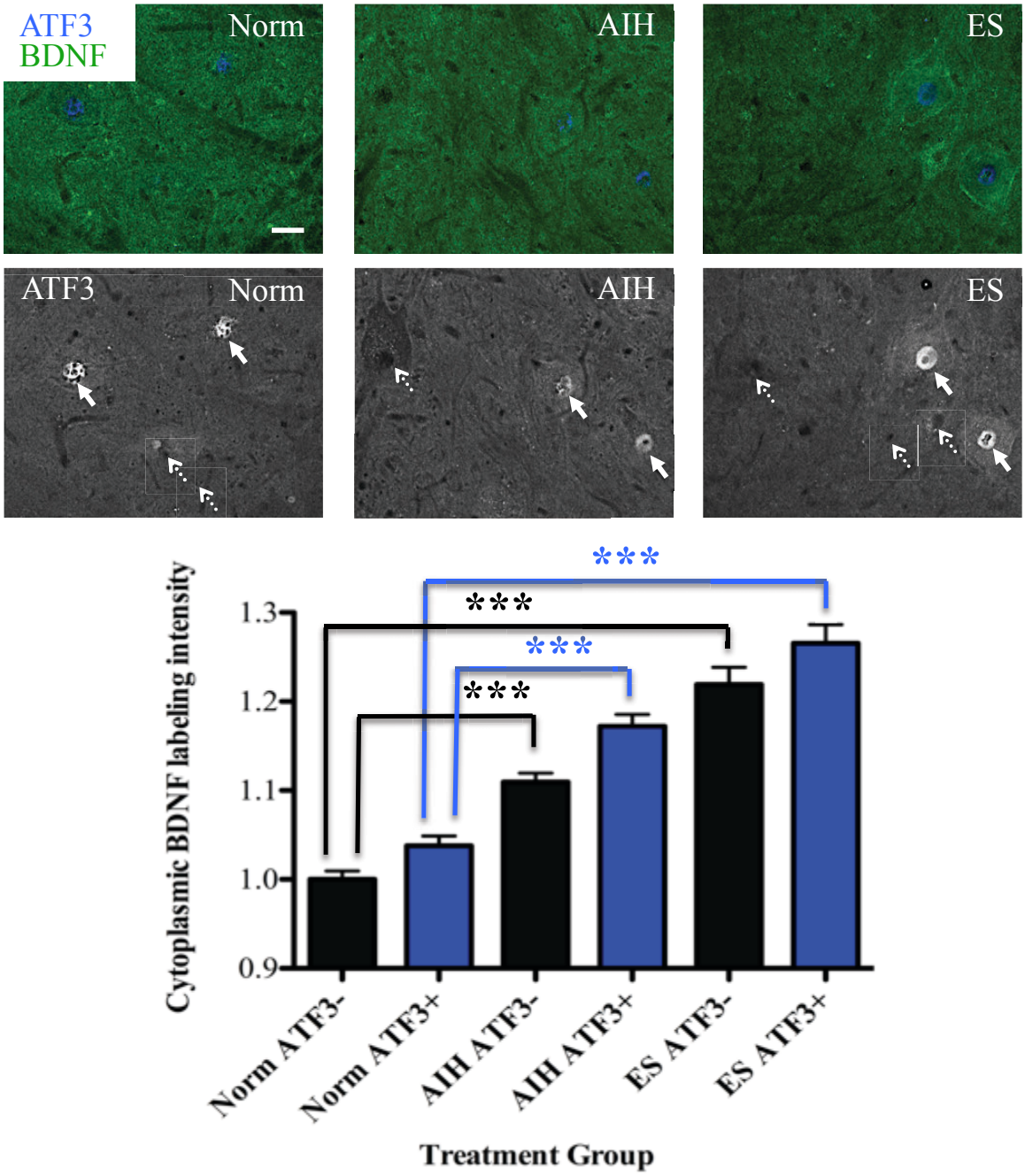

Figure 4.1.2.2 AIH or ES treatment results in increased BDNF protein expression in motor neurons 3 days post nerve repair. Top: Fluorescence photomicrographs of 10 µm lumbar spinal cord sections processed for dual immunofluorescence to detect cytoplasmic BDNF (green) protein levels in injured ATF3 (blue) positive (ATF3+) or uninjured ATF3 negative (ATF3-) motor neurons from rats that underwent tibial nerve repair followed by 2 day normoxia, AIH or 1 hour ES treatment. Arrows identify representative motor neurons with (injured, full arrows) or without (uninjured, dashed arrows) ATF3 positive nuclei. Note: Note: AIH and ES treatment results in increased expression of BDNF in the cytoplasm of injured and uninjured motor neurons as well as

the neuropil compared to normoxia controls. Additionally, as observed in the spinal cord sections processed for GAP43, these sections processed for BDNF show increased expression levels of ATF3 in ES treated injured motor neurons both in the cytoplasm and nucleus compared to AIH and normoxia treatment. Scale bar = 30 μm. Bottom: Graph depicts quantification of relative changes in the cytoplasmic labeling intensity of BDNF in neurons with or without ATF3 positive nuclei in spinal cord from rats treated with either AIH or ES compared to normoxia controls post-tibial nerve repair. The data is normalized to the mean of the motor neurons from the normoxia treatment group without ATF3 positive nuclei (i.e. uninjured). Asterisks indicate significant differences between experimental groups (Kruskal-Wallis test with Dunn's Multiple Comparison test; * $p<0.05$, ** $p<0.01$, *** $p<0.001$; N=340-410 total neurons analyzed from 3 animals per treatment group).

table show the relationship more precisely, with both the ATF3^{+ve} population (injured) and the ATF3^{-ve} population (uninjured) responding to both AIH and ES treatment, compared to normoxia controls. This effect was robust and followed the same pattern irrespective of whether the motor neurons were injured (17% AIH; 27% ES; 4% Norm) or not (11% AIH; 22% ES). This agrees with previously observed increases in BDNF in uninjured motor neurons with AIH treatment (Lovett-Barr et al. 2012, Satriotomo et al. 2012, Baker-Herman et al. 2004, Hassan 2015) or with ES treatment (Al-Majed, Brushart, and Gordon 2000).

4.1.3 Neuronal HIF-1α expression

With AIH treatment, HIF-1α labeling intensity increased in the uninjured ATF3^{-ve} nuclei population and the injured ATF3^{+ve} nuclei population of sensory neurons in the L4 DRG in both the cytoplasm and the nuclei compared to the normoxia treatment group (Figure 4.1.3.1). It appears that there may have been an effect with AIH treatment on expression of HIF-1α in the perineuronal satellite glial cells and the endothelial cells. With ES treatment, it appears that HIF-1α is increased slightly, albeit not as high as the expression level observed with AIH treatment compared to normoxia in both the uninjured ATF3^{-ve} and injured ATF3^{+ve} nuclei sensory neurons in both the cytoplasm and nucleus.

In the L4 region of the spinal cord, the mean immunohistochemical labeling intensity of HIF-1α in the nuclei, as defined by DAPI staining, of the motor neurons of the ATF3^{-ve} populations was significantly increased with either AIH treatment (59%) or ES treatment (64%) compared to normoxia treatment (15%) when normalized to the

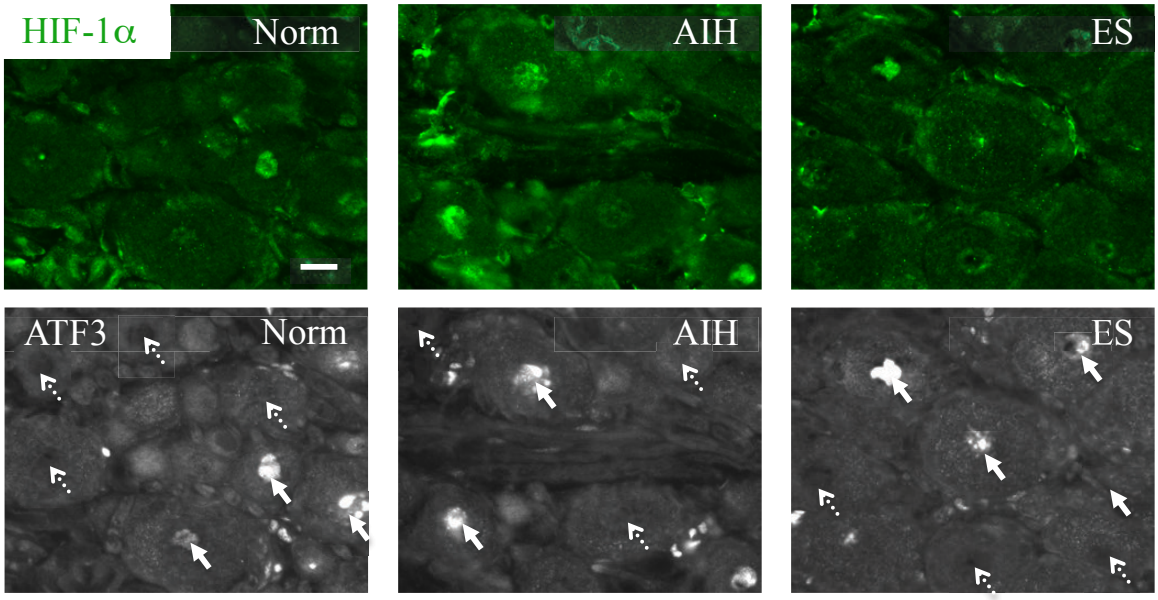

Figure 4.1.3.1 AIH or ES treatment results in increased HIF-1α protein expression in sensory neurons 3 days post nerve repair. Fluorescence photomicrographs of L4 DRG 10 μm sections processed for dual immunofluorescence to detect cytoplasmic and nuclear HIF-1α (green) protein levels in injured ATF3 (white) positive (ATF3+) or uninjured ATF3 negative (ATF3-) sensory neurons from rats that underwent a tibial nerve repair followed by 2 day normoxia (n=3), AIH (n=3) or 1 hour ES treatment (n=3). Arrows identify representative sensory neurons with (injured, full arrows) or without (uninjured, dashed arrows) ATF3 positive nuclei. Note: AIH and ES treatment results in increased expression of HIF-1α in both the cytoplasm and the nucleus compared to normoxia controls in injured and uninjured sensory neurons. Expression of HIF-1α also appears to be increased in the perineuronal satellite glial cells and the endothelial cells in both experimental treatment conditions compared to normoxia controls. Scale bar = 20 μm.

average cytoplasmic HIF-1α expression levels in the ATF3^{-ve} cells in the normoxia treatment group (0%) (Figure 4.1.3.2, Table 4.1.3.2). However, in the cytoplasm of the uninjured motor neurons, only ES treatment (15%) and not AIH treatment (4%), had a significant effect on expression levels compared to normoxia treatment (0%). In the ATF3^{+ve} nuclei motor neuron populations, the results of both treatments were much more pronounced. The mean immunohistochemical labeling intensity in both the cytoplasm and the nuclei of these neurons increased significantly for both AIH treatment (ATF3^{+ve}: 18% cyto, 145% nuc) and ES treatment (ATF3^{+ve}: 24% cyto, 146% nuc) compared to normoxia control treatment (ATF^{+ve}: 4% cyto, 56% nuc). The endothetlial cells, as also observed in the DRG, appeared to have increased expression of HIF-1α with AIH treatment in the spinal cord.

4.1.4 SCG10, GAP43 and BDNF in tibial nerve

The tibial nerve was detached from the sciatic trifurcation and the silastic® tubing was carefully removed to expose the proximal stump of the tibial nerve injury site. The proximal stump was carefully sectioned longitudinally and processed for dual immunofluorescence for the protein of interest (SCG10, GAP43 or BDNF) and βIII tubulin, the latter identifying and being used to demarcate the region of the growing axon front in which the marker of interest immunofluorescence signal intensity was quantified. Further, nerve sections from all three experimental groups were mounted on the same slide to allow processing under identical conditions with pictures used for quantifying alterations in protein expression also taken under identical conditions.

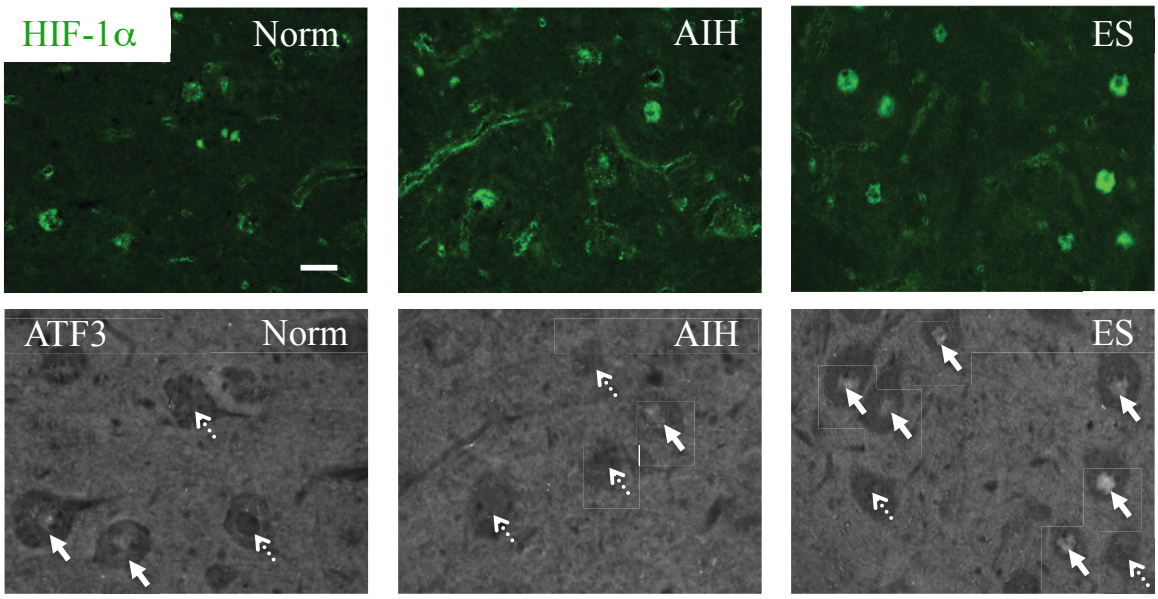
HIF-1α
Norm
AIH
ES
ATF3
Norm
AIH
ES

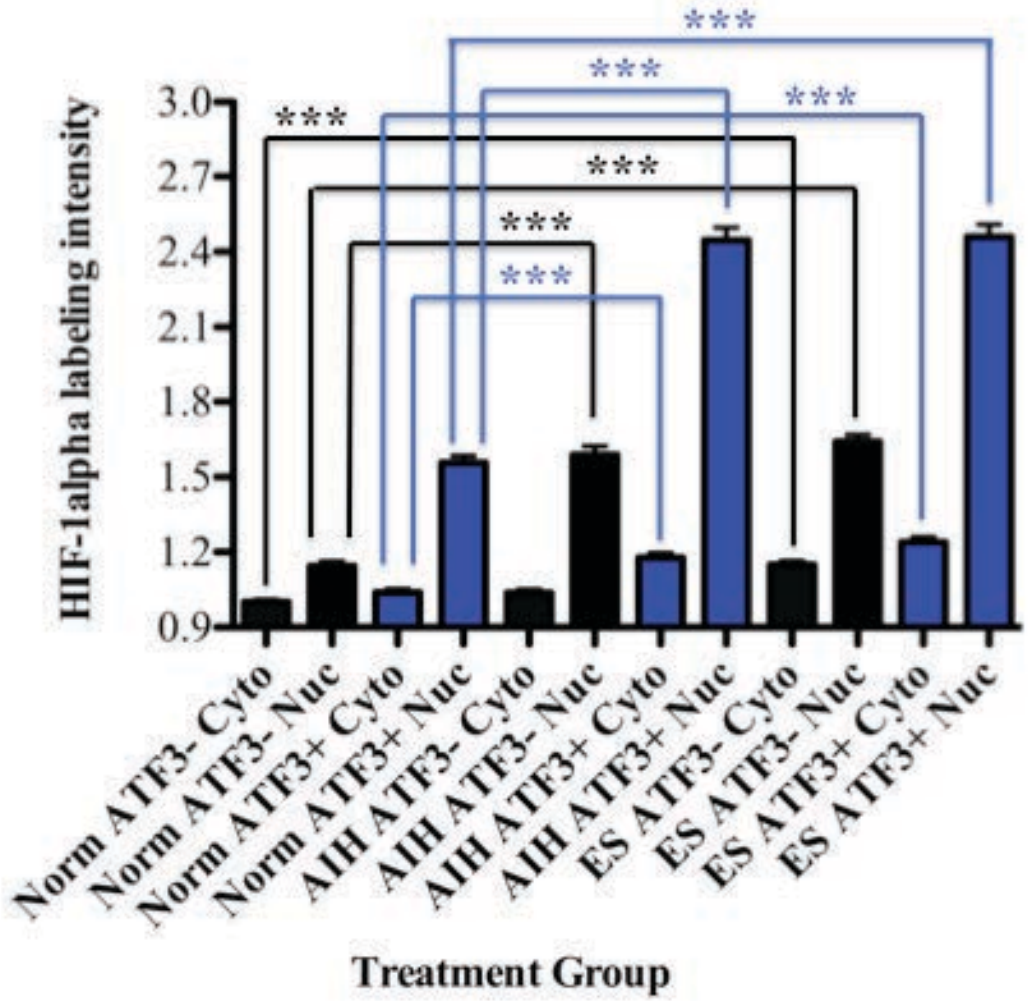
HIF-1alpha labeling intensity
3.0
2.7
2.4
2.1
1.8
1.5
1.2
0.9
***
***
***
***
***
***
Norm ATF3- Cyto
Norm ATF3- Nuc
Norm ATF3+ Cyto
Norm ATF3+ Nuc
AIH ATF3- Cyto
AIH ATF3- Nuc
AIH ATF3+ Cyto
AIH ATF3+ Nuc
ES ATF3- Cyto
ES ATF3- Nuc
ES ATF3+ Cyto
ES ATF3+ Nuc
Treatment Group

Figure 4.1.3.2 AIH and ES treatment results in increased HIF-1α protein expression in motor neurons 3 days post nerve repair. Top: Fluorescence photomicrographs of 10 μm spinal sections processed for dual immunofluorescence to detect cytoplasmic and nuclear HIF-1α (green) protein levels in injured ATF3 (white) positive (ATF3+) or uninjured ATF3 negative (ATF3-) motor neurons from rats that underwent tibial nerve repair followed by 2 day normoxia, AIH or 1 hour ES treatment. Arrows identify representative motor neurons with (injured, full arrows) or without (uninjured, dashed arrows) ATF3 positive nuclei. Note: AIH and ES treatment results in increased expression of HIF-1α in both the cytoplasm and the nucleus compared to normoxia controls in injured motor neurons. AIH treatment results in increased expression of HIF-1α in the nucleus and ES treatment results in increased expression of HIF-1α in both the cytoplasm and the nucleus compared to normoxia controls in uninjured motor neurons. Additionally, a notable increase in expression of HIF-1α is observed in the endothelial cells with AIH treatment, with a slight increase observed with ES treatment compared to normoxia controls. Scale bar = 30 μm. Bottom: Graph depicts quantification of relative changes in the cytoplasmic and nuclear immunofluorescence levels for HIF-1α in motor neurons with or without ATF3 positive nuclei in lumbar spinal cord from rats treated with either AIH or ES and compared to normoxia controls post-tibial nerve repair. The data is normalized to the mean of the motor neurons from the normoxia treatment group without ATF3 positive nuclei (i.e. uninjured). Asterisks indicate significant differences between experimental groups (Kruskal-Wallis test with Dunn's Multiple Comparison test; *$p<0.05$, ** $p<0.01$, *** $p<0.001$; N= 322-387 total neurons analyzed from 3 animal per treatment group).

Cytoplasmic HIF-1α in Motor Neurons			
Treatment	**Normoxia**	**AIH**	**ES**
Mean immunofluorescence signal intensity ATF3^{+ve} cells	1.04 +/- 0.0141 s.e.m.	1.18 +/- 0.0201 s.e.m.	1.24 +/- 0.0210 s.e.m.
# of cells	173	164	165
# of animals	3	3	3
Significance (p)	-	$p<0.001$	$p<0.001$
Mean immunofluorescence signal intensity ATF3^{-ve} cells	1.00 +/- 0.0109 s.e.m.	1.04 +/- 0.0146 s.e.m.	1.15 +/- 0.0159 s.e.m.
# of cells	214	158	175
# of animals	3	3	3
Significance (p)	-	$p>0.05$	$p<0.001$
Nuclear HIF-1α in Motor Neurons			
Treatment	**Normoxia**	**AIH**	**ES**
Mean immunofluorescence signal intensity ATF3^{+ve} cells	1.56 +/- 0.0295 s.e.m.	2.45 +/- 0.0497 s.e.m.	2.46 +/- 0.0484 s.e.m.
# of cells	173	164	165
# of animals	3	3	3
Significance (p)	-	$p<0.001$	$p<0.001$
Mean immunofluorescence signal intensity ATF3^{-ve} cells	1.15 +/- 0.0191 s.e.m.	1.59 +/- 0.0201 s.e.m.	1.64 +/- 0.0286 s.e.m.
# of cells	214	158	175
# of animals	3	3	3
Significance (p)	-	$p<0.001$	$p<0.001$

Table 4.1.3.2 In the L4 region of the spinal cord, the mean immunohistochemical labeling intensity of HIF-1α in the nuclei of the motor neurons of the ATF3^{-ve} populations was significantly increased with either AIH treatment or ES treatment compared to normoxia treatment (Figure 4.1.3.2). However, in the cytoplasm of the motor neurons, only ES treatment, not AIH treatment, had a significant effect on expression levels compared to normoxia treatment. In the ATF3^{+ve} nuclei motor neuron populations, the results of both treatments were much more pronounced. The mean immunohistochemical labeling intensity in both the nucleus and the cytoplasm increased significantly with both AIH treatment and ES treatment compared to normoxia treatment.

Differences between the treatment groups were observed; AIH and ES treatment as normalized to the normoxia control group showed significant increases in levels of GAP43 (16% AIH; 34% ES) and SCG10 (45% AIH; 83% ES) immunofluorescence detected; while for BDNF protein expression ES showed a modest increase in BDNF (8%) immunolabeling intensity, whereas AIH treatment did not (Figure 4.1.4, Table 4.1.4).

Unlike GAP43 and SCG10, BDNF expression was notably dispersed throughout the nerve region proximal to injury and not primarily confined to the growing axon front in both experimental treatment groups, (Figure 4.1.4) raises the possibility of altered retrograde or anterograde axonal transport for this protein, relative to the other two examined.

4.2 Impact of AIH or ES versus normoxia treatment on tibial nerve regeneration

4.2.1 Retrograde labeling of regenerating sensory and motor neurons

The tibial nerve was exposed to 2% FG in saline solution in a Vaseline well, a technique previously used by colleagues for dye uptake (Al-Majed et al. 2000). The topographic distribution of the fluorescent FG positive motor neurons contributing to the tibial nerve was within the upper two thirds of the lateral aspect of the ventral horn of the spinal cord (Figure 4.2.1). There was significant variability (25%) in the total number of FG-labeled motor neurons (1150 +/- 296) indicating that an increase in the size of the mould used for spinal cord sections reduce the likelihood of missing some motor neurons at the most rostral or caudal portions in some animals. Alternatively, processing the spinal cord in two separate sections to be able to increase the length of the spinal cord

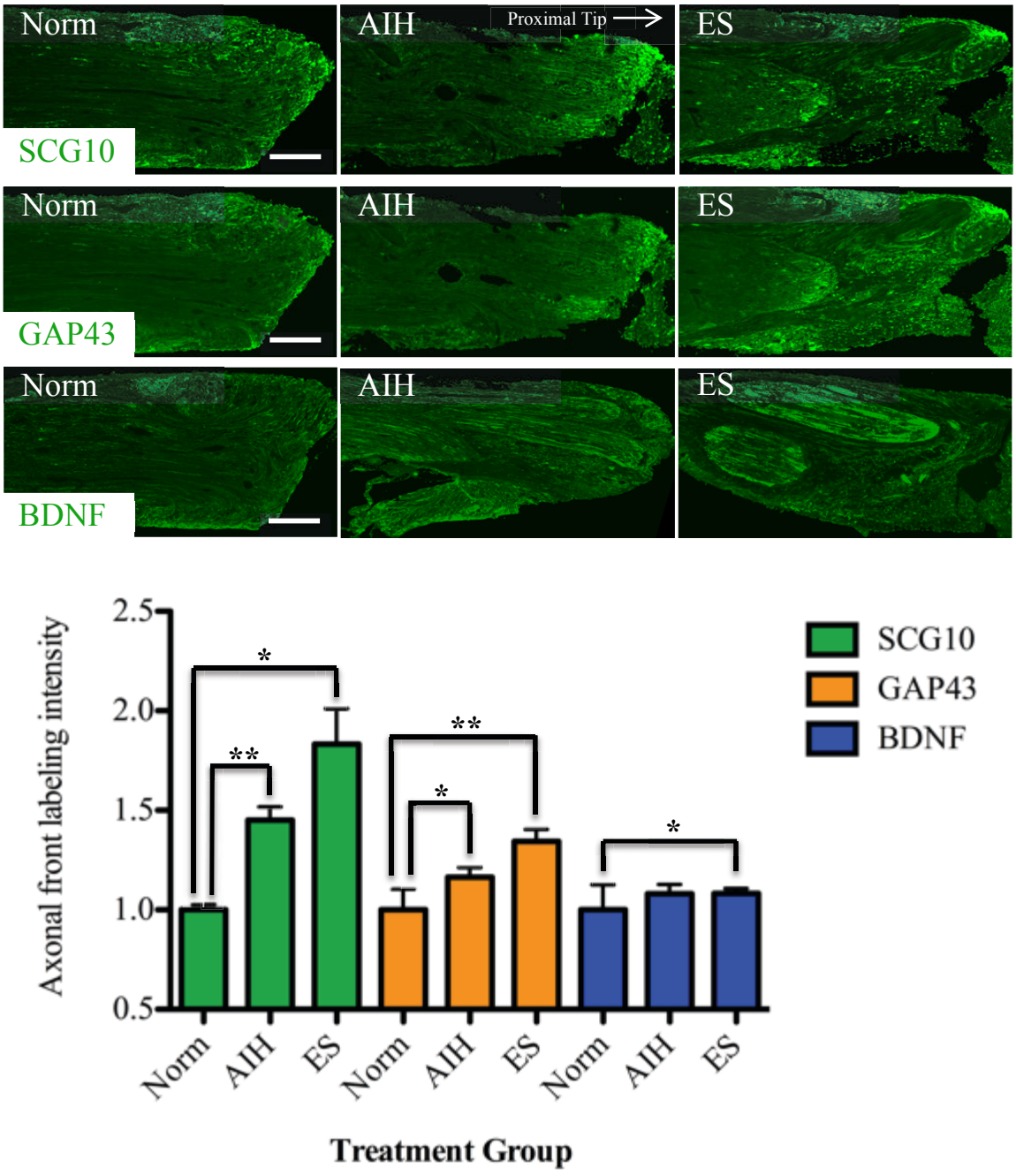

Figure 4.1.4 AIH or ES treatment results in increased SCG10, GAP43 and BDNF protein expression in the tibial nerve proximal tip 3 days post nerve repair. Top: Fluorescence photomicrographs of 10 μm tibial nerve sections processed for dual immunofluorescence to detect SCG10, GAP43 and BDNF (all green) and βIIItubulin (not shown) protein levels in rats that underwent tibial nerve repair followed by 2 day normoxia, AIH or 1 hour ES treatment. This portion of the tibial nerve is encapsulated within the silastic tubing and sutured to the distal stump which may shift or detach during processing. The distal stumps can be observed in some of the AIH and ES photomicrographs above. Note: SCG10 and GAP43 appear more prominent at the

proximal tip. BDNF appears throughout the proximal nerve as well as at the proximal tip. Scale bars = 1 mm Bottom: Graph depicts quantification of relative changes in the axonal immunofluorescence levels at the proximal tip (as identified by an established threshold of increased βIIItubulin labeling) of SCG10, GAP43 and BDNF from rats treated with either AIH or ES and compared to normoxia controls post-tibial nerve repair. The data is normalized to the mean labeling intensity from the normoxia treatment group. Asterisks indicate significant differences between experimental groups (Kruskal-Wallis test with Dunn's Multiple Comparison test; * $p<0.05$, ** $p<0.01$, *** $p<0.001$; N= 4 animals per treatment group).

SCG10 in Proximal Stump			
Treatment	**Normoxia**	**AIH**	**ES**
Mean immunofluorescence signal intensity	1.00 +/- 0.0278 s.e.m.	1.45 +/- 0.0673 s.e.m	1.83 +/- 0.1784 s.e.m.
# of animals	4	4	4
Significance (p)	-	$p<0.01$	$p<0.05$
GAP43 in Proximal Stump			
Treatment	**Normoxia**	**AIH**	**ES**
Mean immunofluorescence signal intensity	1.00 +/- 0.1035 s.e.m.	1.16 +/- 0.0487 s.e.m.	1.34 +/- 0.0596 s.e.m.
# of animals	4	4	4
Significance (p)	-	$p<0.05$	$p<0.01$
BDNF in Proximal Stump			
Treatment	**Normoxia**	**AIH**	**ES**
Mean immunofluorescence signal intensity	1.00 +/- 0.1255 s.e.m.	1.08 +/- 0.0460 s.e.m.	1.08 +/- 0.0238 s.e.m.
# of animals	4	4	4
Significance (p)	-	$p>0.05$	$p<0.05$

Table 4.1.4 The mean immunohistochemical labeling intensity of SCG10 expression with AIH treatment or ES treatment normalized to normoxia treatment increased significantly. The mean labeling intensity of GAP43 expression with AIH treatment or ES treatment normalized to normoxia treatment increased significantly. The mean labeling intensity of BDNF expression with ES treatment normalized to normoxia treatment increased significantly. With AIH treatment, it did not.

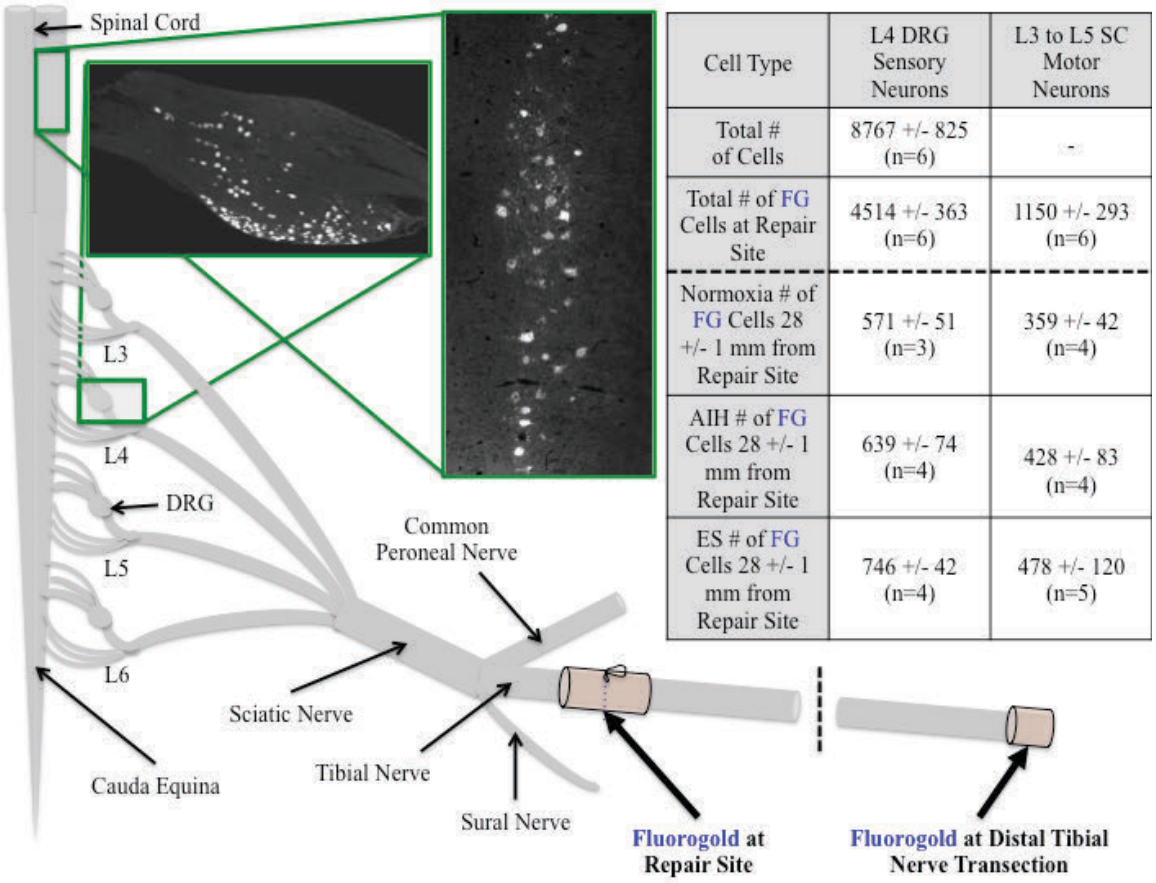

Cell Type	L4 DRG Sensory Neurons	L3 to L5 SC Motor Neurons
Total # of Cells	8767 +/- 825 (n=6)	-
Total # of FG Cells at Repair Site	4514 +/- 363 (n=6)	1150 +/- 293 (n=6)
Normoxia # of FG Cells 28 +/- 1 mm from Repair Site	571 +/- 51 (n=3)	359 +/- 42 (n=4)
AIH # of FG Cells 28 +/- 1 mm from Repair Site	639 +/- 74 (n=4)	428 +/- 83 (n=4)
ES # of FG Cells 28 +/- 1 mm from Repair Site	746 +/- 42 (n=4)	478 +/- 120 (n=5)

Figure 4.2.1 Impact of AIH or ES treatment on numbers of regenerating motor and sensory neurons following tibial nerve repair. Top Left: Fluorescence photomicrographs of 10 μm sections of the right L3 to L5 spinal cord and the right L4 DRG processed for visualization of the FG (white labeled cells) retrograde tracer distribution in rats that underwent tibial nerve repair followed by 2 day normoxia, AIH or 1 hour ES treatment. The tibial nerve was transected and the proximal stump soaked in FG for an hour before it was repaired (n=6) to establish baseline numbers of motor and sensory neurons contributing to the tibial nerve in the L3 to L5 spinal cord and the L4 DRG. The animals were killed 30 days post nerve repair and every 2nd 10 μm section was counted. A second group of animals underwent tibial nerve repair followed by 2 day normoxia (n=4), AIH (n=4) or 1 hour ES treatment (n=5) and at 25 days post-nerve repair, the tibial nerve was transected 28 +/- 1 mm distal from the repair site and the stump was soaked in FG for an hour. The animals were also killed 30 days post nerve repair and every 2nd 10 μm section was counted. Top Right: Table shows the total number of sensory neurons in the L4 DRG, the total number of FG (repair site) labeled motor neurons from the L3 to L5 spinal cord, the total number of FG (repair site) labeled sensory neurons in the L4 DRG, the number of FG labeled regenerated (distal tibial nerve) motor and sensory neurons in animals treated with 2 day normoxia, AIH or 1 hour ES. Note: FG labeled regenerated motor and sensory neurons are not significantly different between treatment groups.

section collected from L2 to L6 is an option. This variability in in the numbers of retrogradely motor neurons neurons was not evident in the sensory neuron counts from L4 DRG examined. The fluorescent FG positive sensory neurons were largely uniformly distributed throughout the ganglia save for the dorsal region and one small lateral portion having very few fluorescent cells (data not shown). Quantification of the FG-labeled cells revealed consistent total number of sensory neurons contributing to the tibial nerve with low variability (4514 +/- 363, 8% variability), also reflected in the low variability observed for the total number (FG labeled and unlabeled) of L4 ganglia sensory neurons (8767 +/- 825, 9% variability) in adult Lewis male rats of the same age and similar weight (average 347 grams +/- 38 grams) (Figure 4.2.1).

For assessment of regeneration at long-term time-points, exposure of the lower tibial nerve to 2% FG in saline solution, the Vaseline well technique was initially attempted. Unfortunately, due to the small size of the nerve and the lack of a position to place the Vaseline well below the level of the nerve to prevent capillary action, the dye ended up being taken up systemically. Therefore, a 4 mm silastic cuff with medical grade silicon glue plug on one end was employed (Elzinga et al. 2015). There was some difficulty isolating all of the collateral sprouting branches of the regenerating tibial nerve as we observed multiple branches arising at the level where the gastrocnemius and soleus muscles begin to transition to the Achilles tendon and as they proceed distally, become deeply intertwined with capillaries branching from the posterior tibial artery. FG dye visualization at the level of the sensory and motor neuron cell bodies when introduced 28 +/ 1 mm from the repair site was low to moderate compared to visualization when introduced at the repair site. Quantification of the FG-labeled motor neurons in the

ventral horn of the L3 to L5 segments of spinal cord revealed that an average 359 +/- 42 (normoxia n=4), 428 +/- 83 (AIH n=4) and 478 +/- 120 motor neurons (ES n=5) axons regenerated a minimum distance of 28 +/- 1 mm distal to the tibial nerve repair site 25 days post-repair. While elevated numbers of regenerating motor neurons were detected in the two treatment groups relative to normoxia controls, they did not reach statistical significance (normoxia n=4; AIH n=4; and ES n=5; Figure 4.2.1). Similarly, the numbers of retrogradely labeled regenerating L4 DRG neurons ipsilateral to lesion were not significantly different, despite also being elevated in the two treatment groups (normoxia 571 +/- 51 n=3; AIH 639 +/- 74 n=4; and ES 746 +/- 42 FG n=4).

4.2.2 Regeneration of tibial nerve axons

One μm semi-thin cross section of the tibial nerve from a 3 mm sample taken at 20 mm from the original repair site (the center or the location of the suture knot on the silastic® tube) or 25 mm from the sciatic trifurcation was photographed and quantified at the light microscopy level from each animal. Despite being taken at the same anatomical distance from the repair site and with no significant variances in weight existing between animals throughout the experiment, the regenerated tibial nerve cross sections revealed 2 ES, 2 Norm and 3 AIH animals had a single fascicled tibial nerve, 2 ES and 2 Norm animals had a bi-fascicular tibial nerve and 1 AIH had a tri-fascicular tibial, all of which were encased in continuous connective tissue (Figure 4.2.2). Initial qualitative observations of the distribution and density of myelinated axons lead us to attempt to do a preliminary quantification and classification. Quantification included heavily myelinated and lightly myelinated axonal profiles. Due to the limitations of light microscopy,

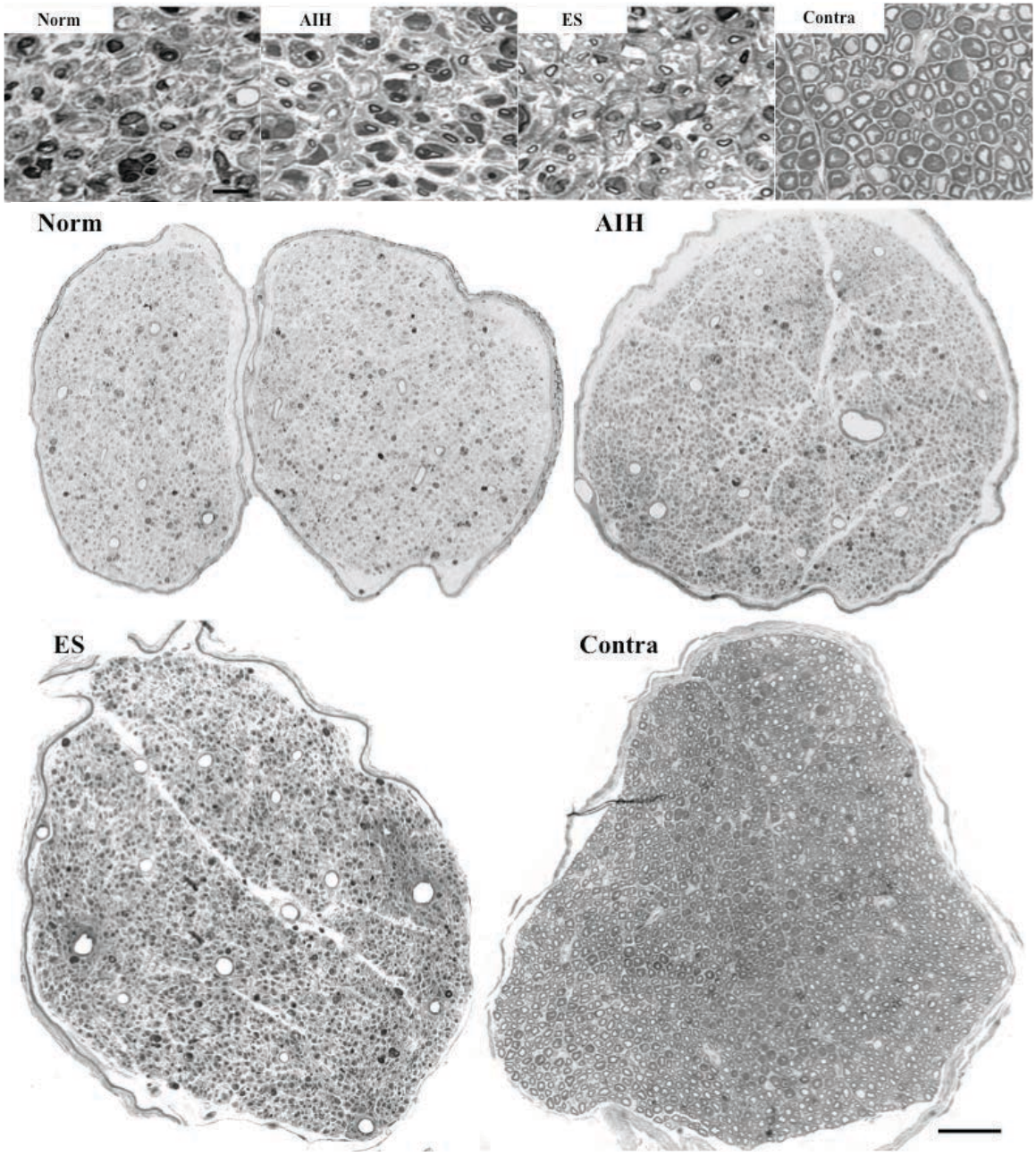

Average # of Tibial Visible Regenerated Myelinated Axons per Animal			
Treatment	Norm (n=4)	AIH (n=4)	ES (n=4)
# of myelinated axons	1684 +/- 81 s.e.m.	2007 +/- 36 s.e.m.	2042 +/- 70 s.e.m.
Significance	-	$p<0.05$	$p<0.01$

Figure 4.2.2 Impact of AIH or ES treatment on numbers of regenerating axonal fibers following tibial nerve repair. Top and Middle: Bright field photomicrographs of transverse 1 μm toluidine blue counterstained semi-thin sections of contralateral or ipsilateral tibial nerve 20 mm from the repair site 25 days following tibial nerve repair in rats that underwent 2 day normoxia, AIH or 1 hour ES treatment with magnified view on the top and the full montage in the middle. Scale bars: 5 and 200 μm respectively. Bottom: Table shows the total number of myelinated axons from the regenerated tibial nerves. Significant differences were observed in the number of myelinated profiles between AIH and Norm treatment groups and between ES and Norm treatment groups. Unmyelinated and very heavily myelinated profiles were not quantified. One 1 μm semi-thin section from each animal was counted in 12 animals total (normoxia n=4, AIH n=4, ES n=4).

unmyelinated axons could not be assessed. Thus, only the total of light and medium myelinated profiles' analyses are shown (Figure 4.2.2) with a significant difference in myelinated profiles between AIH (n=4) compared to Norm (n=4) treatment as well as ES (n=4) compared to Norm (n=4) treatment. It is noted that in order to differentiate the unmyelinated morphological structures from lipid globules or macrophage debris, additional processing with immunofluorescence for neurofilament proteins will need to be done. Furthermore, heavily myelinated profiles appear very similar to degenerating neuronal profiles at the light microscopy level and thus, we were unable to decipher between them for the purpose of this study. We did however quantify them and ES treatment (95 +/- 15) appears to have significantly more heavily myelinated axons or degenerating axon profiles than AIH (37 +/- 3) or Norm (47 +/- 4) treatment groups (Figure 4.2.2). Castro, Negredo, and Avendano (2008) showed that with toluidine blue staining, under a light microscope, certain axonal profiles may appear as heavily myelinated whereas when the same section is viewed at the electron microscopy level, it becomes evident that these are in fact degenerating profiles. Thus, subsequent processing and quantification will need to be done on these nerve cross sections to conclude with any accuracy as to what is happening in regards to heavily myelinated, unmyelinated nerve fibers and degenerating profiles. Further investigation is warranted, but beyond the scope of this thesis.

4.3 Impact of AIH or ES versus normoxia treatment on regeneration- and pain-associated behavioural responses

For the initial two weeks post-surgery, it was challenging to have the rats position their right hind limb down on the testing surface. With a tibial nerve injury, rats typically evert their footpad so that the lateral portion (digits 4 and 5) only contacts the ground with rats guarding it and/or choosing to hop with the other three limbs rather than fully set the right hind limb down. In the cases when some of the rats would not set their right hind limb down on the testing surface (Von Frey and Hargreaves) after a 20 minute period, a treat was given to all the rats from above that required them to stand on their hind limbs and use their forelimbs to retrieve it. Once the treat was consumed, the testing resumed as their hind limbs would remain on the testing surface after they returned to a quadruped position.

The development of neuropathic pain states after a variety of nerve injuries in experimental rats has been shown to be strain specific by numerous researchers (DeLeo and Rutkowski 2000, Wiesenfeld and Hallin 1981, Lee, Chung, and Chung 1997, Herradon et al. 2008). Amongst all of the strains, our experimental strain, the Lewis rat, is seemingly one of the more responsive to neuropathic pain from nerve injuries. Following a priming trigeminal nerve injury, the Lewis strain demonstrated an accelerated development of hind paw mechano-allodynia and mechanohyperalgesia after a sciatic nerve chronic constriction injury compared to the Sprague-Dawley and Sabra strains (Benoliel, Eliav, and Tal 2002). With the same injury, without priming, the Lewis strain has sustained mechanical allodynia for much longer than the Fischer 344 strain of rats (Herradon et al. 2008). Thus, we believe that in addition to being a rat strain that

responds to AIH treatment, it is an ideal strain, due to its heightened sensitivity, to test any possible neuropathic side effect of the AIH treatment.

4.3.1 Thermal hyperalgesia at mid-term

Because of the previously identified impact of BDNF on neuropathic pain states and thermal hyperalgesia (Uchida, Matsushita, and Ueda 2013), it was imperative to determine whether or not the observed AIH- and ES-induced significant increases in BDNF expression levels in peripheral nerves were creating a physiological heightened sensitivity to nociceptive input.

Mid-term thermal hyperalgesia analysis revealed no statistically significant differences between the right hind limbs (injured), the left hind limbs (non-injured) nor one to the other, in tibial nerve repaired animals subjected to normoxia, AIH or ES treatments [N=6 tests x 5 trials per hind limb in 14 animals total (uninjured control n=2, normoxia n=4, AIH n=4, ES n=4); Figure 4.3.1]. Additionally, the anticipated change in withdrawal time of the right hind limb from the infrared heat source immediately post-tibial nerve repair on day 4 was not observed as all animals including the non-injured control animals performed similarly (control: 11.16 sec. +/- 2.50 s.e.m., normoxia: 10.80 +/- 1.86, AIH: 11.76 +/- 2.32 and ES: 8.80 +/- 0.92). It appears that thermal sensory nociceptive input from the footpad is not significantly affected with this tibial nerve injury and repair model. Thermal hyperalgesia testing was repeated in the long-term study to support or discount the phenomenon observed with this study.

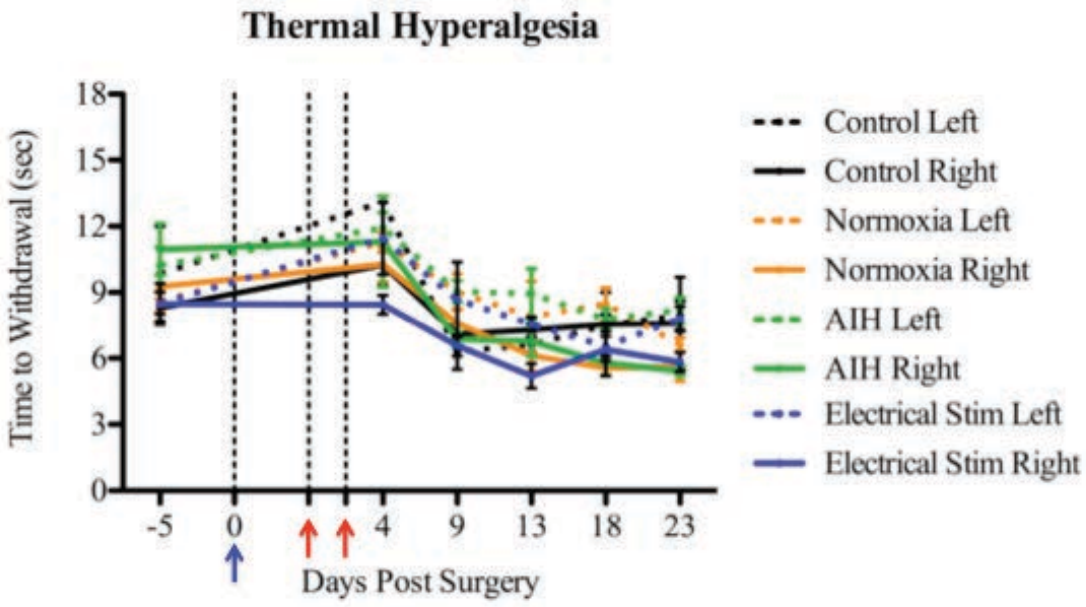

Figure 4.3.1 AIH and ES treatments do not increase thermal hypersensitivity in tibial nerve repaired animals. Graph depicting temporal differences in mean withdrawal time (seconds) tested by Hargreaves infrared apparatus as a function of 2 day normoxia, AIH or 1 hour ES treatment in the right (injured) and the left (uninjured) hind limbs. Tibial nerve transection and repair was performed on Day 0 with one baseline measurement taken during the week prior. ES (blue arrow) was done immediately after tibial repair. AIH or normoxia was administered on days 2 and 3 (red arrows). Note: There were no statistically different withdrawal times between groups during any of the testing time points from baseline to 25 days post-injury (N=6 tests x 5 trials per hind limb in 14 animals total (uninjured control n=2, normoxia n=4, AIH n=4, ES n=4)).

4.3.2 Mechanical hyperalgesia at mid-term

Unlike the thermal hyperalgesia testing results, mechanical hyperalgesia was significantly affected by tibial nerve repair surgery with a decrease in withdrawal pressure observed in the three treatment groups by an average of 20 grams on day 5 compared to baseline (normoxia $p<0.01$, AIH $p<0.0001$, ES $p<0.001$) (Figure 4.3.2). No recovery to baseline withdrawal pressure nor statistically significant differences were observed between the normoxia, AIH or ES treatment groups over the 25 day testing period (N=6 tests x 4 trials per hind limb in 14 animals total (uninjured control n=2, normoxia n=4, AIH n=4, ES n=4)). Therefore, mechanical hyperalgesia was retested during the long-term study to observe whether any mechanical proprioceptive recovery may occur at a later time-point.

4.3.3 Ladder crossing test at mid-term

It was anticipated that AIH might improve horizontal ladder walking ability in peripherally injured Lewis rats as 7 days of AIH has been shown to reduce forelimb footslip errors when administered 4 weeks post-spinal cord injury in the same strain. This recovery was maintained at 1 and 3 weeks after the daily AIH treatments (Lovett-Barr et al. 2012). In the present study, there were no significant differences observed in the mean percentage of correct steps on the horizontal ladder task between the treatment groups at 3 weeks post-injury (N=3 tests per week x 10 crossings in 14 animals total (uninjured control n=2, normoxia n=4, AIH n=4, ES n=4)) (Figure 4.3.3). Immediately after the tibial nerve repair (week 1 day 1), a significant decrease in the correct steps with the right hind limb was observed in the three treatment groups but this margin of error was quickly

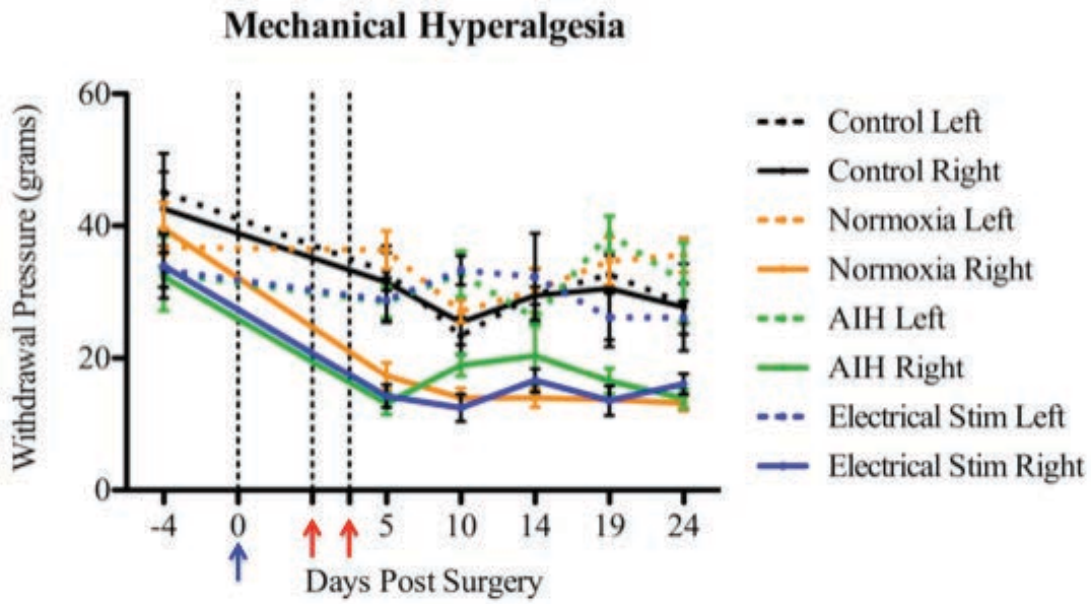

Figure 4.3.2 AIH and ES treatments do not increase mechanical hypersensitivity in tibial nerve repaired animals. Graph depicting temporal differences in mean withdrawal pressure (grams) tested by Von Frey fiber as a function of 2 day normoxia, AIH or 1 hour ES treatment in the right (injured) and the left (uninjured) hind limbs. Tibial nerve transection and repair was performed on Day 0 with one baseline measurement taken during the week prior. ES (blue arrow) was done immediately after tibial repair. AIH or normoxia was administered on days 2 and 3 (red arrows). Note: There were no statistically different withdrawal pressures between groups during any of the testing time points from baseline to 25 days post-injury (N=6 tests x 4 trials per hind limb in 14 animals total (uninjured control n=2, normoxia n=4, AIH n=4, ES n=4)).

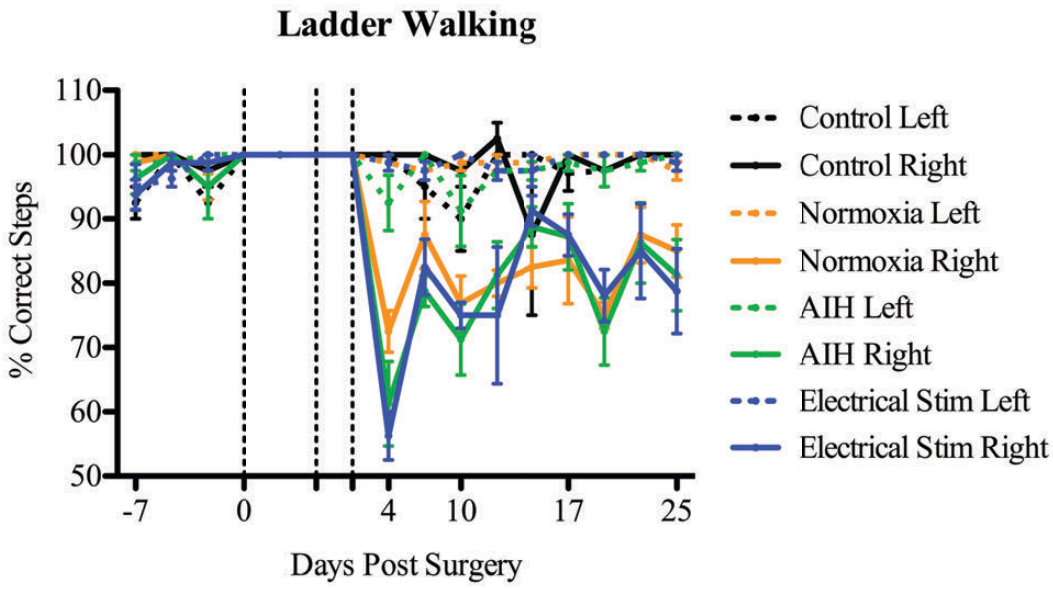

Figure 4.3.3 AIH and ES treatments do not improve the percent correct steps in tibial nerve repaired animals. Graph depicting temporal differences in mean % correct steps on ladder walking as a function of 2 day normoxia, 2 day AIH or 1 hour ES treatment in the right (injured) and the left (uninjured) hind limbs. Tibial nerve transection and repair was performed on Day 0 with three baseline measurements taken during the week prior. ES (blue arrow) was done immediately after tibial repair. AIH or normoxia was administered on days 2 and 3 (red arrows). Note: There were no statistically different percent correct steps between groups during any of the testing time points from baseline to 25 days post-injury (N=3 tests per week x 10 crossings in 14 animals total (uninjured control n=2, normoxia n=4, AIH n=4, ES n=4)).

rectified by 20% the next testing session. All treatment groups demonstrated a similar pattern in the ladder-walking task throughout the 25 days testing session as no significant differences were observed between groups. In the left hind limb, the percentage of correct steps was above 95%. In contrast, with the reduced use of the right hind limb, the rats appeared rather unstable in their forelimb grasps on the horizontal ladder, generating a wide range of correct steps versus incorrect steps with no particular pattern by both forelimbs throughout the 25 days. It is believed that differences in treatments groups in right hind limb performance on the horizontal ladder task may be observed at a later time point.

4.3.4 Walking footprint analysis at mid-term

The magnitude of tibial nerve reinnervation in relation to right hind limb footpad positioning was shown to not be very advanced as only an insignificant slight average improvement was observed in the tibial nerve index function 25 days post injury compared to previous testing sessions (Figure 4.3.4). Despite the minor change in toe spread and footpad positioning, no significant differences of the tibial nerve index function were observed between the two treatment groups, AIH and ES, compared to the normoxia control group (N=3 tests per week x 3 prints per hind limb in 14 animals total (uninjured control n=2, normoxia n=4, AIH n=4, ES n=4)) (Figure 4.3.4). It is believed that with additional time to regenerate of a few weeks, significant differences may be observed. Accordingly, the long-term investigation of 10 weeks was undertaken.

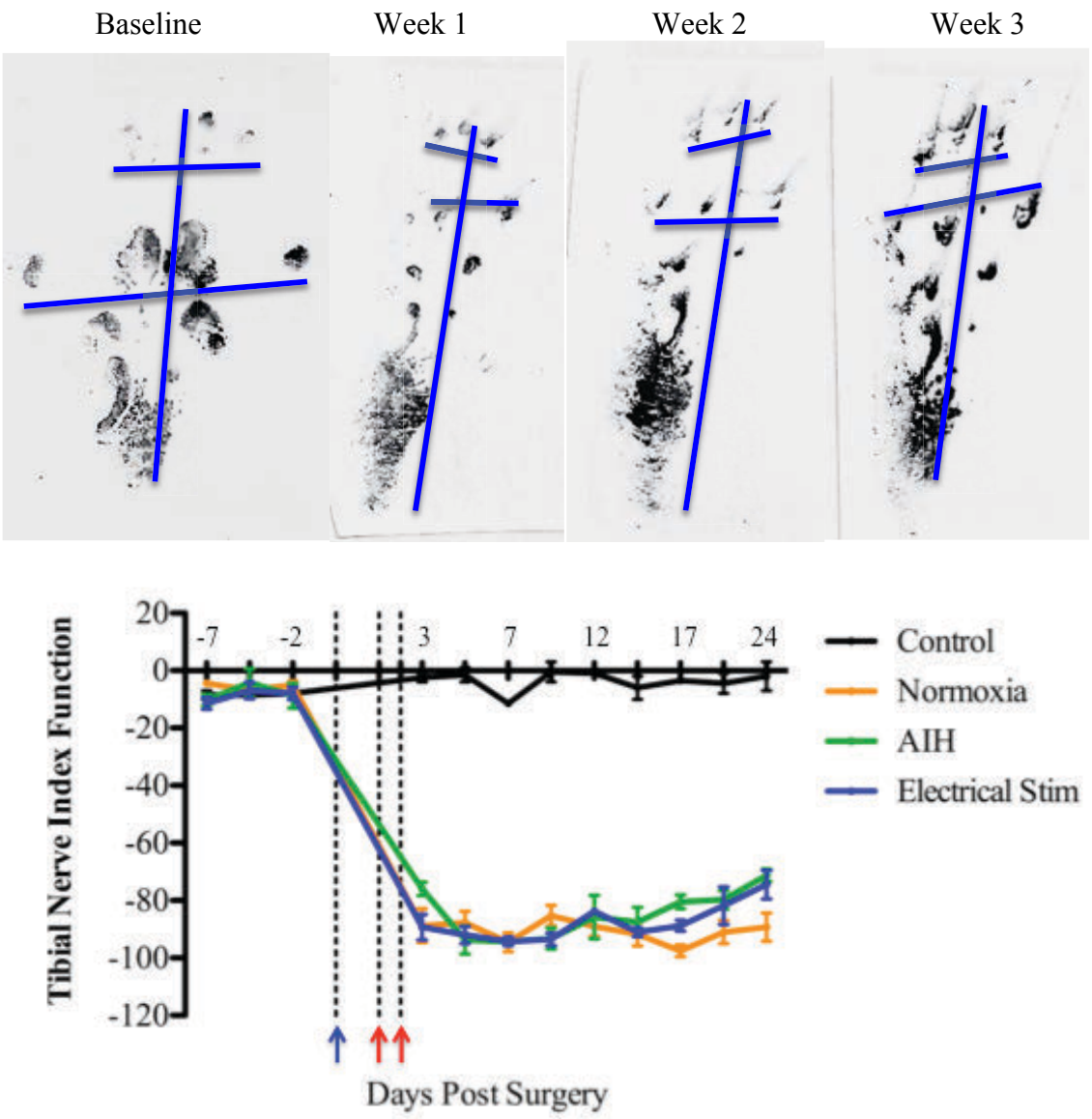

Figure 4.3.4 Impact of AIH or ES treatment on tibial nerve index functional recovery in tibial repaired animals. Top: Representative footprints from ES treatment rats ipsilateral to repair (days post repair as indicated). Blue lines show representative length of print, 1st to 5th toe spread and 2nd to 4th toe spread measurements. Bottom: Graph depicting temporal differences in tibial nerve index function in relation to 2 day normoxia, AIH or 1 hour ES treatment. Tibial nerve transection and repair was performed on Day 0 with three baseline measurements taken during the week prior. ES (blue arrow) was done immediately after tibial repair. AIH or normoxia was administered on days 2 and 3 (red arrows). Note: Three weeks post-injury, the tibial nerve index function for the ES and AIH treatment groups are not significantly different from the normoxia treatment group (N=3 tests per week x 3 prints per hind limb in 14 animals total (uninjured control n=2, normoxia n=4, AIH n=4, ES n=4)).

4.3.5 Thermal hyperalgesia at long-term

The results of the thermal hyperalgesia testing session extended to 10 weeks confirmed the observations from the mid-term study. There were no statistically significant differences in thermal hyperalgesia as indicated by withdrawal times from an infrared Hargreaves heat source between groups during any of the testing time points from injury to ten weeks post-injury (N=1 test per week x 5 trials per hind limb in 18 animals total (uninjured control n=4, normoxia n=5, AIH n=5, ES n=4)) (Figure 4.3.5). However, unlike the mid-term study that showed a slight overall decrease in the withdrawal time between baseline and day 23 of testing, the long-term study showed an overall acclimatization to the testing apparatus as evidenced by the average withdrawal time steadily increasing 1.72 seconds after 3 weeks and 5.57 seconds after 10 weeks from baseline. Immediately after the tibial nerve repair, on week 1, there was a negligible change in withdrawal time, decreasing it an average of 0.46 seconds compared to baseline. Once again, there were no differences observed between the right and left hind limbs in any of the treatment conditions so it appears that the tibial nerve repair model does not affect thermal hyperalgesia.

4.3.6 Mechanical hyperalgesia at long-term

Similar to the mid-term mechanical hyperalgesia testing session, all three treatment groups, normoxia, AIH and ES, showed no significant differences in withdrawal pressure during any of the treatment days over the course of the long-term study (N=1 test per week x 4 trials per hind limb in 18 animals total (uninjured control n=4, normoxia n=5, AIH n=5, ES n=4)) (Figure 4.3.6). Unlike the mid-term results, the

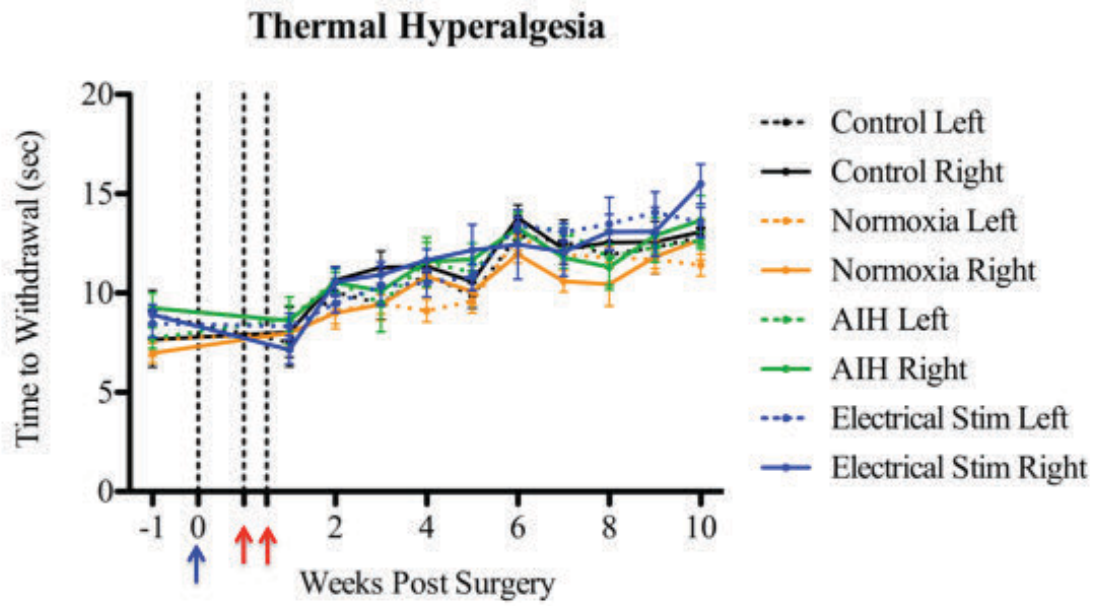

Figure 4.3.5 AIH and ES treatments do not increase thermal hypersensitivity in tibial nerve repaired animals. Graph depicting temporal differences in withdrawal time (seconds) tested by Hargreaves infrared apparatus as a function of 2 day normoxia, AIH or 1 hour ES treatment in the right (injured) and the left (uninjured) hind limbs. Tibial nerve transection and repair was performed on Day 0 with baseline measurements taken during the week prior. ES (blue arrow) was done immediately after tibial repair. AIH or normoxia was administered on days 2 and 3 (red arrows). Note: There were no statistically significant differences in thermal hyperalgesia as indicated by withdrawal times from an infrared Hargreaves heat source between groups during any of the testing time points from injury to ten weeks post-injury (N=1 test per week x 5 trials per hind limb in 18 animals total (uninjured control n=4, normoxia n=5, AIH n=5, ES n=4)). The tibial nerve injury had a small impact on withdrawal time, decreasing it an average of 0.46 seconds compared to baseline on the first week of testing. As time progressed, all treatment groups became further acclimatized to the testing apparatus as evidenced by the average withdrawal time steadily increasing 5.57 seconds from baseline after 10 weeks.

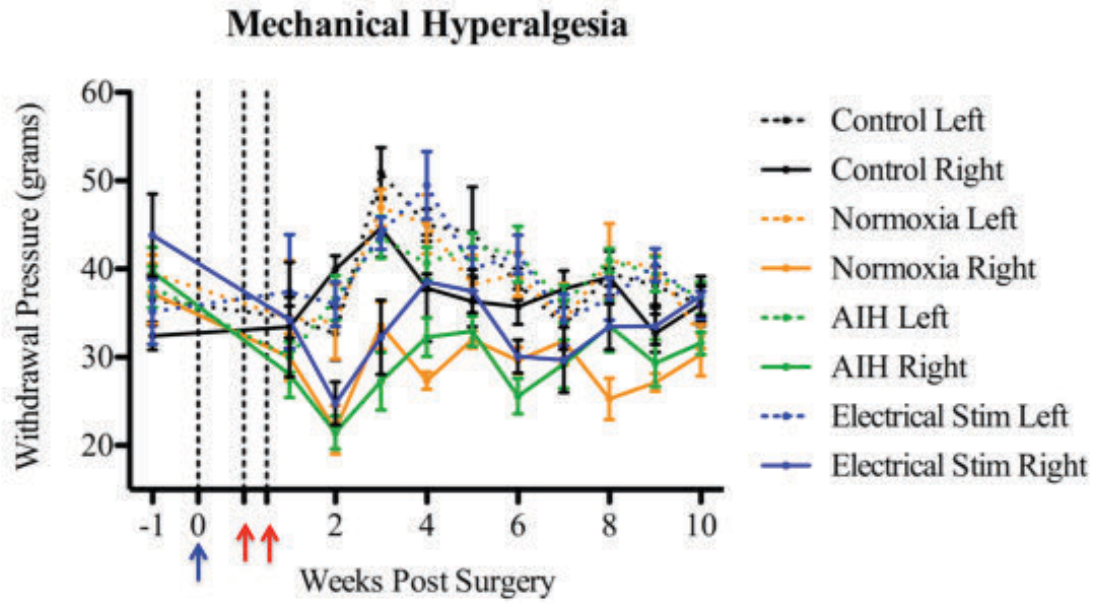

Figure 4.3.6 AIH and ES treatments do not increase mechanical hypersensitivity in tibial nerve repaired animals. Graph depicting temporal differences in withdrawal pressure (grams) tested by Von Frey fiber as a function of 2 day normoxia, AIH or 1 hour ES treatment in the right (injured) and the left (uninjured) hind limbs. Tibial nerve transection and repair was performed on Day 0 with baseline measurements taken during the week prior. ES (blue arrow) was done immediately after tibial repair. AIH or normoxia was administered on days 2 and 3 (red arrows). Note: There were no statistically different withdrawal pressures between groups during any of the testing time points from injury to ten weeks post-injury (N=1 test per week x 4 trials per hind limb in 18 animals total (uninjured control n=4, normoxia n=5, AIH n=5, ES n=4)).

lowest average withdrawal pressure was observed on week 2 after the tibial nerve repair rather than the previously observed week 1. By week 10, the right hind limb withdrawal pressures from the Von Frey fiber do not return to pre-tibial nerve repair levels, remaining lower in all treatment groups.

4.3.7 Ladder crossing test at long-term

Due to the lack of statistically significant differences between the treatment groups on all of the other behavioural tests as well as the mid-term results, only three time-points from this data set were evaluated on the ladder crossing during the long-term study. It was hypothesized that horizontal ladder walking performance may approximate baseline performance after 10 weeks but this proved to not be the case. In addition to not regaining full function, no statistically significant differences were observed between the treatment groups (N=2 tests per week x 10 crossings in 18 animals total (uninjured control n=4, normoxia n=5, AIH n=5, ES n=4)) (Figure 4.3.7). Because of the balancing required to avoid putting the right hind limb fully down with each stride, observations were made, akin to those noted for the mid-term study, that the accuracy of forelimb placement was affected non-specifically over the course of the long-term study.

4.3.8 Walking footprint analysis test at long-term

Following the completion of footprint analysis, it was concluded that footprints were biased in that they were selected for ‘full prints’ where the animal had slowed down its stride and placed its hock more firmly down on the testing track resulting in a less smudged and blurred print. The tibial nerve index includes measurements for the length

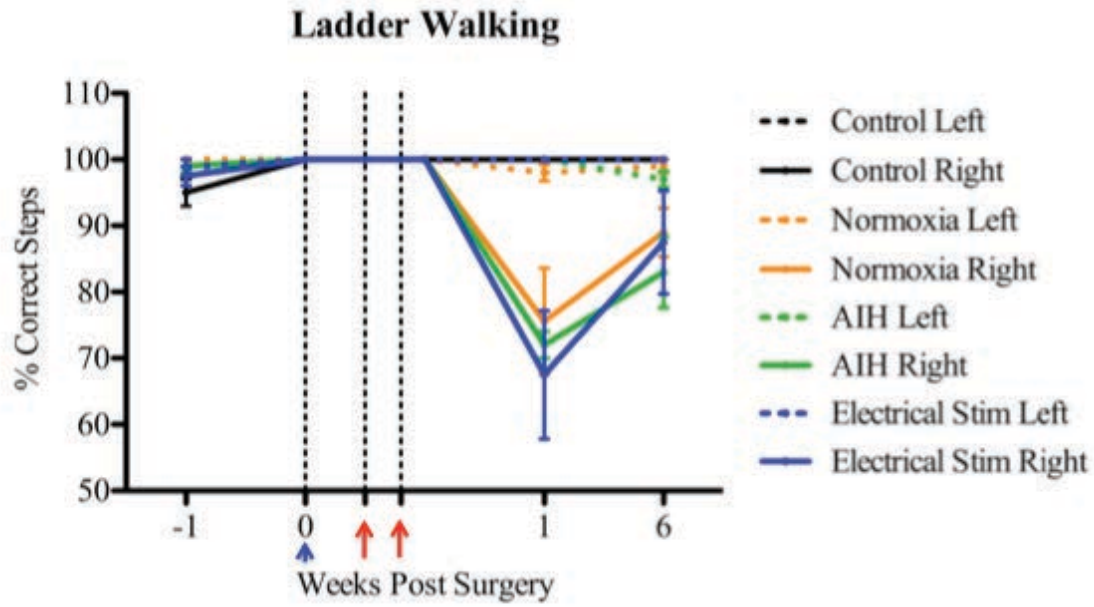

Figure 4.3.7 AIH and ES treatments do not improve the percent correct steps in the hind limbs of tibial nerve repaired animals. Graph depicting temporal differences in % correct steps on ladder walking as a function of 2 day normoxia, AIH or 1 hour ES treatment in the right (injured) and the left (uninjured) hind limbs. Tibial nerve transection and repair was performed on Day 0 with baseline measurements taken during the week prior. ES (blue arrow) was done immediately after tibial repair. AIH or normoxia was administered on days 2 and 3 (red arrows). Note: There were no statistically different percent correct steps between groups during any of the testing time points from injury to 6 weeks post-injury (N=2 tests per week x 10 crossings in 18 animals total (uninjured control n=4, normoxia n=5, AIH n=5, ES n=4)).

of print, length of full toe spread from digits one to five and intermediate toe spread from digits two to four. Thus, for the long-term footprint analysis, the toe spread was used as an indication of regeneration likely due to reinnervation of the tibialis posterior, flexor hallucis longus and the flexor digitorum longus muscles, all contributing to supination of the foot, reversing the pathological pronation of the foot seen with a tibial nerve injury, and possible footpad sensory reinnervation.

Normalized toe spread analysis showed the treatment groups performed similarly until week 5 post-tibial nerve repair (N=2 tests per week x 3 prints per hind limb in 18 animals total (uninjured control n=4, normoxia n=5, AIH n=5, ES n=4) (Figure 4.3.8). From week 5 onwards, the ES treatment group was significantly different from the normoxia treatment group as the difference in toe spread in their hind paws (between their injured right hind paw and their uninjured left hind paw) was significantly reduced except for time-point week 7.5 and week 10.5. At the week 6 and week 7 time points, the AIH treatment group's difference in toe spread was significantly different from the normoxia treatment group ($p<0.001$ and $p<0.05$ respectively). It is of note that it does not appear that any of our treatment groups were trending towards full functional recovery of their right hind paw with not a single time point, even after 10 weeks having less than 7 mm difference in toe spread from left to right when uninjured rats average 1 to 2 mm.

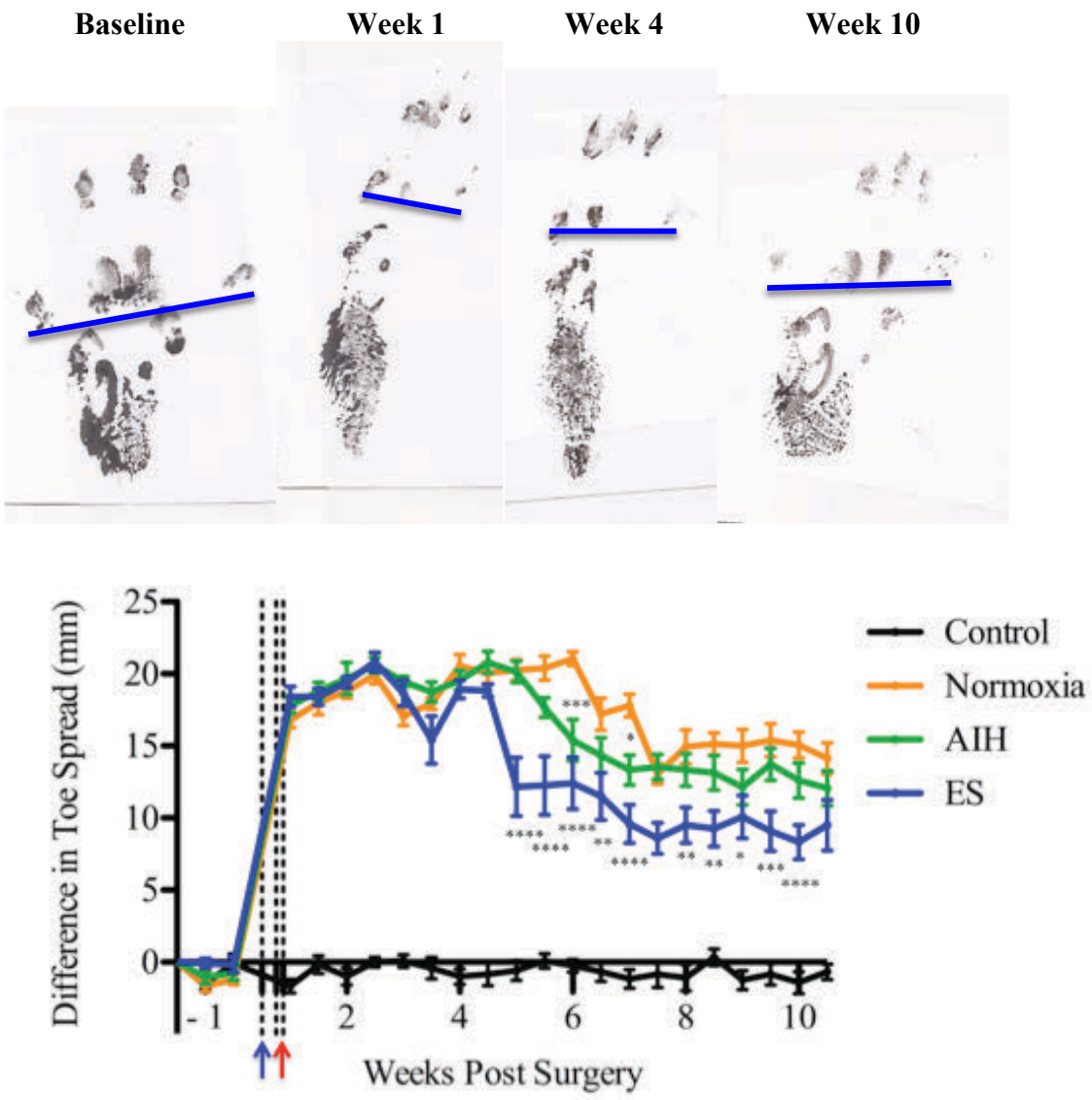

Figure 4.3.8 Impact of AIH or ES treatment on hind limb toe spread functional recovery in tibial repaired animals. Top: Representative footprints from ES treatment rats ipsilateral to repair at days post repair as indicated. Blue lines show representative toe spread measurement. Bottom: Graph depicting temporal differences in toe spread measurement relative to baseline as a function of 2 day normoxia, AIH or 1 hour ES treatment. Tibial nerve transection and repair was performed on Day 0 with baseline measurements taken during the week prior. ES (blue arrow) was done immediately after tibial repair. AIH or normoxia was administered on days 2 and 3 (red arrow). Note: Five weeks post-injury, the toe spread for the ES treatment group was significantly different from the control group with a trend toward significance in the AIH group observed from week 6 on. (Kruskal-Wallis test with Dunn's Multiple Comparison test; * $p<0.05$, ** $p<0.01$, *** $p<0.001$; N=2 tests per week x 3 prints per hind limb in 18 animals total (uninjured control n=4, normoxia n=5, AIH n=5, ES n=4).

5. Discussion

This thesis tested the hypothesis that *AIH will serve as an effective adjunct therapy to promote improved regeneration of surgically repaired peripheral nerves in a manner akin to that observed with brief nerve ES.* The experiments herein addressed the biological, morphological and behavioural affects of AIH or ES treatment compared to control normoxia treatment following a peripheral nerve injury and repair involving the tibial nerve. In the first section, the short-term effects of AIH or ES versus normoxia control treatment on RAGs were assessed and quantified. Next, the regenerative potential induced by these experimental and normoxia control treatments was investigated using retrograde fluorescent tracer to label both the regenerating sensory and motor neurons 25 days after repair 28 mm from the original repair site. Finally, a series of behavioural experiments were conducted for each treatment paradigm on two timelines, 25 days and 10 weeks, to assess the changes in the anatomical positioning of the rats' hind limb when walking, as well as changes in sensory innervation of the footpad in terms of responses to thermal and mechanical stimuli.

5.1 Summary of major findings

The results of this thesis revealed that: 1) 2 days of AIH or 1 hour immediate ES treatment significantly increases RAGs in the repaired peripheral nerve, tibial nerve-associated neuronal cell bodies and in some cases, non-associated neuronal cell bodies in the DRG and spinal cord regions examined; 2) AIH or ES treatment significantly increases the numbers of regenerated myelinated axonal profiles observed 25 days post-injury 20 mm from the repair site; 3) AIH or ES treatment do not elevate neuropathic

pain states associated with the nerve injury and repair, as assessed by mechanical- and thermal- hyperalgesia behavioural tests; 4) AIH or ES treatment promote the reestablishment of toe spread during the stance phase of walking in the recovering hind limb post-repair.

5.2 RAG changes with AIH and ES treatment

The robust changes in RAG expression in response to AIH or ES relative to the normoxia controls were observed 72 hours post-tibial nerve transection and repair (one hour after completion of the 2nd AIH treatment) and included elevated GAP43, BDNF, ATF-3, HIF-1α and SCG10. These alterations were observed in associated sensory and motor neuron cell bodies and in some cases, even in non-associated neurons (i.e. not contributing to the tibial nerve) in the L4 DRG and lumbar spinal cord levels examined. The timeframe of the observed response is consistent with the rapid activation of injury-associated transcription factors and subsequent expression of target regeneration-associated proteins that drive or modulate the repair of the injured axons (reviewed in Raivich 2011) and that were previously reported to be induced in response to ES at the same time-point in our previous studies (Geremia et al. 2007, Al-Majed, Brushart, and Gordon 2000, Al-Majed et al. 2000).

Of the regeneration-associated factors investigated, SCG10 has the most rapid response post-injury. Shin et al. (2012) have reported that levels increase dramatically and selectively in the sensory versus motor axons proximal to injury within an hour following a peripheral nerve transection, and continue to rise until 3 hours post-injury when they plateau, with labeling observed in the central region of individual growth

cones by 5 hours (Shin, Geisler, and DiAntonio 2014). My investigations confirm that SCG10 levels are still elevated 72 hours post-repair, and significantly increased by both treatment modalities, ES and AIH, at the growing axon front. In contrast, we did not observe any discernible SCG10 labeling in the distal tibial nerve stump in 72 hour injured and repaired nerves, consistent with the reported 80% decrease in SCG10 observed only 3 hours post-injury likely due to its selective loss in response to JNK-dependent degradation (Shin et al. 2012). Thus, relative to other markers of axon regeneration which remain fragmented in the distal nerve stump, such as βIII-tubulin or neurofilament (Beirowski et al. 2005), SCG10 cleanly labels the regenerating sensory axon front. Further, as SCG10 is a destabilizing factor linked to efficient axon outgrowth, the dynamic axon state induced by its elevated expression in response to ES and AIH likely benefits regrowth of the injured axons (Morii, Shiraishi-Yamaguchi, and Mori 2006), the former consistent with that previously reported in response to long term potentiation events in hippocampal pathways (Peng, Derrick, and Martinez 2003, 2004).

With a similar time frame of upregulation as SCG10 post-injury, the transcription factor HIF-1α is normally quickly degraded by the ubiquitin-proteasome system in the non-injured cell under conditions of normoxia (at atmospheric oxygen levels), having a half life of only approximately 5 minutes (Salceda and Caro 1997). However, under hypoxic conditions, HIF-1α is activated within the cell, translocated from the cytoplasm to the nucleus where it forms the HIF heterodimer complex protein by binding with HIF-1β which is constitutively expressed (Lando et al. 2002, reviewed in Masoud and Li 2015). HIF-1α plays a crucial role in the initiation of an adaptive response by triggering a cascade of transcriptional gene changes, including energy metabolism, cellular

homeostasis and mitochondrial modulation. Using an exogenously administered probe, hypoxyprobe-1, that allows for the *in vivo* monitoring of hypoxic conditions when oxygen levels are below 10 mmHg (Gross et al. 1995), an area of severe hypoxia was observed to co-localize with axons, macrophages and Schwann cells at the injury site and distally within 2 hours and 3 days later, was also evident distal to the lesion site (Lim et al. 2015). In my doctoral studies, I found that that both AIH and ES treatments elevated expression levels of the transcription factor HIF-1α in spinal cord motor neurons beyond that seen in the peripheral nerve and repair only controls +/- normoxia treatment. Hypoxia has been previously shown to induce expression of HIF-1α in a variety of cell types including spinal motor neurons, sensory neurons, endothelial and Schwann cells (Cho et al. 2015, Yang et al. 2014, Satriotomo et al. 2016, Zhang et al. 2013). While the expression levels of HIF-1α in the DRG with AIH or ES treatment were not quantified, a qualitative increase in expression in the cytoplasm and nucleus of injured and uninjured sensory neurons as well as the endothelial cells was observed with both treatment paradigms. While the mechanisms underlying the observed increased expression was not addressed in this thesis, HIF-1α's transcription rate has been shown to be regulated by various signal transduction pathways including that of Ca^{2+} (Mottet et al. 2003). Thus, it is possible that the elevated levels of intracellular Ca^{2+} generated by ES stimulation were sufficient to upregulate HIF-1α to levels comparable to those seen with AIH treatment (Luo et al. 2014, Cheng et al. 2010). Finally, while this study represents the first to examine the regulation of HIF-1α expression in the regenerating peripheral nerve in response to ES, sciatic nerve stimulation or exercise in combination with 8% oxygen hypoxia have both been associated with rises in HIF-1α protein expression in Western

blot analysis in gastrocnemius muscle, however with hypoxia alone, no upregulation is observed (Tang et al. 2004).

The timeline of activation of the transcription factor ATF3 in sensory and motor neurons is rapid, yet dependent on the distance of the axonal injuries. It is described as either not expressed or weakly expressed in non-injured nerve tissue and it is significantly upregulated post-injury in both humans and rodents (Gey et al. 2016, Tsujino et al. 2000). Unlike c-jun, ATF3 is not induced trans-synaptically and is therefore appreciated as an excellent marker of nerve injury (Tsujino et al. 2000). Three days post-injury, it has been shown that the expression levels of roughly 20-25% of the RAGs modulated by a peripheral nerve injury are dependent on ATF3, as demonstrated in a gene-knockout model which also showed impaired regeneration (Gey et al. 2016). In this study, we observed a qualitative increase in ATF3 expression with AIH and even more so with ES treatment. An increase in NGF post-peripheral nerve injury has been shown to be ATF3 dependent (Gey et al. 2016) with NGF being necessary for the sprouting of nerve fibers (Romero et al. 2000).

Exogenous application of growth factors has been demonstrated to increase peripheral nerve regeneration (Boyd and Gordon 2002, 2003). The therapeutic strategies used in this thesis namely ES or AIH both stimulated endogenous production of BDNF which has been shown to be induced rapidly in sensory neurons post-injury (Karchewski et al. 2002) and has also been shown to be critical for the induction of a regenerative state in sensory and motor neurons (Geremia et al. 2010, Verge 2004). In terms of mechanism, BDNF, has been shown to be upregulated in a serotonin-dependent manner with AIH treatment (Baker-Herman et al. 2004) or speculated to be directly elevated by ES

treatment through the activation of L-type voltage sensitive Ca^{2+} channels of the non-N-methyl-D-aspartate subtype of glutamate receptor (Al-Majed, Brushart, and Gordon 2000).

AIH appeared to have a greater effect on neuronal BDNF expression levels, suggesting that AIH works in conjunction with injury factors elevating expression levels beyond that observed with injury alone. This amplified BDNF expression was most notable in the smaller sensory neuron population (<30 μm diameter), the same size neuron that also expresses higher levels two days post-axotomy, relative to other size ranges of injured neurons (Karchewski et al. 2002). AIH treatment also resulted in more modest increases in BDNF expression in the non-injured ($ATF3^{-ve}$) sensory neuron cell bodies within the same section of the L4 ganglia, whereas ES treatment did not, further supporting a systemic impact of AIH.

Injured motor neurons have been shown to increase expression of BDNF following ES treatment as well (Al-Majed, Brushart, and Gordon 2000). Surprisingly, phrenic motor neurons (C3 to C5) and their surrounding neuropil in proximity to an injury (a C2 spinal cord hemi-section) when treated with daily AIH did not further increase their expression of BDNF beyond that observed with injury alone (81% increase) or daily AIH alone (45% increase) compared to uninjured normoxia treated rats (Lovett-Barr 2008). This is in contrast to our findings as we observed a 6% increase in BDNF expression with AIH treatment in injured lumbar motor neurons compared to their uninjured neighbors.

It is believed that the 2 days of AIH treatment investigated in this thesis is near the minimum threshold of hypoxic cycle exposure needed to induce a significant

regenerative response in the peripheral nervous system, with more prolonged treatment perhaps capable of eliciting an even more beneficial effect. With increased exposure to AIH, such as the Satriotomo et al. (2012) protocol of three days of AIH treatment per week for 10 weeks, there is a significant elevation in the expression of VEGF, HIF-1α, as well as, BDNF, its receptor NTRK2 and the phosphorylated form of the NTRK2 receptor in non-respiratory alpha motor neurons (Satriotomo et al. 2016). A more aggressive protocol with respect to reduced oxygen levels (8%) AIH also elicited an approximate 30% increase in expression levels of nuclear HIF-1α in L4 and L5 DRG compared to normoxia controls Cho et al. (2015). It is important to note that Cho et al. (2015) used the same surgical anesthesia as we did, isoflurane, which has been shown to increase levels of *HIF-1α* and inducible nitric oxide synthase mRNA in hippocampal neurons (Li, Zhu, and Jiang 2008). Only 2% of isoflurane anesthesia administered for 30 min, 24 hours prior to transient cerebral ischemia (stroke) was shown to be neuroprotective (Sun et al. 2015). The neuroprotection preconditioned by isoflurane administration is dependent on nitric oxide synthase (Zhao and Zuo 2004) and upregulates *HIF-1α* mRNA in hippocampal neurons (Li, Zhu, and Jiang 2008). This suggests that the systemic effects of AIH treatment, notably the increased expression of HIF-1α, may be confounded when administered shortly after isoflurane anesthesia, as in Cho et al. (2015).

While these responses are promising and consistent with our observed responses, it is still not known whether a threshold effect exists for sensory neurons relative to motor neurons in this response, as was observed for ES following peripheral nerve repair. One hour ES treatment at time of nerve repair, the same time-frame employed in our current study, has previously been shown to elicit the most optimal regeneration response with

ES treatment duration extending beyond this being less beneficial (Geremia et al. 2007), in contrast with motor neurons where ES durations of one hour all the way up to 2 weeks all elicited an optimal regeneration response (Al-Majed et al. 2000). It remains to be determined whether there is a threshold effect for sensory neurons with respect to AIH treatment of injured peripheral nerves.

Notably, the parameters of our current AIH protocol were influenced by clinical investigations of intermittent hypoxia to date that have shown beneficial physiological effects and utilized cycles with 9-14% hypoxic levels, a low number of cycles lasting 15 sec to 4 min each, and less than an hour of total exposure time per session (reviewed in Mateika et al. 2015, Mateika and Sandhu 2011).

5.3 Peripheral nerve regeneration

There are strain differences in how the motor neurons contributing to the tibial nerve distribute segmentally. Employing a combination of light and electron micrographs of naïve rat tibial nerve, taken just distal to the sciatic trifurcation, it was determined that 1000 motor, 3700 sympathetic, 3500 myelinated and 5400 unmyelinated sensory axons contribute to the tibial nerve of male Wistar rats (Schmalbruch 1986). The tibial nerve motor component was described as distributing to spinal segments L4 to L6. In comparison, the tibial nerve in Lewis rats, distributed within the upper two thirds of the lateral aspect of the ventral horn of the spinal cord from L3 to L5. Further, I identified that a total of 1150 +/- 296 (n=6) FG-labeled motor neurons contribute to the tibial nerve. This is roughly in line with the findings of other researchers, with 1144 +/- 163 motor neurons distributing from L1 to L6 (Yu et al. 2016) and 982 +/- 36 motor neurons from

L3 to L6 (Swett et al. 1986) found to contribute to the tibial nerve of adult female Sprague-Dawley rats. Thus, it appears that adult rats, irrespective of strain, have a total of ~1000 to 1150 motor neurons in the tibial nerve, however their cell body spinal segment distribution may indeed be strain specific.

Schmalbruch (1986) counted a total of 8900 sensory axons in the tibial nerve. We observed the tibial from Lewis rats has the majority of its sensory nerve fibers distributing to the L4 DRG (unpublished findings) with 4514 +/- 363 cell bodies labeled (51% of the total number in the ganglia). Swett et al.'s (1991) extensive sciatic nerve branch analysis concluded that the L4 DRG contained 3234 +/- 1098 contributing to the tibial nerve from both male and female Sprague Dawley rats with wide weight variances (120-510 grams). Thus it appears it is difficult to do cross strain comparisons of numbers of DRG neurons contributing to the tibial nerve, as significant inter strain variability exists (Rigaud et al. 2008). There has also been a study published about the lack of morphological symmetry within individual rats with multiple observed variations of bilateral or unilateral thin nerves forming connections from L3 to L4 or L4 to L3 (Asato et al. 2000).

The tibial nerve, directly after the sciatic trifurcation, but proximal to its branch to the medial gastrocnemius muscle, by our assessment, contains axons from 1150 +/- 293 motor neurons (n=6) and 4514 +/- 363 L4 DRG sensory neurons (n=6). We thus performed a tibial nerve injury repair at this location and 25 days later assessed the number of regenerating neurons contributing axons 28 +/- 1 mm distal to the repair site. This revealed that an average of 359 +/- 42 (Norm), 428 +/- 83 (AIH) and 478 +/- 120 (ES) regenerating motor neurons and an average of 571 +/- 51 (Norm), 639 +/- 74 (AIH)

and 746 +/- 42 (ES) regenerating L4 DRG sensory neurons had regenerated to this point with no significant differences noted between treatment paradigms. It is of note that this location is distal to the tibial nerve branches to the medial gastrocnemius muscle, the lateral gastrocnemius, soleus and plantaris muscles, and the tibialis posterior, flexor halluces longus and the flexor digitorum longus muscles and would therefore contain significantly fewer axons. It should ultimately consist of the axons projecting to the two terminal branches of the tibial nerve: the medial plantar nerve and the lateral plantar nerve. Crockett, Harris, and Egger (1987) reported, in uninjured rats, ~180 motor neuron cell bodies located in caudal L5 and rostral L6 spinal levels contributing to the medial plantar nerve and ~310 motor neuron cell bodies distributed throughout L4 to L6 spinal levels contributing to the lateral plantar nerve. Therefore, this would indicate that roughly 87% +/- 17% of motor neurons regenerated with AIH treatment and 97% +/- 24% with ES treatment, both treatments higher than the 73% +/- 9% motor neurons observed with Norm treatment in our model.

5.4 Impact of AIH and ES treatment on behavioural and functional measures of regeneration

Lewis rats have been shown to have diminished hypothalamic-pituitary-adrenal axis activity and have an increased predisposition to developing autoimmunity and chronic inflammation in comparison with the Fischer 344 strain (Fecho and Valtschanoff 2006). When Lewis rats are subjected to a partial sciatic nerve ligation, they develop profound mechanical hyperalgesia and no thermal hyperalgesia, while the Fischer 344 strain acquired just the opposite, thermal hyperalgesia and no mechanical hyperalgesia.

Thus, our observations of no significant differences between the non-injured and injured hind paws in our Lewis rats with regards to thermal hyperalgesia after a tibial nerve transection for 10 weeks post-repair support Fecho and Valtschanoff (2006) strain-specific findings. Correspondingly, significant differences in mechanical hyperalgesia were observed between the hind paws during both time points, 25 days and 10 weeks post-repair.

Nerve debridement, i.e. excision of a small portion of the proximal nerve stump, is recognized as an additional measure during surgery in humans to support nerve regeneration, especially in circumstances of delayed repair (reviewed in Hammert 2013). Modeled in rats as a conditioning lesion, it consists of damaging the nerve typically with a crush lesion, prior to the subsequent nerve injury. When assessed for its regenerative potential, a conditioning lesion has been shown to improve foot print spread as measured by sciatic functional index at 13 days compared to 18 days in non-conditioned rats (Bisby 1985). Rats that had a conditioning lesion to the tibial nerve also had a significant long-term reduction in hypersensitivity to thermal and mechanical stimuli compared to their non-injured hind paws (Moalem-Taylor et al. 2011). A conditioning lesion performed 3 days prior to a nerve crush recently highlighted the role of HIF-1α as a transcriptional regulator, activating the pro-regenerative program, showing a 2 fold increase in axon regeneration (Cho et al. 2015). In our model, no conditioning lesion or nerve debridement was employed at the time of coaptation, as it was performed immediately following transection, a situation that does not exist in a clinical setting. This however permitted the quantification of functional outcomes associated with AIH or ES treatment unencumbered by the decrease or increase in regeneration potential seen in clinical

settings due to a number of varying factors including delay of repair, surrounding necrotic tissue, nerve debridement, regeneration distance as well as increased nerve tension among many others.

We not only saw no significant differences in performance on the ladder crossing test between treatment groups by 10 weeks post-tibial nerve repair, but none fully recovered to baseline accuracy. The rats were observed attempting to avoid putting the right hind limb fully down when crossing, non-specifically affecting the accuracy of the placement of their forelimbs while balancing accordingly. An irregular pattern of ladder peg placement has been used previously for hind limb mobility assessment (Kemp et al. 2010, Metz and Whishaw 2002) whereby the pegs are spaced between 1 to 5 cm from one another and the sequence is switched between each testing session. No behavioural improvement was seen until week 3 onward in the experimental groups compared to the negative control group (Kemp et al. 2010). It is believed that the additional spacing between the pegs and the variability in peg placement would have proven more challenging to the tibial injured rats in this study, such that variations in performance may have been more readily observed.

With ES treatment, we observed a significant partial recovery of the toe spread from week 5 onward relative to normoxia treated rats and with AIH, at the week 6 and week 7 time-points, possibly due to reinnervation of the tibialis posterior, flexor hallucis longus and the flexor digitorum longus muscles, all contributing to supination of the foot, reversing the pathological pronation of the foot seen with a tibial nerve injury. Lewis rats with a tibial nerve repair significantly recover toe spread from 4 to 24 weeks, however they don't fully recuperate; remaining significantly different from non-injured controls

during all assessments from 2 to 24 weeks (Hare 1993). These muscles and the tibial nerve branches that innervate them are distal to the tibial nerve branches for the gastrocnemius, plantaris and soleus muscles that allow the rat to lift its hock, a kinematic variable that decreases print length and is affected by the velocity of the rat. Gait, stance duration and stride length are all factors altered by changes in a rat's locomotion velocity (reviewed in Kemp, Cederna, and Midha 2017). Moradzadeh et al. (2008) also observed significant improvements at week 6 and week 7 in Lewis rats with a tibial nerve transection repaired with an acellular motor nerve graft compared to an acellular sensory nerve graft. However this was measured by a decrease in print length, not an increase in toe spread, potentially identifying when reinnervation of the more proximal gastrocnemius, plantaris and soleus muscles occurred, allowing the rat to effectively lift its hock post-surgery. Significant recovery of print length in Lewis rats occurs from 4 to 24 weeks post-tibial nerve repair with maximal recovery reported to be at 16 weeks (Hare 1993). This supports findings of ES treatment by Pockett and Gavin (1985) that showed with 1 Hz for 15 min to an hour, rats regained their toe spread reflex more quickly, from 10.4 +/- 1.7 days without ES to 4.14 +/- 1.6 days with ES, after a sciatic nerve crush. Additionally, ES treatment has been compared to and combined with treadmill training as a therapy for peripheral nerve injuries in animals and shown to enhance the number of regenerating axon profiles in an androgen receptor-dependent manner (Thompson, Sengelaub, and English 2014). Gordon and Borschel (2016) have recently stated that "both ES and exercise are promising experimental treatments for peripheral nerve injury that seem to be ready to be translated to clinical use". Thus there are a plethora of exciting possibilities to potentially improve peripheral nerve regeneration: ES could be

paired with surgery if performed, AIH could be administered as an inpatient or outpatient therapy and specific exercise could be included in rehabilitation protocols.

5.5 Clinical relevance

The findings in my thesis support the potential for AIH and ES treatment as viable therapies in supporting the regeneration of peripheral nerve injuries. We are aware that our treatment protocol of ES administered at the time of nerve repair, which in our case occurs immediately after a peripheral nerve injury, is not a clinically feasible timeline. However, at the clinical level, ES treatment has already shown to accelerate axonal regeneration when administered immediately following carpal tunnel release (Gordon et al. 2010, Gordon, Brushart, and Chan 2008). When applied to the proximal stump of an injured nerve and immediately repaired nerve, it enhances the regeneration of both sensory and motor neurons as well as their regrowth specificity (Geremia et al. 2007, Al-Majed et al. 2000, Brushart et al. 2005). If treatment is further delayed, it has been shown, in animals, that ES remains a worthwhile treatment modality, increasing the numbers of both motor and sensory neurons when administered at the time of a peripheral direct nerve-to-nerve repair, three months after the initial injury (Elzinga et al. 2015). Thus, ES should be considered therapeutically pertinent to administer immediately following a peripheral nerve repair, whether it is days or months after the initial injury. Beyond direct nerve stimulation, stimulation of target tissue such as muscle is also being explored (Willand et al. 2016, Willand et al. 2015).

AIH is also seemingly ready for the same bench to bedside transition, as a novel therapy for peripheral nerve injuries. Its affect on the central nervous system is currently

being investigated in long-term clinical trials in patients with partial spinal cord injuries (Clinical Trials Gov. #NCT02274116 and #NCT03071393) with promising initial findings. Additionally, 15 cycles of 90 second hypoxic episodes of 9% oxygen alternated with normoxic 21% oxygen (total time per treatment of 45 min) as a non-severe 5 times/first week followed by 3 times/week for 3 weeks treatment protocol in humans has been demonstrated to not elicit any visual or verbal memory impairment during or after (Navarrete-Opazo et al. 2016). Our studies further support this translation to the clinical level of investigation with data demonstrating no deleterious effects on thermal or mechanical sensation of rat footpads. Notably, a new clinical trial is also examining sensory function in healthy adult humans with AIH (Clinical Trials Gov. #NCT03283072). Similar to the studies in animals describing outcomes with delayed ES treatment, our research group investigated AIH treatment administered 4 weeks after a partial spinal cord injury in a rat (Prosser-Loose et al. 2015). It was shown to improve forelimb function when combined with task training. After the successful completion of the clinical trials, it is fair to conclude that clinical inquiries into AIH's effect on the peripheral nervous system should be the next logical step in establishing its potential as a non-invasive alternative to ES treatment for peripheral nerve injuries. Finally, due to the systemic impacts of AIH, it is possible that the positive combinatorial impacts of ES and hypoxia on muscle responses associated with favorable repair described in Tang et al. (2004) and AIH on neuronal responses (current thesis; Cho et al. 2015), work in combination to promote the favorable impacts of AIH observed in this thesis on nerve regeneration. In support of the potential for manipulation of both neuronal and target tissue to promote peripheral nerve regeneration outcomes, it has recently been shown that

electrical muscle stimulation (Willand et al. 2015) and electrical nerve stimulation (reviewed in Gordon, Eva, and Borschel 2015) can both improve motor neuron regeneration, thus opening the avenue toward exploring combinatorial ES treatments.

In the course of our experiments supporting a promising potential for AIH in enhancing nerve repair, we also gained insight into the biological variability in physiological response to AIH treatment, which indicates that not all people may respond in an equivalent manner to AIH. We observed no discernible alteration in the RAG response in initial studies of 1 or 2 day AIH performed on the Wistar strain of rat, a strain commonly used in the Verge lab to study nerve repair and the impact of ES. Thus, we switched to the Lewis strain of rat used by Dr. Muir's group, due to their consistent response to AIH treatment following central nervous system injuries and their calm disposition for behavioural work. Prominent research groups in the field of AIH primarily use an in-house Sprague Dawley strain and the Lewis strain of rats (Baker-Herman et al. 2010, Lovett-Barr et al. 2012). Different inbred rat strains including Brown-Norway, Fischer, Lewis and Piebald-viral-Glaxo, showed differences in phrenic LTF responses with AIH (Golder et al. 2005). In humans, following AIH treatment, there appear to not be any sex differences in the observed increased magnitude of LTF minute ventilation, but depression of parasympathetic activity and increases in sympathovagal balance compared to baseline were found to be significantly different in men, but not women (Wadhwa et al. 2008). Some age, sex and hormone differences in the development of LTF after AIH have also been reported in rats (Zabka, Behan, and Mitchell 2001b, a, Zabka, Mitchell, and Behan 2006). Thus, careful documentation of phenotypic response, the potential variability in short-term and long-term effects, to AIH in future clinical trials

will help to establish dose parameters based on age, sex and hormone levels among other health markers.

5.6 Conclusions and future directions

In conclusion, we have shown that AIH mirrors many of the beneficial effects of electrical nerve stimulation on peripheral nerve repair outcomes, highlighting its potential for clinical translation as a non-invasive means to effect better regeneration of the injured peripheral nerve.

AIH and ES treatment increased the expression of RAGs and showed some significant changes in regenerative capacity in a tibial nerve injury repair animal model. It has been argued that regeneration of the tibial nerve is difficult to assess in terms of the neuromuscular system as it innervates a large range of muscles having multiple functions in the hind limb (reviewed in Gordon and Borschel 2016). Thus, other clinically relevant peripheral nerve pathology models such as entrapment of the median nerve within the carpal tunnel, the ulnar nerve in the post-condylar groove or the sciatic nerve within the piriformis muscle could further elucidate the potential benefits of AIH and ES in fine motor movement and gross limb function.

Analysis of the motor neurons and sensory neurons as well as their axons that contribute to the regenerating tibial nerve 25 days after a tibial nerve repair provided insightful preliminary data on the potential reinnervation of the medial and plantar nerves and should be replicated to increase the total number of animals. FG was introduced 28 +/- 1 mm from the repair site, which lies approximately 5 mm proximal to the bifurcation of the medial and lateral plantar nerves. The tibial nerve contributes the majority of the

innervation of the rat hind limb footpad via the medial and lateral plantar nerves. Limitations were observed in the footpad measurements presented given the decreased prints lengths erroneously selected for analysis. With further food reward encouragement, as rats increase their pace, they lift their hock thus decreasing their print length. This testing parameter modification could potentially provide future data for the early reinnervation of the gastrocnemius, plantaris and soleus muscles separate from the toe spread data we collected that more accurately represents the possible distal reinnervation of the tibialis posterior, flexor hallucis longus and the flexor digitorum longus muscles which all contribute to supination of the foot. In addition to future footprint analysis, collection and sectioning of the footpad could provide information regarding reinnervation. With respect to this, the regenerating nerve fiber types could be visualized with an ankyrin-b antibody, as Aβ and all of the cutaneous mechanoreceptor fibers including hair follicle receptors and Meissner and Pacinian corpuscles as well as Aδ and C fibers, express ankyrin-β at the axon terminals (Engelhardt et al. 2013). Thus, skin reinnervation could potentially be quantified in a spatial manner, proximal to distal. In addition to the suggested footprint analysis modifications and collecting supplementary sensory reinnervation data from the footpads, regenerative outcomes in the motor component of this model could also be further analysed with respect to quantifying re-established neuromuscular junctions, muscle fiber size and muscle weights, as in Jonsson et al. (2013).

An AIH protocol with more than 2 days of treatment should be examined to see if it further increases the demonstrated benefits on peripheral nerve regeneration to a level rivaling that seen with the more invasive ES treatment protocol, thereby making it a

viable treatment option. Repair strategies employed in this thesis could also be combined with those of Willand et al. (2015), which demonstrate an enhanced regenerative capacity in response to ES of target muscle. In this instance, the hypothesis to be tested would be that AIH coupled with ES of the nerve at the time of repair and ES of the target muscle would further improve functional outcomes after a peripheral nerve injury. Finally, the increasing numbers of clinical trials involving other nervous system pathologies speak to the promise of AIH as a therapeutic intervention and support the need for further research examining its potential in peripheral nerve repair. Current AIH-based clinical trials examine systemic inflammation and brain function imaging (Clinical Trials Gov.#NCT03453697), circulating progenitor cells and cognitive functioning in patients with traumatic brain injuries (#NCT02083445) and functional recovery in patients with partial spinal cord injuries (#NCT01272336, #NCT01272349, #NCT02274116, #NCT03071393, #NCT02973438, #NCT03433599, #NCT03262766).

6. References

Al-Majed, A. A., T. M. Brushart, and T. Gordon. 2000. "Electrical stimulation accelerates and increases expression of BDNF and trkB mRNA in regenerating rat femoral motoneurons." *Eur J Neurosci* 12 (12):4381-90. doi: ejn1341 [pii].

Al-Majed, A. A., C. M. Neumann, T. M. Brushart, and T. Gordon. 2000. "Brief electrical stimulation promotes the speed and accuracy of motor axonal regeneration." *J Neurosci* 20 (7):2602-8.

Artico, M., L. Cervoni, F. Nucci, and R. Giuffre. 1996. "Birthday of peripheral nervous system surgery: the contribution of Gabriele Ferrara (1543-1627)." *Neurosurgery* 39 (2):380-2; discussion 382-3.

Asato, F., M. Butler, H. Blomberg, and T. Gordh. 2000. "Variation in rat sciatic nerve anatomy: implications for a rat model of neuropathic pain." *J Peripher Nerv Syst* 5 (1):19-21.

Astorino, T. A., E. T. Harness, and A. C. White. 2015. "Efficacy of Acute Intermittent Hypoxia on Physical Function and Health Status in Humans with Spinal Cord Injury: A Brief Review." *Neural Plast* 2015:409625. doi: 10.1155/2015/409625.

Bach, K. B., and G. S. Mitchell. 1996. "Hypoxia-induced long-term facilitation of respiratory activity is serotonin dependent." *Respir Physiol* 104 (2-3):251-60.

Badia, J., A. Pascual-Font, M. Vivo, E. Udina, and X. Navarro. 2010. "Topographical distribution of motor fascicles in the sciatic-tibial nerve of the rat." *Muscle Nerve* 42 (2):192-201. doi: 10.1002/mus.21652.

Bain, J. R., S. E. Mackinnon, and D. A. Hunter. 1989. "Functional evaluation of complete sciatic, peroneal, and posterior tibial nerve lesions in the rat." *Plast Reconstr Surg* 83 (1):129-38.

Baker, T. L., D. D. Fuller, A. G. Zabka, and G. S. Mitchell. 2001. "Respiratory plasticity: differential actions of continuous and episodic hypoxia and hypercapnia." *Respir Physiol* 129 (1-2):25-35. doi: S0034568701002808 [pii].

Baker, T. L., and G. S. Mitchell. 2000. "Episodic but not continuous hypoxia elicits long-term facilitation of phrenic motor output in rats." *J Physiol* 529 Pt 1:215-9.

Baker-Herman, T. L., R. W. Bavis, J. M. Dahlberg, A. Z. Mitchell, J. E. Wilkerson, F. J. Golder, P. M. Macfarlane, J. J. Watters, M. Behan, and G. S. Mitchell. 2010. "Differential expression of respiratory long-term facilitation among inbred rat strains." *Respir Physiol Neurobiol* 170 (3):260-7. doi: 10.1016/j.resp.2009.12.008.

Baker-Herman, T. L., D. D. Fuller, R. W. Bavis, A. G. Zabka, F. J. Golder, N. J. Doperalski, R. A. Johnson, J. J. Watters, and G. S. Mitchell. 2004. "BDNF is necessary and sufficient for spinal respiratory plasticity following intermittent hypoxia." *Nat Neurosci* 7 (1):48-55. doi: 10.1038/nn1166.

Baker-Herman, T. L., and G. S. Mitchell. 2002. "Phrenic long-term facilitation requires spinal serotonin receptor activation and protein synthesis." *J Neurosci* 22 (14):6239-46. doi: 20026595
22/14/6239 [pii].

Baloh, R. H., H. Enomoto, E. M. Johnson, Jr., and J. Milbrandt. 2000. "The GDNF family ligands and receptors - implications for neural development." *Curr Opin Neurobiol* 10 (1):103-10.

Battiston, B., I. Papalia, P. Tos, and S. Geuna. 2009. "Chapter 1: Peripheral nerve repair and regeneration research: a historical note." *Int Rev Neurobiol* 87:1-7. doi: 10.1016/S0074-7742(09)87001-3.

Batty, N. J., K. K. Fenrich, and K. Fouad. 2017. "The role of cAMP and its downstream targets in neurite growth in the adult nervous system." *Neurosci Lett* 652:56-63. doi: 10.1016/j.neulet.2016.12.033.

Beirowski, B., R. Adalbert, D. Wagner, D. S. Grumme, K. Addicks, R. R. Ribchester, and M. P. Coleman. 2005. "The progressive nature of Wallerian degeneration in wild-type and slow Wallerian degeneration (WldS) nerves." *BMC Neurosci* 6:6. doi: 10.1186/1471-2202-6-6.

Bennett, D. L., G. J. Michael, N. Ramachandran, J. B. Munson, S. Averill, Q. Yan, S. B. McMahon, and J. V. Priestley. 1998. "A distinct subgroup of small DRG cells express GDNF receptor components and GDNF is protective for these neurons after nerve injury." *J Neurosci* 18 (8):3059-72.

Benoliel, R., E. Eliav, and M. Tal. 2002. "Strain-dependent modification of neuropathic pain behaviour in the rat hindpaw by a priming painful trigeminal nerve injury." *Pain* 97 (3):203-12.

Berger, S., and L. Lavie. 2011. "Endothelial progenitor cells in cardiovascular disease and hypoxia--potential implications to obstructive sleep apnea." *Transl Res* 158 (1):1-13. doi: 10.1016/j.trsl.2010.12.008.

Bisby, M. A. 1985. "Enhancement of the conditioning lesion effect in rat sciatic motor axons after superimposition of conditioning and test lesions." *Exp Neurol* 90 (2):385-94.

Blumenfeld, H. 2011. *Neuroanatomy through Clinical Cases with ebook*: Sinauer.

Bomze, H. M., K. R. Bulsara, B. J. Iskandar, P. Caroni, and J. H. Skene. 2001. "Spinal axon regeneration evoked by replacing two growth cone proteins in adult neurons." *Nat Neurosci* 4 (1):38-43. doi: 10.1038/82881.

Boyd, J. G., and T. Gordon. 2002. "A dose-dependent facilitation and inhibition of peripheral nerve regeneration by brain-derived neurotrophic factor." *Eur J Neurosci* 15 (4):613-26.

Boyd, J. G., and T. Gordon. 2003. "Glial cell line-derived neurotrophic factor and brain-derived neurotrophic factor sustain the axonal regeneration of chronically axotomized motoneurons in vivo." *Exp Neurol* 183 (2):610-9.

Boyer, R. B., K. W. Sexton, C. L. Rodriguez-Feo, R. Nookala, A. C. Pollins, N. L. Cardwell, K. Y. Tisdale, L. B. Nanney, R. B. Shack, and W. P. Thayer. 2015. "Adjuvant neurotrophic factors in peripheral nerve repair with chondroitin sulfate proteoglycan-reduced acellular nerve allografts." *J Surg Res* 193 (2):969-77. doi: 10.1016/j.jss.2014.09.023.

Brushart, T. M., J. Gerber, P. Kessens, Y. G. Chen, and R. M. Royall. 1998. "Contributions of pathway and neuron to preferential motor reinnervation." *J Neurosci* 18 (21):8674-81.

Brushart, T. M., R. Jari, V. Verge, C. Rohde, and T. Gordon. 2005. "Electrical stimulation restores the specificity of sensory axon regeneration." *Exp Neurol* 194 (1):221-9. doi: S0014-4886(05)00077-4 [pii]
10.1016/j.expneurol.2005.02.007.
Brushart, T. M., and M. M. Mesulam. 1980. "Alteration in connections between muscle and anterior horn motoneurons after peripheral nerve repair." *Science* 208 (4444):603-5.
Burchiel, K. J. 1984. "Spontaneous impulse generation in normal and denervated dorsal root ganglia: sensitivity to alpha-adrenergic stimulation and hypoxia." *Exp Neurol* 85 (2):257-72.
Castro, J., P. Negredo, and C. Avendano. 2008. "Fiber composition of the rat sciatic nerve and its modification during regeneration through a sieve electrode." *Brain Res* 1190:65-77. doi: 10.1016/j.brainres.2007.11.028.
Chakrabarty, A.S., Chakrabarty, K. 2006. *Fundamentals of Respiratory Physiology*. New Delhi, India: I.K. International Publishing House Pvt. Ltd.
Chan, J. R., J. M. Cosgaya, Y. J. Wu, and E. M. Shooter. 2001. "Neurotrophins are key mediators of the myelination program in the peripheral nervous system." *Proc Natl Acad Sci U S A* 98 (25):14661-8. doi: 10.1073/pnas.251543398
251543398 [pii].
Cheng, L. Z., N. Lu, Y. Q. Zhang, and Z. Q. Zhao. 2010. "Ryanodine receptors contribute to the induction of nociceptive input-evoked long-term potentiation in the rat spinal cord slice." *Mol Pain* 6:1. doi: 10.1186/1744-8069-6-1.
Cho, Y., J. E. Shin, E. E. Ewan, Y. M. Oh, W. Pita-Thomas, and V. Cavalli. 2015. "Activating Injury-Responsive Genes with Hypoxia Enhances Axon Regeneration through Neuronal HIF-1alpha." *Neuron* 88 (4):720-34. doi: 10.1016/j.neuron.2015.09.050.
Chong, M. S., M. Fitzgerald, J. Winter, M. Hu-Tsai, P. C. Emson, U. Wiese, and C. J. Woolf. 1992. "GAP-43 mRNA in Rat Spinal Cord and Dorsal Root Ganglia Neurons: Developmental Changes and Re-expression Following Peripheral Nerve Injury." *Eur J Neurosci* 4 (10):883-95.
Cosgaya, J. M., J. R. Chan, and E. M. Shooter. 2002. "The neurotrophin receptor p75NTR as a positive modulator of myelination." *Science* 298 (5596):1245-8. doi: 10.1126/science.1076595
298/5596/1245 [pii].
Coull, J. A., S. Beggs, D. Boudreau, D. Boivin, M. Tsuda, K. Inoue, C. Gravel, M. W. Salter, and Y. De Koninck. 2005. "BDNF from microglia causes the shift in neuronal anion gradient underlying neuropathic pain." *Nature* 438 (7070):1017-21. doi: nature04223 [pii]
10.1038/nature04223.
Crockett, D. P., S. L. Harris, and M. D. Egger. 1987. "Plantar motoneuron columns in the rat." *J Comp Neurol* 265 (1):109-18. doi: 10.1002/cne.902650108.
Crowley, C., S. D. Spencer, M. C. Nishimura, K. S. Chen, S. Pitts-Meek, M. P. Armanini, L. H. Ling, S. B. McMahon, D. L. Shelton, A. D. Levinson, and et al. 1994. "Mice lacking nerve growth factor display perinatal loss of sensory and sympathetic neurons yet develop basal forebrain cholinergic neurons." *Cell* 76 (6):1001-11. doi: 0092-8674(94)90378-6 [pii].

Dale, E. A., F. Ben Mabrouk, and G. S. Mitchell. 2014. "Unexpected benefits of intermittent hypoxia: enhanced respiratory and nonrespiratory motor function." *Physiology (Bethesda)* 29 (1):39-48. doi: 10.1152/physiol.00012.2013.

Dale-Nagle, E. A., M. S. Hoffman, P. M. MacFarlane, I. Satriotomo, M. R. Lovett-Barr, S. Vinit, and G. S. Mitchell. 2010. "Spinal plasticity following intermittent hypoxia: implications for spinal injury." *Ann N Y Acad Sci* 1198:252-9. doi: 10.1111/j.1749-6632.2010.05499.x

NYAS5499 [pii].

Daroff, R.B., J. Jankovic, J.C. Mazziotta, and S.L. Pomeroy. 2015. *Bradley's Neurology in Clinical Practice E-Book*: Elsevier Health Sciences.

DeLeo, J. A., and M. D. Rutkowski. 2000. "Gender differences in rat neuropathic pain sensitivity is dependent on strain." *Neurosci Lett* 282 (3):197-9.

Devor, M., R. Govrin-Lippmann, I. Frank, and P. Raber. 1985. "Proliferation of primary sensory neurons in adult rat dorsal root ganglion and the kinetics of retrograde cell loss after sciatic nerve section." *Somatosens Res* 3 (2):139-67.

Djouhri, L., R. Newton, S. R. Levinson, C. M. Berry, B. Carruthers, and S. N. Lawson. 2003. "Sensory and electrophysiological properties of guinea-pig sensory neurones expressing Nav 1.7 (PN1) Na+ channel alpha subunit protein." *J Physiol* 546 (Pt 2):565-76. doi: PHY_026559 [pii].

Elzinga, K., N. Tyreman, A. Ladak, B. Savaryn, J. Olson, and T. Gordon. 2015. "Brief electrical stimulation improves nerve regeneration after delayed repair in Sprague Dawley rats." *Exp Neurol* 269:142-53. doi: 10.1016/j.expneurol.2015.03.022.

Engelhardt, M., S. Vorwald, J. M. Sobotzik, V. Bennett, and C. Schultz. 2013. "Ankyrin-B structurally defines terminal microdomains of peripheral somatosensory axons." *Brain Struct Funct* 218 (4):1005-16. doi: 10.1007/s00429-012-0443-0.

Fang, X., L. Djouhri, J. A. Black, S. D. Dib-Hajj, S. G. Waxman, and S. N. Lawson. 2002. "The presence and role of the tetrodotoxin-resistant sodium channel Na(v)1.9 (NaN) in nociceptive primary afferent neurons." *J Neurosci* 22 (17):7425-33. doi: 22/17/7425 [pii].

Fecho, K., and J. G. Valtschanoff. 2006. "Acute inflammatory and neuropathic pain in Lewis and Fischer rats." *J Neuroendocrinol* 18 (7):504-13. doi: 10.1111/j.1365-2826.2006.01442.x.

Franz, C. K., B. Singh, J. A. Martinez, D. W. Zochodne, and R. Midha. 2013. "Brief transvertebral electrical stimulation of the spinal cord improves the specificity of femoral nerve reinnervation." *Neurorehabil Neural Repair* 27 (3):260-8. doi: 10.1177/1545968312461717.

Fu, S. Y., and T. Gordon. 1995. "Contributing factors to poor functional recovery after delayed nerve repair: prolonged axotomy." *J Neurosci* 15 (5 Pt 2):3876-85.

Fu, S. Y., and T. Gordon. 1997. "The cellular and molecular basis of peripheral nerve regeneration." *Mol Neurobiol* 14 (1-2):67-116. doi: 10.1007/BF02740621.

Fuller, D. D., K. B. Bach, T. L. Baker, R. Kinkead, and G. S. Mitchell. 2000. "Long term facilitation of phrenic motor output." *Respir Physiol* 121 (2-3):135-46.

Fuller, D. D., S. M. Johnson, E. B. Olson, Jr., and G. S. Mitchell. 2003. "Synaptic pathways to phrenic motoneurons are enhanced by chronic intermittent hypoxia after cervical spinal cord injury." *J Neurosci* 23 (7):2993-3000.

Gaudet, A. D., P. G. Popovich, and M. S. Ramer. 2011. "Wallerian degeneration: gaining perspective on inflammatory events after peripheral nerve injury." *J Neuroinflammation* 8:110. doi: 10.1186/1742-2094-8-110.

Geremia, N. M., T. Gordon, T. M. Brushart, A. A. Al-Majed, and V. M. Verge. 2007. "Electrical stimulation promotes sensory neuron regeneration and growth-associated gene expression." *Exp Neurol* 205 (2):347-59. doi: S0014-4886(07)00042-8 [pii]
10.1016/j.expneurol.2007.01.040.

Geremia, N. M., L. M. Pettersson, J. C. Hasmatali, T. Hryciw, N. Danielsen, D. J. Schreyer, and V. M. Verge. 2010. "Endogenous BDNF regulates induction of intrinsic neuronal growth programs in injured sensory neurons." *Exp Neurol* 223 (1):128-42. doi: S0014-4886(09)00285-4 [pii]
10.1016/j.expneurol.2009.07.022.

Gey, M., R. Wanner, C. Schilling, M. T. Pedro, D. Sinske, and B. Knoll. 2016. "Atf3 mutant mice show reduced axon regeneration and impaired regeneration-associated gene induction after peripheral nerve injury." *Open Biol* 6 (8). doi: 10.1098/rsob.160091.

Ghergherehchi, C. L., G. D. Bittner, R. L. Hastings, M. Mikesh, D. C. Riley, R. C. Trevino, T. Schallert, W. P. Thayer, S. R. Sunkesula, T. A. Ha, N. Munoz, M. Pyarali, A. Bansal, A. D. Poon, A. T. Mazal, T. A. Smith, N. S. Wong, and P. J. Dunne. 2016. "Effects of extracellular calcium and surgical techniques on restoration of axonal continuity by polyethylene glycol fusion following complete cut or crush severance of rat sciatic nerves." *J Neurosci Res* 94 (3):231-45. doi: 10.1002/jnr.23704.

Golder, F. J., and G. S. Mitchell. 2005. "Spinal synaptic enhancement with acute intermittent hypoxia improves respiratory function after chronic cervical spinal cord injury." *J Neurosci* 25 (11):2925-32. doi: 25/11/2925 [pii]
10.1523/JNEUROSCI.0148-05.2005.

Golder, F. J., A. G. Zabka, R. W. Bavis, T. Baker-Herman, D. D. Fuller, and G. S. Mitchell. 2005. "Differences in time-dependent hypoxic phrenic responses among inbred rat strains." *J Appl Physiol* 98 (3):838-44. doi: 00984.2004 [pii]
10.1152/japplphysiol.00984.2004.

Gomez-Sanchez, J. A., L. Carty, M. Iruarrizaga-Lejarreta, M. Palomo-Irigoyen, M. Varela-Rey, M. Griffith, J. Hantke, N. Macias-Camara, M. Azkargorta, I. Aurrekoetxea, V. G. De Juan, H. B. Jefferies, P. Aspichueta, F. Elortza, A. M. Aransay, M. L. Martinez-Chantar, F. Baas, J. M. Mato, R. Mirsky, A. Woodhoo, and K. R. Jessen. 2015. "Schwann cell autophagy, myelinophagy, initiates myelin clearance from injured nerves." *J Cell Biol* 210 (1):153-68. doi: 10.1083/jcb.201503019.

Gordon, T., N. Amirjani, D. C. Edwards, and K. M. Chan. 2010. "Brief post-surgical electrical stimulation accelerates axon regeneration and muscle reinnervation without affecting the functional measures in carpal tunnel syndrome patients." *Exp Neurol* 223 (1):192-202. doi: S0014-4886(09)00407-5 [pii]
10.1016/j.expneurol.2009.09.020.

Gordon, T., and G. H. Borschel. 2016. "The use of the rat as a model for studying peripheral nerve regeneration and sprouting after complete and partial nerve injuries." *Exp Neurol*. doi: 10.1016/j.expneurol.2016.01.014.
Gordon, T., T. M. Brushart, and K. M. Chan. 2008. "Augmenting nerve regeneration with electrical stimulation." *Neurol Res* 30 (10):1012-22. doi: 10.1179/174313208X362488.
Gordon, T., P. Eva, and G. H. Borschel. 2015. "Delayed peripheral nerve repair: methods, including surgical 'cross-bridging' to promote nerve regeneration." *Neural Regen Res* 10 (10):1540-4. doi: 10.4103/1673-5374.167747.
Gordon, T., E. Udina, V. M. Verge, and E. I. de Chaves. 2009. "Brief electrical stimulation accelerates axon regeneration in the peripheral nervous system and promotes sensory axon regeneration in the central nervous system." *Motor Control* 13 (4):412-41.
Gottlieb, J. D., A. R. Schwartz, J. Marshall, P. Ouyang, L. Kern, V. Shetty, M. Trois, N. M. Punjabi, C. Brown, S. S. Najjar, and S. S. Gottlieb. 2009. "Hypoxia, not the frequency of sleep apnea, induces acute hemodynamic stress in patients with chronic heart failure." *J Am Coll Cardiol* 54 (18):1706-12. doi: 10.1016/j.jacc.2009.08.016.
Griffin, M.F., M. Malahias, S. Hindocha, and Wasim S. Khan. 2014. "Peripheral Nerve Injury: Principles for Repair and Regeneration." *The Open Orthopaedics Journal* 8:199-203. doi: 10.2174/1874325001408010199.
Gross, M. W., U. Karbach, K. Groebe, A. J. Franko, and W. Mueller-Klieser. 1995. "Calibration of misonidazole labeling by simultaneous measurement of oxygen tension and labeling density in multicellular spheroids." *Int J Cancer* 61 (4):567-73.
Hammert, Warren C. 2013. *Peripheral Nerve Conditions: Using Evidence to Guide Treatment, An Issue of Hand Clinics*. 1st ed. Vol. 29-3: Elsevier.
Han, N., C. G. Xu, T. B. Wang, Y. H. Kou, X. F. Yin, P. X. Zhang, and F. Xue. 2015. "Electrical stimulation does not enhance nerve regeneration if delayed after sciatic nerve injury: the role of fibrosis." *Neural Regen Res* 10 (1):90-4. doi: 10.4103/1673-5374.150714.
Hanani, M. 2005. "Satellite glial cells in sensory ganglia: from form to function." *Brain Res Brain Res Rev* 48 (3):457-76. doi: S0165-0173(04)00127-4 [pii]
10.1016/j.brainresrev.2004.09.001.
Hare, G.M.T., Evans, P.J., Mackinnon, S.E., Best, T.J., Midha, R., Szalai, J.P., Hunter, D.A. 1993. "Walking track analysis: Utilization of individual footprint parameters." *Ann Plast Surg* 30:147-153.
Hassan, A.U. 2015. "Intermittent hypoxia induces spinal plasticity in rats with cervical spinal cord injury." PhD, Veterinary Biomedical Sciences, University of Saskatchewan.
Hayashi, F., S. K. Coles, K. B. Bach, G. S. Mitchell, and D. R. McCrimmon. 1993. "Time-dependent phrenic nerve responses to carotid afferent activation: intact vs. decerebellate rats." *Am J Physiol* 265 (4 Pt 2):R811-9.
Henrich, M., R. Paddenberg, R. V. Haberberger, A. Scholz, M. Gruss, G. Hempelmann, and W. Kummer. 2004. "Hypoxic increase in nitric oxide generation of rat sensory neurons requires activation of mitochondrial complex II and voltage-

gated calcium channels." *Neuroscience* 128 (2):337-45. doi: 10.1016/j.neuroscience.2004.06.057.
Herradon, G., L. Ezquerra, T. Nguyen, C. Wang, A. Siso, B. Franklin, L. Dilorenzo, J. Rossenfeld, I. Silos-Santiago, and L. F. Alguacil. 2008. "Noradrenergic and opioidergic alterations in neuropathy in different rat strains." *Neurosci Lett* 438 (2):186-9. doi: 10.1016/j.neulet.2008.03.095.
Hoffmann, P., D. Buck-Gramcko, and J. D. Lubahn. 1993. "The Hoffmann-Tinel sign. 1915." *J Hand Surg Br* 18 (6):800-5.
Janjua, M. Z., and S. K. Leong. 1984. "Organization of neurons forming the femoral, sciatic, common peroneal and tibial nerves in rats and monkeys." *Brain Res* 310 (2):311-23.
Jessen, K. R., and R. Mirsky. 2005. "The origin and development of glial cells in peripheral nerves." *Nat Rev Neurosci* 6 (9):671-82. doi: 10.1038/nrn1746.
Jessen, K. R., and R. Mirsky. 2016. "The repair Schwann cell and its function in regenerating nerves." *J Physiol* 594 (13):3521-31. doi: 10.1113/JP270874.
Jonsson, S., R. Wiberg, A. M. McGrath, L. N. Novikov, M. Wiberg, L. N. Novikova, and P. J. Kingham. 2013. "Effect of delayed peripheral nerve repair on nerve regeneration, Schwann cell function and target muscle recovery." *PLoS One* 8 (2):e56484. doi: 10.1371/journal.pone.0056484.
Kandel, Eric, J. H. Schwartz, and Thomas Jessell. 2000. *Principles of Neural Science*: McGraw-Hill Medical.
Karchewski, L. A., K. A. Gratto, C. Wetmore, and V. M. Verge. 2002. "Dynamic patterns of BDNF expression in injured sensory neurons: differential modulation by NGF and NT-3." *Eur J Neurosci* 16 (8):1449-62. doi: 2205 [pii].
Kemp, S. W., J. Alant, S. K. Walsh, A. A. Webb, and R. Midha. 2010. "Behavioural and anatomical analysis of selective tibial nerve branch transfer to the deep peroneal nerve in the rat." *Eur J Neurosci* 31 (6):1074-90. doi: 10.1111/j.1460-9568.2010.07130.x.
Kemp, S. W., P. S. Cederna, and R. Midha. 2017. "Comparative outcome measures in peripheral regeneration studies." *Exp Neurol* 287 (Pt 3):348-357. doi: 10.1016/j.expneurol.2016.04.011.
Kilding, A. E., B. P. Dobson, and E. Ikeda. 2016. "Effects of Acutely Intermittent Hypoxic Exposure on Running Economy and Physical Performance in Basketball Players." *J Strength Cond Res* 30 (7):2033-42. doi: 10.1519/JSC.0000000000001301.
Koerber, H. R., A. W. Seymour, and L. M. Mendell. 1989. "Mismatches between peripheral receptor type and central projections after peripheral nerve regeneration." *Neurosci Lett* 99 (1-2):67-72. doi: 0304-3940(89)90266-8 [pii].
Lando, D., D. J. Peet, D. A. Whelan, J. J. Gorman, and M. L. Whitelaw. 2002. "Asparagine hydroxylation of the HIF transactivation domain a hypoxic switch." *Science* 295 (5556):858-61. doi: 10.1126/science.1068592.
Lee, D. H., K. Chung, and J. M. Chung. 1997. "Strain differences in adrenergic sensitivity of neuropathic pain behaviors in an experimental rat model." *Neuroreport* 8 (16):3453-6.

Li, Q. F., Y. S. Zhu, and H. Jiang. 2008. "Isoflurane preconditioning activates HIF-1alpha, iNOS and Erk1/2 and protects against oxygen-glucose deprivation neuronal injury." *Brain Res* 1245:26-35. doi: 10.1016/j.brainres.2008.09.069.

Lim, T. K., X. Q. Shi, J. M. Johnson, M. B. Rone, J. P. Antel, S. David, and J. Zhang. 2015. "Peripheral nerve injury induces persistent vascular dysfunction and endoneurial hypoxia, contributing to the genesis of neuropathic pain." *J Neurosci* 35 (8):3346-59. doi: 10.1523/JNEUROSCI.4040-14.2015.

Lin, S. Y., W. J. Chang, C. S. Lin, C. Y. Huang, H. F. Wang, and W. H. Sun. 2011. "Serotonin receptor 5-HT2B mediates serotonin-induced mechanical hyperalgesia." *J Neurosci* 31 (4):1410-8. doi: 31/4/1410 [pii]
10.1523/JNEUROSCI.4682-10.2011.

Lovett-Barr, M. R. 2008. "Intermittent hypoxia induces plasticity in spinal synaptic pathways to phrenic motor neurons: a potential therapeutic approach to spinal cord injury?" PhD, Neuroscience, Wisconsin-Madison.

Lovett-Barr, M. R., I. Satriotomo, G. D. Muir, J. E. Wilkerson, M. S. Hoffman, S. Vinit, and G. S. Mitchell. 2012. "Repetitive intermittent hypoxia induces respiratory and somatic motor recovery after chronic cervical spinal injury." *J Neurosci* 32 (11):3591-600. doi: 10.1523/JNEUROSCI.2908-11.2012
32/11/3591 [pii].

Luo, B., J. Huang, L. Lu, X. Hu, Z. Luo, and M. Li. 2014. "Electrically induced brain-derived neurotrophic factor release from Schwann cells." *J Neurosci Res* 92 (7):893-903. doi: 10.1002/jnr.23365.

MacKinnon, S. E. , and A.L. Dellon. 1988. Classification of nerve injuries as the basis for treatment. In *Surgery of the Peripheral Nerve*, edited by S. E. MacKinnon, Dellon, A.L. New York: Thieme.

Mahamed, S., and G. S. Mitchell. 2007. "Is there a link between intermittent hypoxia-induced respiratory plasticity and obstructive sleep apnoea?" *Exp Physiol* 92 (1):27-37. doi: 10.1113/expphysiol.2006.033720.

Mahamed, S., and G. S. Mitchell. 2008. "Respiratory long-term facilitation: too much or too little of a good thing?" *Adv Exp Med Biol* 605:224-7. doi: 10.1007/978-0-387-73693-8_39.

Masoud, G. N., and W. Li. 2015. "HIF-1alpha pathway: role, regulation and intervention for cancer therapy." *Acta Pharm Sin B* 5 (5):378-89. doi: 10.1016/j.apsb.2015.05.007.

Mateika, J. H., M. El-Chami, D. Shaheen, and B. Ivers. 2015. "Intermittent hypoxia: a low-risk research tool with therapeutic value in humans." *J Appl Physiol (1985)* 118 (5):520-32. doi: 10.1152/japplphysiol.00564.2014.

Mateika, J. H., and K. S. Sandhu. 2011. "Experimental protocols and preparations to study respiratory long term facilitation." *Respir Physiol Neurobiol* 176 (1-2):1-11. doi: 10.1016/j.resp.2011.01.007.

McGuire, M., Y. Zhang, D. P. White, and L. Ling. 2002. "Effect of hypoxic episode number and severity on ventilatory long-term facilitation in awake rats." *J Appl Physiol* 93 (6):2155-61. doi: 10.1152/japplphysiol.00405.2002
00405.2002 [pii].

McGuire, M., Y. Zhang, D. P. White, and L. Ling. 2004. "Serotonin receptor subtypes required for ventilatory long-term facilitation and its enhancement after chronic

intermittent hypoxia in awake rats." *Am J Physiol Regul Integr Comp Physiol* 286 (2):R334-41. doi: 10.1152/ajpregu.00463.2003
00463.2003 [pii].
Metz, G. A., and I. Q. Whishaw. 2002. "Cortical and subcortical lesions impair skilled walking in the ladder rung walking test: a new task to evaluate fore- and hindlimb stepping, placing, and co-ordination." *J Neurosci Methods* 115 (2):169-79.
Miletic, G., and V. Miletic. 2002. "Increases in the concentration of brain derived neurotrophic factor in the lumbar spinal dorsal horn are associated with pain behavior following chronic constriction injury in rats." *Neurosci Lett* 319 (3):137-40.
Millan, M. J. 1999. "The induction of pain: an integrative review." *Prog Neurobiol* 57 (1):1-164. doi: S0301-0082(98)00048-3 [pii].
Mitchell, G. S., T. L. Baker, S. A. Nanda, D. D. Fuller, A. G. Zabka, B. A. Hodgeman, R. W. Bavis, K. J. Mack, and E. B. Olson, Jr. 2001. "Invited review: Intermittent hypoxia and respiratory plasticity." *J Appl Physiol* 90 (6):2466-75.
Mitchell, G. S., and S. M. Johnson. 2003. "Neuroplasticity in respiratory motor control." *J Appl Physiol* 94 (1):358-74. doi: 10.1152/japplphysiol.00523.2002
94/1/358 [pii].
Moalem-Taylor, G., M. Li, H. N. Allbutt, A. Wu, and D. J. Tracey. 2011. "A preconditioning nerve lesion inhibits mechanical pain hypersensitivity following subsequent neuropathic injury." *Mol Pain* 7:1. doi: 10.1186/1744-8069-7-1.
Moradzadeh, A., G. H. Borschel, J. P. Luciano, E. L. Whitlock, A. Hayashi, D. A. Hunter, and S. E. Mackinnon. 2008. "The impact of motor and sensory nerve architecture on nerve regeneration." *Exp Neurol* 212 (2):370-6. doi: 10.1016/j.expneurol.2008.04.012.
Morii, H., Y. Shiraishi-Yamaguchi, and N. Mori. 2006. "SCG10, a microtubule destabilizing factor, stimulates the neurite outgrowth by modulating microtubule dynamics in rat hippocampal primary cultured neurons." *J Neurobiol* 66 (10):1101-14. doi: 10.1002/neu.20295.
Mottet, D., G. Michel, P. Renard, N. Ninane, M. Raes, and C. Michiels. 2003. "Role of ERK and calcium in the hypoxia-induced activation of HIF-1." *J Cell Physiol* 194 (1):30-44. doi: 10.1002/jcp.10176.
Navarrete-Opazo, A., J. Alcayaga, D. Testa, and A. L. Quinteros. 2016. "Intermittent Hypoxia Does not Elicit Memory Impairment in Spinal Cord Injury Patients." *Arch Clin Neuropsychol* 31 (4):332-42. doi: 10.1093/arclin/acw012.
Navarrete-Opazo, A., and G. S. Mitchell. 2014. "Therapeutic potential of intermittent hypoxia: a matter of dose." *Am J Physiol Regul Integr Comp Physiol* 307 (10):R1181-97. doi: 10.1152/ajpregu.00208.2014.
Ozon, S., A. Maucuer, and A. Sobel. 1997. "The stathmin family -- molecular and biological characterization of novel mammalian proteins expressed in the nervous system." *Eur J Biochem* 248 (3):794-806.
Pannese, E. 1960. "Observations on the morphology, submicroscopic structure and biological properties of satellite cells (s.c.) in sensory ganglia of mammals." *Z Zellforsch Mikrosk Anat* 52:567-97.
Pannese, E. 1981. "The satellite cells of the sensory ganglia." *Adv Anat Embryol Cell Biol* 65:1-111.

Peng, H., B. E. Derrick, and J. L. Martinez, Jr. 2003. "Identification of upregulated SCG10 mRNA expression associated with late-phase long-term potentiation in the rat hippocampal Schaffer-CA1 pathway in vivo." *J Neurosci* 23 (16):6617-26.
Peng, H., B. E. Derrick, and J. L. Martinez, Jr. 2004. "Time-course study of SCG10 mRNA levels associated with LTP induction and maintenance in the rat Schaffer-CA1 pathway in vivo." *Brain Res Mol Brain Res* 120 (2):182-7.
Pettersson, L. M., N. M. Geremia, Z. Ying, and V. M. Verge. 2014. "Injury-associated PACAP expression in rat sensory and motor neurons is induced by endogenous BDNF." *PLoS One* 9 (6):e100730. doi: 10.1371/journal.pone.0100730.
Pierchala, L. A., A. S. Mohammed, K. Grullon, J. H. Mateika, and M. S. Badr. 2008. "Ventilatory long-term facilitation in non-snoring subjects during NREM sleep." *Respir Physiol Neurobiol* 160 (3):259-66. doi: S1569-9048(07)00289-3 [pii]
10.1016/j.resp.2007.10.008.
Pockett, S., and R. M. Gavin. 1985. "Acceleration of peripheral nerve regeneration after crush injury in rat." *Neurosci Lett* 59 (2):221-4.
Prabhakar, N. R. 2001. "Oxygen sensing during intermittent hypoxia: cellular and molecular mechanisms." *J Appl Physiol* 90 (5):1986-94.
Prosser-Loose, E. J., A. Hassan, G. S. Mitchell, and G. D. Muir. 2015. "Delayed Intervention with Intermittent Hypoxia and Task Training Improves Forelimb Function in a Rat Model of Cervical Spinal Injury." *J Neurotrauma* 32 (18):1403-12. doi: 10.1089/neu.2014.3789.
Raivich, G. 2011. "Transcribing the path to neurological recovery-From early signals through transcription factors to downstream effectors of successful regeneration." *Ann Anat* 193 (4):248-58. doi: 10.1016/j.aanat.2011.01.010.
Rigaud, M., G. Gemes, M. E. Barabas, D. I. Chernoff, S. E. Abram, C. L. Stucky, and Q. H. Hogan. 2008. "Species and strain differences in rodent sciatic nerve anatomy: implications for studies of neuropathic pain." *Pain* 136 (1-2):188-201. doi: 10.1016/j.pain.2008.01.016.
Romero, M. I., N. Rangappa, L. Li, E. Lightfoot, M. G. Garry, and G. M. Smith. 2000. "Extensive sprouting of sensory afferents and hyperalgesia induced by conditional expression of nerve growth factor in the adult spinal cord." *J Neurosci* 20 (12):4435-45.
Salceda, S., and J. Caro. 1997. "Hypoxia-inducible factor 1alpha (HIF-1alpha) protein is rapidly degraded by the ubiquitin-proteasome system under normoxic conditions. Its stabilization by hypoxia depends on redox-induced changes." *J Biol Chem* 272 (36):22642-7.
Santosa, K. B., N. J. Jesuraj, A. Viader, M. MacEwan, P. Newton, D. A. Hunter, S. E. Mackinnon, and P. J. Johnson. 2013. "Nerve allografts supplemented with schwann cells overexpressing glial-cell-line-derived neurotrophic factor." *Muscle Nerve* 47 (2):213-23. doi: 10.1002/mus.23490.
Satriotomo, I., E. A. Dale, J. M. Dahlberg, and G. S. Mitchell. 2012. "Repetitive acute intermittent hypoxia increases expression of proteins associated with plasticity in the phrenic motor nucleus." *Exp Neurol* 237 (1):103-15. doi: 10.1016/j.expneurol.2012.05.020
S0014-4886(12)00231-2 [pii].

Satriotomo, I., N. L. Nichols, E. A. Dale, A. T. Emery, J. M. Dahlberg, and G. S. Mitchell. 2016. "Repetitive acute intermittent hypoxia increases growth/neurotrophic factor expression in non-respiratory motor neurons." *Neuroscience* 322:479-88. doi: 10.1016/j.neuroscience.2016.02.060.

Schmalbruch, H. 1986. "Fiber composition of the rat sciatic nerve." *Anat Rec* 215 (1):71-81. doi: 10.1002/ar.1092150111.

Schreyer, D. J., and J. H. Skene. 1991. "Fate of GAP-43 in ascending spinal axons of DRG neurons after peripheral nerve injury: delayed accumulation and correlation with regenerative potential." *J Neurosci* 11 (12):3738-51.

Seddon, H.J. 1948a. "A classification of nerve injuries." *Br Med J* 2:237-39.

Seddon, H.J. 1948b. "War injuries of peripheral nerves." *Br J Surg War Surg* 2 (Suppl):325.

Seddon, H.J. 1954. Peripheral nerve injuries. London: HMSO: Medical Research Council Special Report Series.

Semenza, G. L., M. K. Nejfelt, S. M. Chi, and S. E. Antonarakis. 1991. "Hypoxia-inducible nuclear factors bind to an enhancer element located 3' to the human erythropoietin gene." *Proc Natl Acad Sci U S A* 88 (13):5680-4.

Shin, J. E., S. Geisler, and A. DiAntonio. 2014. "Dynamic regulation of SCG10 in regenerating axons after injury." *Exp Neurol* 252:1-11. doi: 10.1016/j.expneurol.2013.11.007.

Shin, J. E., B. R. Miller, E. Babetto, Y. Cho, Y. Sasaki, S. Qayum, E. V. Russler, V. Cavalli, J. Milbrandt, and A. DiAntonio. 2012. "SCG10 is a JNK target in the axonal degeneration pathway." *Proc Natl Acad Sci U S A* 109 (52):E3696-705. doi: 10.1073/pnas.1216204109.

Shinder, V., and M. Devor. 1994. "Structural basis of neuron-to-neuron cross-excitation in dorsal root ganglia." *J Neurocytol* 23 (9):515-31.

Singh, B., Q. G. Xu, C. K. Franz, R. Zhang, C. Dalton, T. Gordon, V. M. Verge, R. Midha, and D. W. Zochodne. 2012. "Accelerated axon outgrowth, guidance, and target reinnervation across nerve transection gaps following a brief electrical stimulation paradigm." *J Neurosurg* 116 (3):498-512. doi: 10.3171/2011.10.JNS11612.

Smeyne, R. J., R. Klein, A. Schnapp, L. K. Long, S. Bryant, A. Lewin, S. A. Lira, and M. Barbacid. 1994. "Severe sensory and sympathetic neuropathies in mice carrying a disrupted Trk/NGF receptor gene." *Nature* 368 (6468):246-9. doi: 10.1038/368246a0.

Snell, R.S. 2010. *Clinical Neuroanatomy*: Wolters Kluwer Health/Lippincott Williams & Wilkins.

Sun, M., B. Deng, X. Zhao, C. Gao, L. Yang, H. Zhao, D. Yu, F. Zhang, L. Xu, L. Chen, and X. Sun. 2015. "Isoflurane preconditioning provides neuroprotection against stroke by regulating the expression of the TLR4 signalling pathway to alleviate microglial activation." *Sci Rep* 5:11445. doi: 10.1038/srep11445.

Sunderland, S. 1951. "A classification of peripheral nerve injuries producing loss of function." *Brain* 74:491-516.

Sunderland, S. 1978. *Nerves and nerve injuries*. 2nd edition ed. New York: Churchill Livingstone.

Swett, J. E., Y. Torigoe, V. R. Elie, C. M. Bourassa, and P. G. Miller. 1991. "Sensory neurons of the rat sciatic nerve." *Exp Neurol* 114 (1):82-103. doi: 0014-4886(91)90087-S [pii].

Swett, J. E., R. P. Wikholm, R. H. Blanks, A. L. Swett, and L. C. Conley. 1986. "Motoneurons of the rat sciatic nerve." *Exp Neurol* 93 (1):227-52.

Szynkaruk, M., S. W. Kemp, M. D. Wood, T. Gordon, and G. H. Borschel. 2013. "Experimental and clinical evidence for use of decellularized nerve allografts in peripheral nerve gap reconstruction." *Tissue Eng Part B Rev* 19 (1):83-96. doi: 10.1089/ten.TEB.2012.0275.

Tajdaran, K., T. Gordon, M. D. Wood, M. S. Shoichet, and G. H. Borschel. 2016. "A glial cell line-derived neurotrophic factor delivery system enhances nerve regeneration across acellular nerve allografts." *Acta Biomater* 29:62-70. doi: 10.1016/j.actbio.2015.10.001.

Tang, K., E. C. Breen, H. Wagner, T. D. Brutsaert, M. Gassmann, and P. D. Wagner. 2004. "HIF and VEGF relationships in response to hypoxia and sciatic nerve stimulation in rat gastrocnemius." *Respir Physiol Neurobiol* 144 (1):71-80. doi: 10.1016/j.resp.2004.04.009.

Tender, G. C., Y. Y. Li, and J. G. Cui. 2010. "Brain-derived neurotrophic factor redistribution in the dorsal root ganglia correlates with neuropathic pain inhibition after resiniferatoxin treatment." *Spine J* 10 (8):715-20. doi: S1529-9430(10)00285-8 [pii]
10.1016/j.spinee.2010.03.029.

Thompson, N. J., D. R. Sengelaub, and A. W. English. 2014. "Enhancement of peripheral nerve regeneration due to treadmill training and electrical stimulation is dependent on androgen receptor signaling." *Dev Neurobiol* 74 (5):531-40. doi: 10.1002/dneu.22147.

Tinel, J. 1915. "Le signe du 'fourmillement' dans les lesions des nerfs periphiques." *Presse Med* 23:388-89.

Trumbower, R. D., A. Jayaraman, G. S. Mitchell, and W. Z. Rymer. 2012. "Exposure to acute intermittent hypoxia augments somatic motor function in humans with incomplete spinal cord injury." *Neurorehabil Neural Repair* 26 (2):163-72. doi: 1545968311412055 [pii]
10.1177/1545968311412055.

Tsujino, H., E. Kondo, T. Fukuoka, Y. Dai, A. Tokunaga, K. Miki, K. Yonenobu, T. Ochi, and K. Noguchi. 2000. "Activating transcription factor 3 (ATF3) induction by axotomy in sensory and motoneurons: A novel neuronal marker of nerve injury." *Mol Cell Neurosci* 15 (2):170-82. doi: 10.1006/mcne.1999.0814.

Uchida, H., Y. Matsushita, and H. Ueda. 2013. "Epigenetic regulation of BDNF expression in the primary sensory neurons after peripheral nerve injury: implications in the development of neuropathic pain." *Neuroscience* 240:147-54. doi: 10.1016/j.neuroscience.2013.02.053.

Udina, E., M. Furey, S. Busch, J. Silver, T. Gordon, and K. Fouad. 2008. "Electrical stimulation of intact peripheral sensory axons in rats promotes outgrowth of their central projections." *Exp Neurol* 210 (1):238-47. doi: S0014-4886(07)00415-3 [pii]
10.1016/j.expneurol.2007.11.007.

Vargas, M. E., Y. Yamagishi, M. Tessier-Lavigne, and A. Sagasti. 2015. "Live Imaging of Calcium Dynamics during Axon Degeneration Reveals Two Functionally Distinct Phases of Calcium Influx." *J Neurosci* 35 (45):15026-38. doi: 10.1523/JNEUROSCI.2484-15.2015.

Verge, V. M., K. A. Gratto, L. A. Karchewski, and P. M. Richardson. 1996. "Neurotrophins and nerve injury in the adult." *Philos Trans R Soc Lond B Biol Sci* 351 (1338):423-30. doi: 10.1098/rstb.1996.0038.

Verge, V. M., P. M. Richardson, Z. Wiesenfeld-Hallin, and T. Hokfelt. 1995. "Differential influence of nerve growth factor on neuropeptide expression in vivo: a novel role in peptide suppression in adult sensory neurons." *J Neurosci* 15 (3 Pt 1):2081-96.

Verge, V. M., W. Tetzlaff, M. A. Bisby, and P. M. Richardson. 1990. "Influence of nerve growth factor on neurofilament gene expression in mature primary sensory neurons." *J Neurosci* 10 (6):2018-25.

Verge, V.M.K., Geremia, L.M.F., Petterssoon, M.E., Danielsen, N. . 2004. "Endogenous BDNF regulates injury/regeneration-associated gene expression in adult motor neurons." Society for Neuroscience.

Villiere, V., and E. M. McLachlan. 1996. "Electrophysiological properties of neurons in intact rat dorsal root ganglia classified by conduction velocity and action potential duration." *J Neurophysiol* 76 (3):1924-41.

Vinit, S., M. R. Lovett-Barr, and G. S. Mitchell. 2009. "Intermittent hypoxia induces functional recovery following cervical spinal injury." *Respir Physiol Neurobiol* 169 (2):210-7. doi: 10.1016/j.resp.2009.07.023

S1569-9048(09)00220-1 [pii].

Wadhwa, H., C. Gradinaru, G. J. Gates, M. S. Badr, and J. H. Mateika. 2008. "Impact of intermittent hypoxia on long-term facilitation of minute ventilation and heart rate variability in men and women: do sex differences exist?" *J Appl Physiol (1985)* 104 (6):1625-33. doi: 10.1152/japplphysiol.01273.2007.

Waller, A. 1850. Experiments on the section of the glossopharyngeal and hypoglossal nerves of the frog, and observations of the alterations produced thereby in the structure of their primitive fibres. edited by Soc. PTR. London.

Wang, Y., Z. Zhao, Z. Ren, B. Zhao, L. Zhang, J. Chen, W. Xu, S. Lu, Q. Zhao, and J. Peng. 2012. "Recellularized nerve allografts with differentiated mesenchymal stem cells promote peripheral nerve regeneration." *Neurosci Lett* 514 (1):96-101. doi: 10.1016/j.neulet.2012.02.066.

Weil, J. V. 2003. "Variation in human ventilatory control-genetic influence on the hypoxic ventilatory response." *Respir Physiol Neurobiol* 135 (2-3):239-46. doi: S156990480300048X [pii].

Wenjin, W., L. Wenchao, Z. Hao, L. Feng, W. Yan, S. Wodong, F. Xianqun, and D. Wenlong. 2011. "Electrical stimulation promotes BDNF expression in spinal cord neurons through Ca(2+)- and Erk-dependent signaling pathways." *Cell Mol Neurobiol* 31 (3):459-67. doi: 10.1007/s10571-010-9639-0.

Wiesenfeld, Z., and R. G. Hallin. 1981. "Influence of nerve lesions, strain differences and continuous cold stress on chronic pain behavior in rats." *Physiol Behav* 27 (4):735-40.

Wilber, R. L., J. Stray-Gundersen, and B. D. Levine. 2007. "Effect of hypoxic "dose" on physiological responses and sea-level performance." *Med Sci Sports Exerc* 39 (9):1590-9. doi: 10.1249/mss.0b013e3180de49bd.

Wilkerson, J. E., and G. S. Mitchell. 2009. "Daily intermittent hypoxia augments spinal BDNF levels, ERK phosphorylation and respiratory long-term facilitation." *Exp Neurol* 217 (1):116-23. doi: 10.1016/j.expneurol.2009.01.017
S0014-4886(09)00039-9 [pii].

Willand, M. P., C. D. Chiang, J. J. Zhang, S. W. Kemp, G. H. Borschel, and T. Gordon. 2015. "Daily Electrical Muscle Stimulation Enhances Functional Recovery Following Nerve Transection and Repair in Rats." *Neurorehabil Neural Repair* 29 (7):690-700. doi: 10.1177/1545968314562117.

Willand, M. P., J. P. Lopez, H. de Bruin, M. Fahnestock, M. Holmes, and J. R. Bain. 2011. "A New System and Paradigm for Chronic Stimulation of Denervated Rat Muscle." *J Med Biol Eng* 31 (2):87-92. doi: 10.5405/jmbe.828.

Willand, M. P., E. Rosa, B. Michalski, J. J. Zhang, T. Gordon, M. Fahnestock, and G. H. Borschel. 2016. "Electrical muscle stimulation elevates intramuscular BDNF and GDNF mRNA following peripheral nerve injury and repair in rats." *Neuroscience* 334:93-104. doi: 10.1016/j.neuroscience.2016.07.040.

Witzel, C., C. Rohde, and T. M. Brushart. 2005. "Pathway sampling by regenerating peripheral axons." *J Comp Neurol* 485 (3):183-90. doi: 10.1002/cne.20436.

Yang, D., L. Gao, T. Wang, Z. Qiao, Y. Liang, and P. Zhang. 2014. "Hypoxia triggers endothelial endoplasmic reticulum stress and apoptosis via induction of VLDL receptor." *FEBS Lett* 588 (23):4448-56. doi: 10.1016/j.febslet.2014.09.046.

Ying, Z., V. Misra, and V. M. Verge. 2014. "Sensing nerve injury at the axonal ER: activated Luman/CREB3 serves as a novel axonally synthesized retrograde regeneration signal." *Proc Natl Acad Sci U S A* 111 (45):16142-7. doi: 10.1073/pnas.1407462111.

Yu, Y., P. Zhang, N. Han, Y. Kou, X. Yin, and B. Jiang. 2016. "Collateral development and spinal motor reorganization after nerve injury and repair." *Am J Transl Res* 8 (7):2897-911.

Zabka, A. G., M. Behan, and G. S. Mitchell. 2001a. "Long term facilitation of respiratory motor output decreases with age in male rats." *J Physiol* 531 (Pt 2):509-14.

Zabka, A. G., M. Behan, and G. S. Mitchell. 2001b. "Selected contribution: Time-dependent hypoxic respiratory responses in female rats are influenced by age and by the estrus cycle." *J Appl Physiol (1985)* 91 (6):2831-8. doi: 10.1152/jappl.2001.91.6.2831.

Zabka, A. G., G. S. Mitchell, and M. Behan. 2006. "Conversion from testosterone to oestradiol is required to modulate respiratory long-term facilitation in male rats." *J Physiol* 576 (Pt 3):903-12. doi: 10.1113/jphysiol.2006.114850.

Zhang, J., Y. Xiong, L. X. Lu, H. Wang, Y. F. Zhang, F. Fang, Y. L. Song, and H. Jiang. 2013. "AQP1 expression alterations affect morphology and water transport in Schwann cells and hypoxia-induced up-regulation of AQP1 occurs in a HIF-1alpha-dependent manner." *Neuroscience* 252:68-79. doi: 10.1016/j.neuroscience.2013.08.006.

Zhang, J. Y., X. G. Luo, C. J. Xian, Z. H. Liu, and X. F. Zhou. 2000. "Endogenous BDNF is required for myelination and regeneration of injured sciatic nerve in rodents." *Eur J Neurosci* 12 (12):4171-80. doi: ejn1312 [pii].

Zhao, P., and Z. Zuo. 2004. "Isoflurane preconditioning induces neuroprotection that is inducible nitric oxide synthase-dependent in neonatal rats." *Anesthesiology* 101 (3):695-703.

Zigmond, R. E. 2012. "Cytokines that promote nerve regeneration." *Exp Neurol* 238 (2):101-6. doi: 10.1016/j.expneurol.2012.08.017.

Zochodne, D. W. 2012. "The challenges and beauty of peripheral nerve regrowth." *J Peripher Nerv Syst* 17 (1):1-18. doi: 10.1111/j.1529-8027.2012.00378.x.